



**HAL**  
open science

# Design and characterization of adaptive geometry composite structures using 3D multilayer woven reinforcements

Zakariya Zubair

► **To cite this version:**

Zakariya Zubair. Design and characterization of adaptive geometry composite structures using 3D multilayer woven reinforcements. Mechanics [physics]. Université de Haute Alsace - Mulhouse, 2020. English. NNT : 2020MULH2983 . tel-03690947

**HAL Id: tel-03690947**

**<https://theses.hal.science/tel-03690947v1>**

Submitted on 8 Jun 2022

**HAL** is a multi-disciplinary open access archive for the deposit and dissemination of scientific research documents, whether they are published or not. The documents may come from teaching and research institutions in France or abroad, or from public or private research centers.

L'archive ouverte pluridisciplinaire **HAL**, est destinée au dépôt et à la diffusion de documents scientifiques de niveau recherche, publiés ou non, émanant des établissements d'enseignement et de recherche français ou étrangers, des laboratoires publics ou privés.

Year 2020

**Université de Haute Alsace (UHA)**

**Laboratoire de Physique et Mécanique Textiles LPMT (ED269)**

# **THESIS**

A thesis submitted to fulfil the requirement for the degree of Doctor of Philosophy (Ph.D) in  
Mechanics

Submitted by: Zakariya ZUBAIR

17 July 2020

---

**Design and characterization of adaptive geometry composite  
structures using 3D multilayer woven reinforcements**

**Conception et caractérisation de structures composites à  
géométrie adaptative à l'aide de renforts tissés multicouches 3D**

---

Jury Members:

Professeur Damien Soulat  
Professeur Jean François Ganghoffer  
Professeur Bernard Durand  
Professeur Gildas L'Hostis  
directeur de thèse

Gemtex, ENSAIT de Roubaix  
LEM3, Université de Lorraine  
LPMT, Université de Haute Alsace  
LPMT, Université de Haute Alsace

Rapporteur  
Rapporteur  
Examineur  
Examineur,

## **Acknowledgement**

First of all, I want to express my deep gratitude to my supervisor Dr. Gildas L'Hostis for giving me the opportunity to perform my doctorate research work under his kind supervision. I also grateful to Dr. Jean-Yves Drean and Muhammad Zubair (Father) for their valuable guidance, suggestions and encouragement to complete this research work. They motivated me in every way and put all their efforts to provide a favourable working environment. Without their contribution, I couldn't have accomplished my research with this much ease and zest. I, importantly, express my heartiest gratitude to Higher Education Commission (HEC) PAKISTAN for financing me and providing me the opportunity to study abroad and develop new skills. Last but not the least, I am highly grateful to my beloved family, especially my parents who supported me in every way throughout my career. They have always remained a constant source of encouragement and motivation for me.

## **DEDICATION**

This research work is dedicated to my great parent's and my wife.

## List of Abbreviations

ANOVA	Analysis of Variance
ILSS	Interlaminar shear strength
SBST	Short beam shear test
SM	Shape memory
SMP	Shape memory polymer
SMPC	Shape memory polymer composite
SMC	Shape memory composite
SMF	Shape memory function
SME	Shape memory effect
SR	Shape Recovery
SRC	Shape recovery cycle
SRE	Shape recovery effect
$T_a$	Ambient temperature
$T_g$	Glass transition temperature
$T_r$	Recovery temperature
TMDP	Thermomechanical deformation process

## Résumé étendu de la thèse en Français

### Introduction

Les composites à base de polymères à mémoire de forme (SMPC) peuvent être considéré comme des matériaux actifs, car ils combinent les propriétés mécaniques et fonctionnelles typiques des composites avec des propriétés de mémoire de forme. En particulier, les préformes fibreuses tridimensionnelles (3D) ont un potentiel énorme pour le développement de ces composites car elles permettent de combiner leurs capacités de conception 3D et le comportement de polymère à mémoire de forme de la matrice.

Dans ce cadre, ce travail vise à étudier le comportement de la mémoire de forme et les propriétés de récupération de forme d'un type spécifique de composite SMPC multicouche tissé 3D (SMPC 3D) soumis à stimuli thermiques, externe puis interne.

Une série de tests est effectuée sur neuf renforts 3D pour évaluer leurs propriétés mécaniques et physiques puis le renfort qui présente les meilleures performances mécaniques est ensuite utilisée pour fabriquer les échantillons composites SMPC 3D. Des essais comprenant des tests de flexion trois points et de cisaillement inter laminaire sont ensuite réalisés pour étudier leur réponse mécanique pour différentes températures.

Ensuite par des essais spécifiques, la mémoire de forme et la capacité de récupération de forme de ces composite sont étudiées. Un scanner 3D basé sur la projection de franges est utilisé pour acquérir précisément les données géométriques et effectuer une analyse de déformation afin d'évaluer quantitativement la fixité de la forme et les comportements de récupération du composite à mémoire de forme. Enfin, une étude complète portant sur les deux étapes caractéristiques pour un composite à mémoire de forme, la fixation de la forme (fixity) et le retour à la forme initiale (recovery) est présentée. Elle repose sur le développement d'un essais mécanique particulier basé sur un essai de flexion trois point et met en œuvre des composites autonomes, c'est-à-dire comportant une activation thermique interne qui peut être piloté par effet Joule. Les résultats de cette étude sont très prometteurs pour des applications de structures déployables, car ils montrent que ces structures SMPC 3D peuvent retrouver leur forme initiale avec succès et sans apparition

de dommages notables même pour des niveaux de compaction important imposé sur la structure lors de la phase initiale de fixation de la forme.

## **Bibliographie – Chapitre 2**

Les polymères à mémoire de forme (Shape Memory Polymer, SMP) sont une classe de matériaux actifs déformables qui ont une capacité de double forme. Ils ont attiré une attention croissante au cours des dernières décennies en raison de leur importance scientifique et technologique. L'effet de mémoire de forme est un phénomène et non une propriété intrinsèque, ce qui signifie que les polymères ne présentent pas cet effet par eux-mêmes. Les SMP offrent une capacité unique à subir une déformation substantielle de leur forme et à retrouver ensuite la forme permanente d'origine lorsqu'ils sont exposés à un nouveau stimuli. Ces stimuli peuvent être de différents types, tels que la chaleur (thermo-réactif), la chimie (y compris l'eau, chimio-réactif), la lumière (photo-réactif), le pH du milieu (pH-réactif), le courant/tension électrique (électro-réactif), le champ magnétique (magnéto-réactif). Parmi eux, les SMP thermo-réactifs sont toujours le groupe le plus courant et le plus étudié en raison de leur large éventail d'applications. Dans ce travail, nous considérons la stimulation thermique comme un activateur de l'effet de mémoire de forme pour lequel la récupération (recovery) se produit par rapport à une certaine température critique. En fait, il a été prouvé que les matériaux SMP sont des substituts appropriés pour les alliages métalliques à mémoire de forme en raison de leurs avantages inhérents : ils sont bon marché, légers, faciles à mettre en œuvre et offrent une déformabilité plus élevée.

Les SMP sont essentiellement connus pour avoir une double forme, c'est-à-dire la forme originale et la forme déformée. L'architecture moléculaire des polymères facilite en fait cette propriété de mémoire de forme [47]. Les SMP peuvent être considérés comme des copolymères ayant un segment dur et un segment mou (Fig. 1), agissant ainsi respectivement comme une phase fixe et une phase réversible. La fonction de la phase fixe est d'empêcher l'écoulement des chaînes polymères voisines lorsque la contrainte est appliquée. Alors que l'autre phase, responsable de l'élasticité du polymère, subit une déformation temporaire dans le cycle de mémoire de forme. Cette seconde phase réversible remplit la fonction d'un commutateur moléculaire, ce qui permet de stocker la forme déformée en dessous d'une température dite de de transition et, plus tard, de

permettre au polymère de reprendre sa forme pour une température égale ou supérieure à cette température de transition [48].

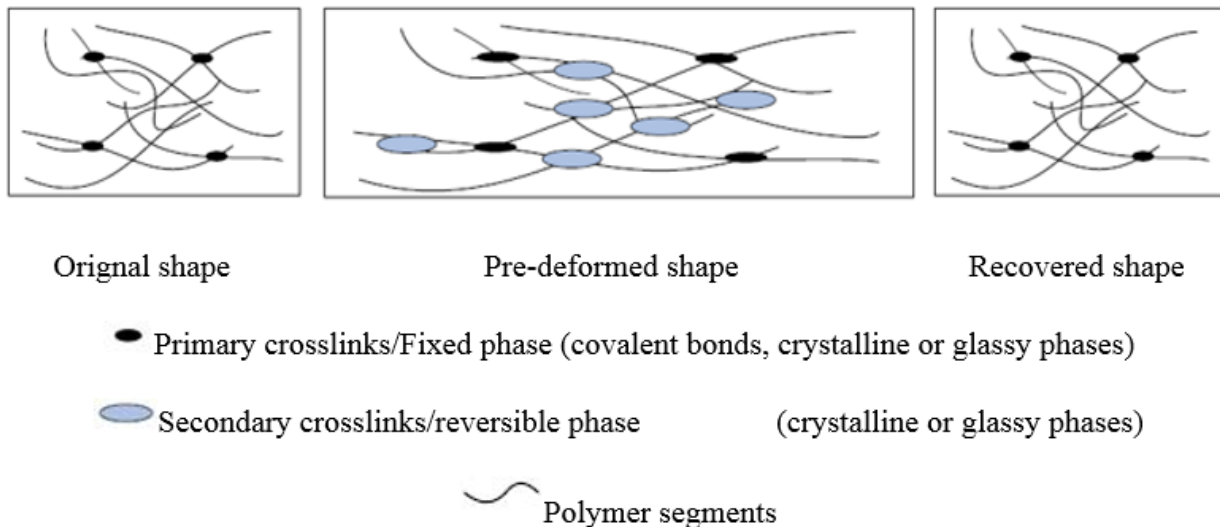


Figure 1: Schématisation du réseau d'un polymère à mémoire de forme [49]

Les SMP peuvent être classés en fonction du nombre de géométries qu'ils peuvent fixer lors de leur phase d'éducation (Duale, Triple ou multiple géométries) mais aussi de leur capacité lors de la phase de recouvrement (recovery) d'aller et venir ou non entre ces différentes géométries et ceci sans une nouvelle étape d'éducation (Fig. 2). On parle alors d'effet simple ou double (One-way ou two-way effect).

Les SMP ont été étudiés pour plusieurs applications potentielles en raison de leur programmation facile (cycle d'éducation), de leur coût et poids réduits ainsi que leur capacité à recouvrir de fortes modifications. Cependant, ils présentent certains inconvénients qui les rendent impossibles à utiliser pour certaines applications. Par exemple, le taux de récupération de la forme sous contrainte des SMP est faible (3 MPa), contrairement à leur homologue métalliques, les SMA (0,5 Gpa). Pour surmonter ce problème, l'utilisation de composites à mémoire de forme (Shape Memory Polymer Composite, SMPC) constitue une alternative. De nombreux travaux ont donc porté sur le couplage des propriétés de mémoire des polymères avec les propriétés mécaniques de différents types de renforts, fibreux ou non, pour élaborer des composites à mémoire de forme. Il a été montré que l'introduction de tout type de renforcement dans le composite peut aider à améliorer sa contrainte d'actionnement ou taux de récupération sous contrainte. Le verre, les



nanoparticules, le Kevlar ou les fils de carbone finement hachés sont quelques exemples de renforcement qui peuvent être utilisés dans une structure composite.

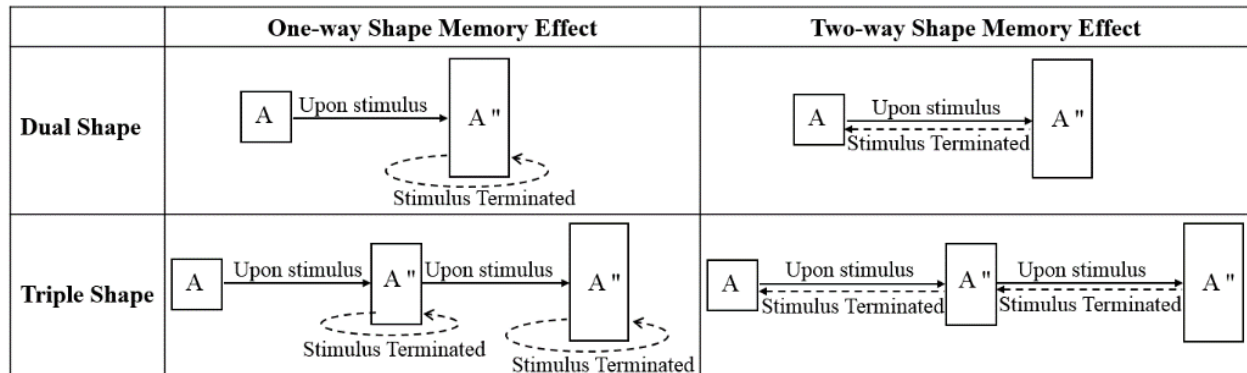


Figure 2: Description du fonctionnement des SMP (modifié de [82])

Dans le domaine des "smart materials", les SMPC occupent un large domaine d'applications allant des engins spatiaux aux véhicules routiers. Dans le domaine aérospatial, des travaux récents ont montré leur potentiel pour le développement de structures déployables. Les propriétés de déploiement sont amplifiées grâce à l'utilisation de structures pliables/origamiques, approches qui permet également de complexifier les changements géométriques.

Ce type de formes complexes a notamment été obtenue à partir d'un composite à base de résine époxy renforcé par des fibres de verre qui offre la possibilité de changer de forme grâce à la liaison dynamique ester illustrée dans la figure 3 [112].

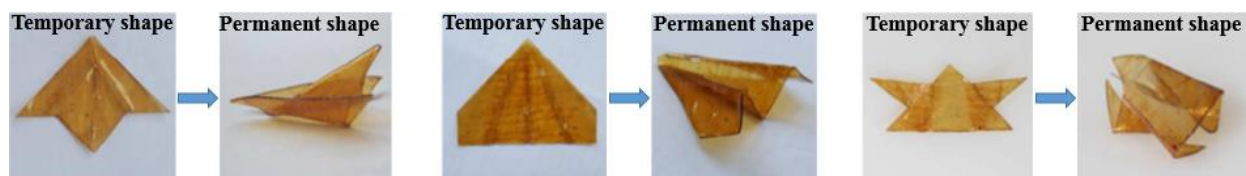


Figure 3: SMPC origamique [112]

Une autre application étudiée est celle d'antennes spatiales déployables (Fig. 4). La forme de l'antenne de type mat, est obtenue par l'enchevêtrement de tissus en fibre de carbone et la matrice utilisée est une epoxy [113].

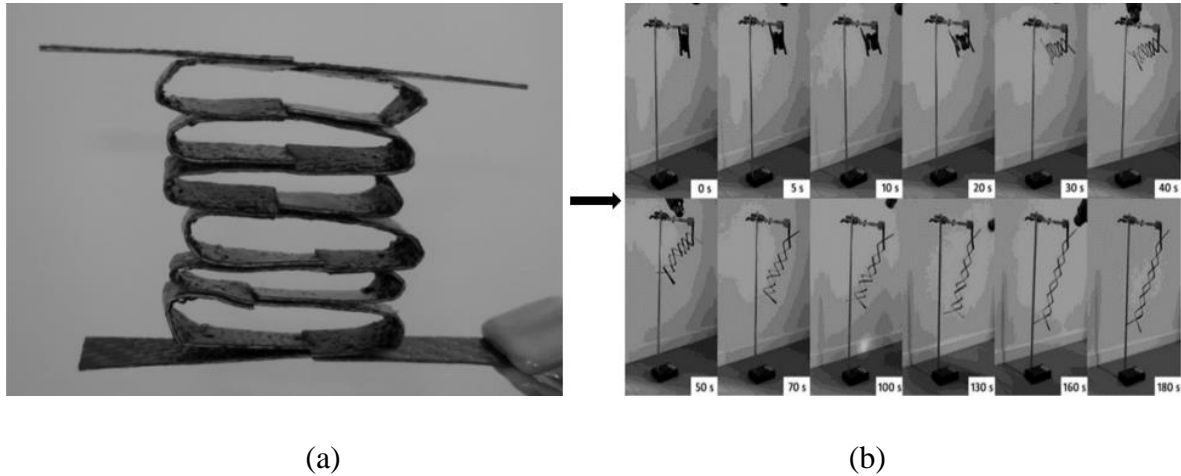


Figure 4 (a) Forme fixée après éducation, (b) différentes étapes du recouvrement [113]

Pour résumer, ce chapitre aborde divers aspects des SMP, et des composites à mémoire de forme (SMPC). Différentes applications potentielles des SMPC y sont décrites.

### Matériel et méthode – Chapitre 3

Ce travail, se décompose en trois grandes étapes. La première porte sur la sélection de renforts à architecture 3D obtenus à partir de structures tissées 3 couches, chacune des couches (supérieure, inférieure et intermédiaire) entrelacées entre elles, possède un tissage différent. Cette sélection repose sur des propriétés de perméabilité à l'air, de flexion et de cisaillement dans le plan de l'étoffe. Le renfort de type A3 24 qui possède un motif à armure toile dans toutes les couches et des densités de remplissage élevées dans les sens de la chaîne et de la trame a été retenu pour la fabrication de SMPC, car bien que présentant une perméabilité plus faible que les autres, il possède à l'inverse les meilleures propriétés en flexion et cisaillement.

Ce choix du renfort est complété par celui de la matrice (SMP) et bien qu'il existe plusieurs types de polymères à mémoire de forme thermoplastiques ou thermodurcissable, nous utilisons dans cette étude une résine époxy. Ceci car les résines à base d'époxy présentent de bonnes propriétés pour la mémoire de forme mais aussi car elles possèdent d'excellentes propriétés thermiques et mécaniques. La matrice époxy est préparée en mélangeant une base époxy Araldite LY 1564 avec des durcisseurs Aradur 3486 et 3487. La résine époxy Araldite LY 1564 a une densité de  $1,1 \text{ g/cm}^3$ , une viscosité de 1200-1400 mPas, et un indice d'époxy de 5,8-6,05 Eq/kg. Ces composants de chez Huntsman sont mélangés dans le rapport de (100/8,5/25,5) - (résine/ durcisseur 1/durcisseur 2).

La seconde étape consiste à fabriquer différents types d'échantillons afin d'étudier les points suivant : les propriétés de mémoire de forme de la matrice seule, du SMPC composé du renfort 3D et de la matrice (SMPC 3D) et enfin du SMPC 3D autonome comportant outre le renfort 3D des fils de carbone qui par effet Joule permet de générer une source interne de chaleur dans le composite.

Afin d'obtenir des épaisseurs contrôlées et un bon placement des renforts, un moule spécial en acier inoxydable (17cm×17cm×2cm) a été réalisé. Le moule se compose de deux parties (inférieure et supérieure). La fermeture du moule et son serrage se font à l'aide de 8 vis, l'épaisseur finale du composite est donnée par la géométrie du moule fermé. Pour le reste de l'étude, ce moule servira à réaliser les trois types de plaques : plaque de résine seule, plaque résine/renfort 3D, plaque résine/renfort 3D/fils de carbone. Après réalisation les éprouvettes nécessaires aux différents essais de caractérisations, sont extraites de ces plaques par une découpe à disque diamant.

La dernière étape consiste à réaliser un ensemble de caractérisation pour mettre en évidence les aptitudes de mise en forme des différents échantillons SMP et SMPC. Pour déterminer les propriétés physico-chimique de la résine et notamment sa température de transition vitreuse ( $T_g$ ), une analyse DSC est réalisée. Ceci permet de définir la plage de température dans laquelle il est nécessaire de se situer pour réaliser la mise en forme. Ces essais de DSC mené sur résine seule sont complétés par des essais de formabilité des échantillons de résine. A partir d'un essai de flexion 3 points leur capacité à admettre de fort rayon de courbure est ainsi étudiée.

Par la suite les essais de caractérisations mécanique sur les SMPC s'organisent suivant des essais relatifs à l'étude de leur déformabilité sous conditionnement libre (pas de mesure d'effort) d'une part et d'autre part sur des essais de flexion 3 points réalisés sur une machine de traction Instron (série 5985) équipée d'une enceinte thermique. Pour ces essais trois capteurs sont utilisés dont les charges limites sont respectivement de 500 N, 2kN et 250 kN.

### **Essais en conditions libre - fold-deploy shape memory test**

Après une étape de chauffage à la température de déformation ( $T_d = T_g + 5^\circ\text{C} - 91^\circ\text{C}$ ), les échantillons SMPC 3D (renfort 3D/epoxy) de géométrie plane et de dimension (170 x 14 x 1,4 mm<sup>3</sup>) sont mis en forme manuellement suivant différentes géométries puis refroidis dans un bain d'eau froide pour fixer la nouvelle forme. Les différentes géométries étudiées induisent dans le

SMPC des effets de flexion de torsion ou les combinent (forme en U, S, M et en spirale). Après fixation de la forme souhaitée, les échantillons sont ensuite réchauffés à la température de recouvrance ( $T_r = T_d$ ) pour analyser leur capacité à recouvrir leur géométrie initiale. Cette procédure est réalisée trois fois par échantillons puis leurs surfaces sont observées par MEB pour identifier l'existence de dommages.

### **Etude fine des propriétés de mise en forme libre**

Les paramètres les plus importants pour quantifier les propriétés de mémoire de forme sont la récupération de la forme et la fixité de la forme. La récupération de la forme quantifie la capacité du matériau composite SMPC à retrouver sa forme originale tandis que la fixité de la forme quantifie la capacité du matériau à fixer une forme temporaire. Afin d'obtenir une mesure fine des changements géométrique entre les différentes géométries caractéristiques du cycle du SMPC 3D (géométries initiale, imposée, fixée puis recouverte) une numérisation 3D de chacune d'entre elles est réalisée. La technique utilisée est celle de la projection de frange, le dispositif expérimental est un scanner GOM ATOS Core MV135 (Fig.5) avec un volume de mesure de 135mm×100mm×100mm et une résolution de caméra de 2448×2050 pixels.

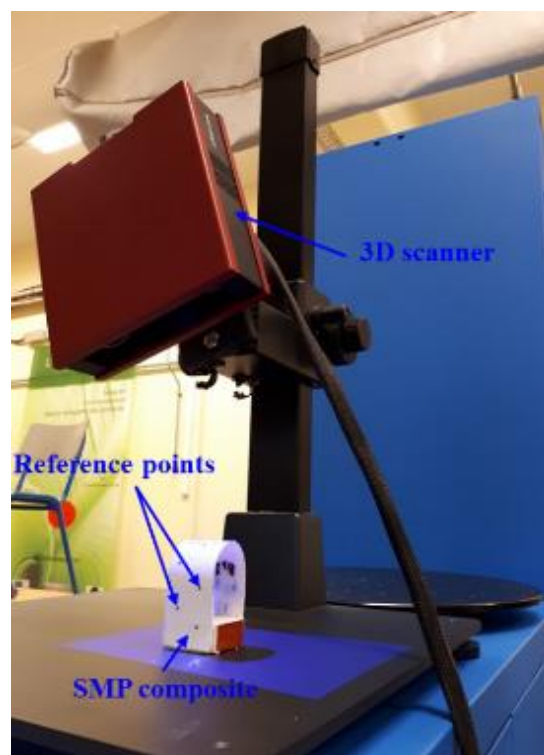


Figure 5: Dispositif de numérisation 3D

### **Flexion en température**

Afin d'établir le comportement en flexion des échantillons SMPC et en fonction de la température (25°C, 40°C et 60 °C), une série d'essais menée sur 5 échantillons (pour chaque température) a été réalisée en suivant la norme ISO 14125:1998. Après essais les échantillons sont observé par MEB pour analyse des dommages.

### **Cisaillement inter laminaire (ILSS)**

Pour évaluer le comportement des composites SMPC 3D pour de fortes courbures imposées, et plus particulièrement leur résistance au cisaillement suivant l'épaisseur, les échantillons sont soumis à un essai d'ILSS en fonction de la température (25°C, 60°C et 80 °C) et conformément à la norme NF EN ISO 14130. L'ILSS est déterminée en effectuant un essai de flexion trois points sur appuis rapprochés pour une série de trois échantillons (par température). Après essais les échantillons sont observé par MEB pour analyse des dommages.

### **Test complet sur composite autonome**

Les SMPC 3D intègrent dans cette partie les fils de carbones qui permettent de générer par effet Joule une source interne de chaleur. Pour cet essai un dispositif expérimental spécifique a été mis en place. Le montage de flexion 3 points est complété par un générateur de courant connecté à l'échantillon SMPC et par un système d'acquisition de températures mesurées par trois thermocouples disposés sur la surface supérieure du SMPC (Fig. 6). Un cycle thermomécanique d'éducation et de recouvrance a été programmé sur la machine de traction. A partir de la géométrie initiale, ce cycle contient les étapes suivantes :

- Une étape de chauffe à  $T_d$  avec maintien d'une pré-charge de 0.1N
- Une étape de chargement conduisant à la géométrie imposée (forme en U)
- Une étape de refroidissement avec maintien de la géométrie (géométrie déformée)
- Un retour à la pré-charge de 0.1N (géométrie fixée)
- Une étape de chauffe à  $T_r=T_d$  avec maintien d'une pré-charge de 0.1N, pour la recouvrance

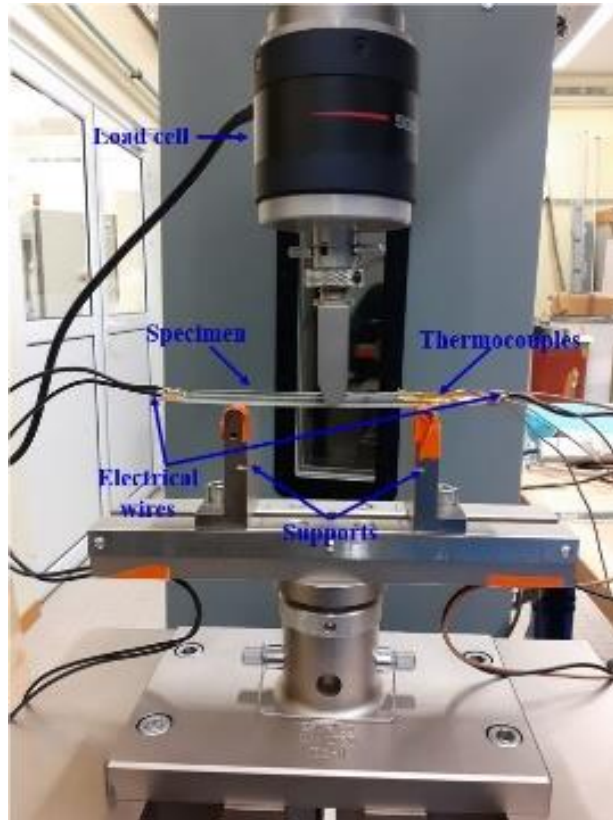


Figure 6: Dispositif d'essai avec capteur de 500N (classe 0.5)

## Résultats et discussion – Chapitre 4

Les principaux résultats obtenus dans ce travail et relatif aux propriétés de mémoire de forme des composites à renfort 3D se résume de la manière suivante :

### Essais en conditions libre et étude fine des propriétés de mise en forme

La figure 7 présente la récupération de la géométrie initiale pour trois géométries fixées complexes (géométrie en M, en torsion et en spirale). La première géométrie basée sur des effets de flexion met 31 secondes pour revenir à sa forme plane initiale (Fig. 7-a). Pour la seconde les effets de torsions gèrent les effets mémoire et le temps de recouvrance est égal à 34 s, temps équivalent au précédent (Fig. 7-b). La géométrie en spirale est la plus complexe car le comportement de mémoire fait appel à de la torsion combinée à de la flexion, le temps nécessaire à la recouvrance est ici de 49 s (Fig. 7-c). Les observations MEB de ces échantillons après trois cycle (éducation-recouvrance) n'ont pas permis de visualiser des dommages sur leurs surfaces et ceci quel que soit



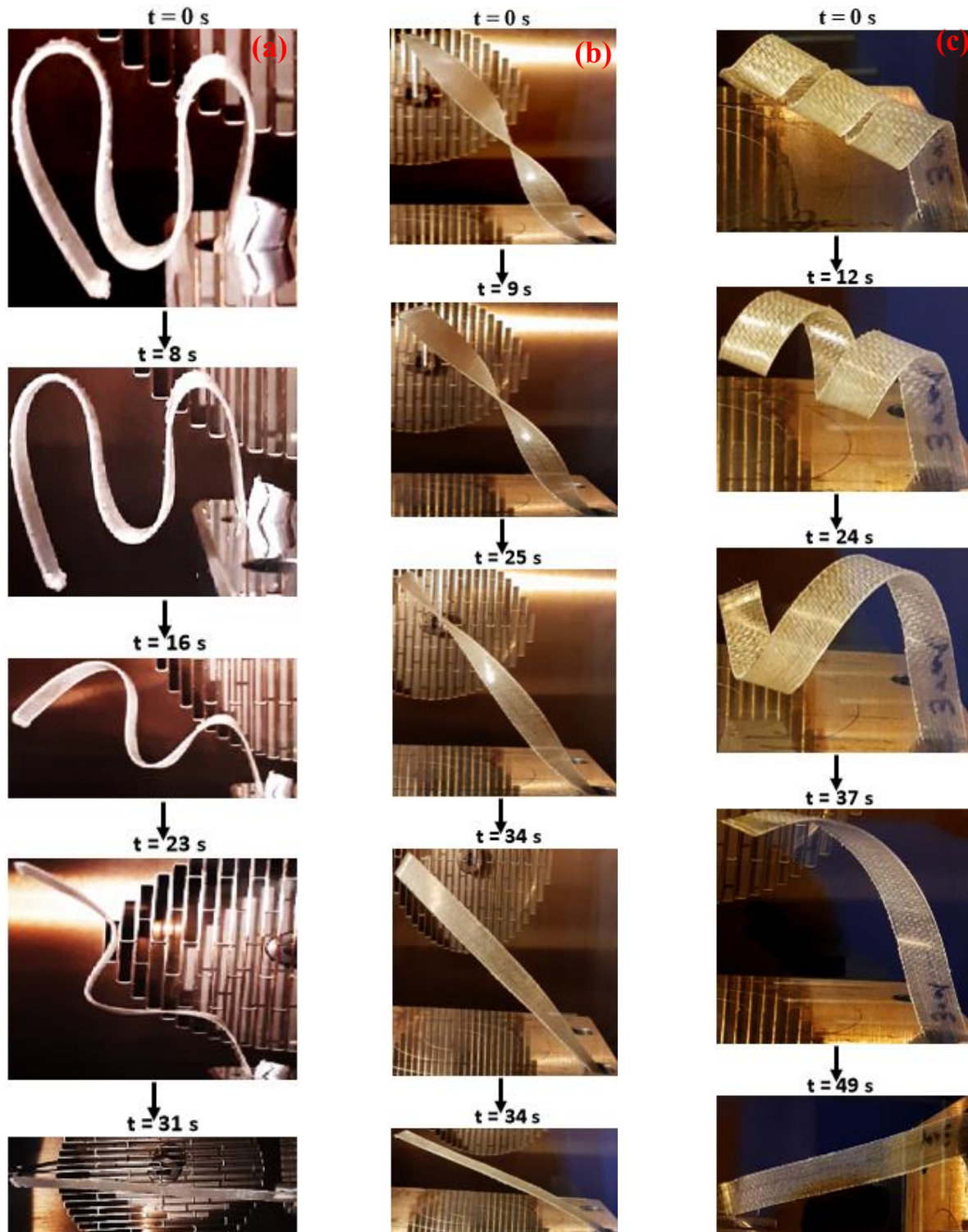


Figure 7 : Recouvrance en fonction du temps. (a) M-shaped, (b) twisted et (c) spiral configuration

la forme fixée après éducation. Ceci montre la capacité pour les composites SMPC 3D développés dans ce travail à admettre après éducation des forme complexe pour la géométrie fixée. On note également que le temps de recouvrance est lié aux effets induits lors de la mise en forme initiale, effets de torsion et de flexion et particulière si ceux-ci sont combinés.

Pour l'étude des propriétés fines de mise en forme et pour une géométrie en forme de boucle (loop geometry), les différentes géométries, formes originales, déformées, temporaires et récupérées sont obtenues à partir d'un nuage de points issu de l'opération de scan 3D (Fig. 8). La performance de l'étape de recouvrance c'est-à-dire la capacité du SMPC 3D à retrouver sa géométrie initiale est évaluée en comparant les géométries numérisées de la forme initiale avec celle de la forme recouvrée (Fig. 9).

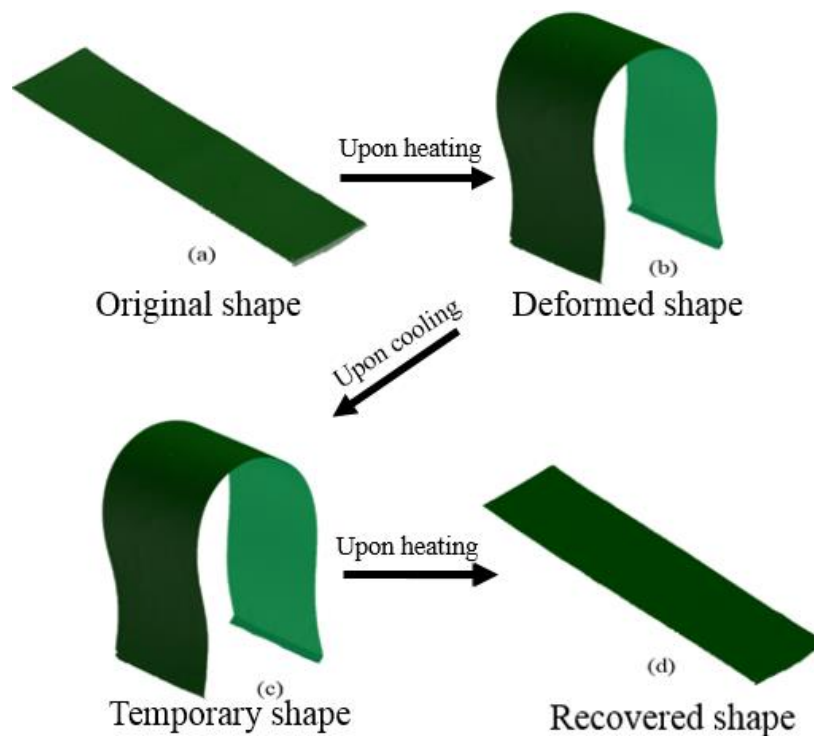


Figure 8: Scan 3D du composite SMP lors du test du cycle à mémoire de forme (a) Original shape, (b) deformed shape (c) temporary and (d) recovered shape

On peut observer à l'exclusion de deux zones singulières (différence égale à 0.3 mm et -1.25 mm) que l'ensemble de l'échantillon a récupéré sa forme initiale. Cette comparaison de géométrie est également réalisée pour estimer la capacité du SMPC 3D à fixer la géométrie après éducation (Fig. 9 - a), différence entre la géométrie déformée (en bleu) et la géométrie fixée (en vert).



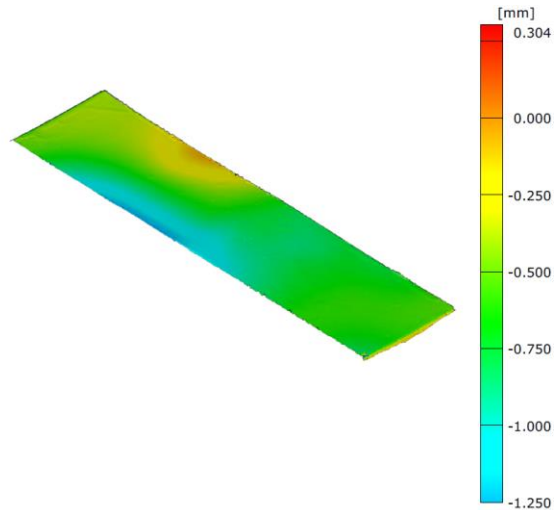


Figure 9: Carte d'écart de déplacement entre la géométrie initiale et recouvrée

La figure 9 - b montre que les valeurs d'écart varient de 0 à  $\pm 2,50$  mm. Sur la partie supérieure, la forme fixée conserve parfaitement ses dimensions, puisque les valeurs d'écart sont nulles. Alors qu'il y a un changement sur la partie inférieure qui atteint 2,50 mm à l'extrémité. Cette différence peut être attribuée à la déformation résiduelle induite par l'effet de la relaxation de la contrainte pendant le cycle de programmation, et particulièrement dans les zones sujettes aux plus grandes déformations.

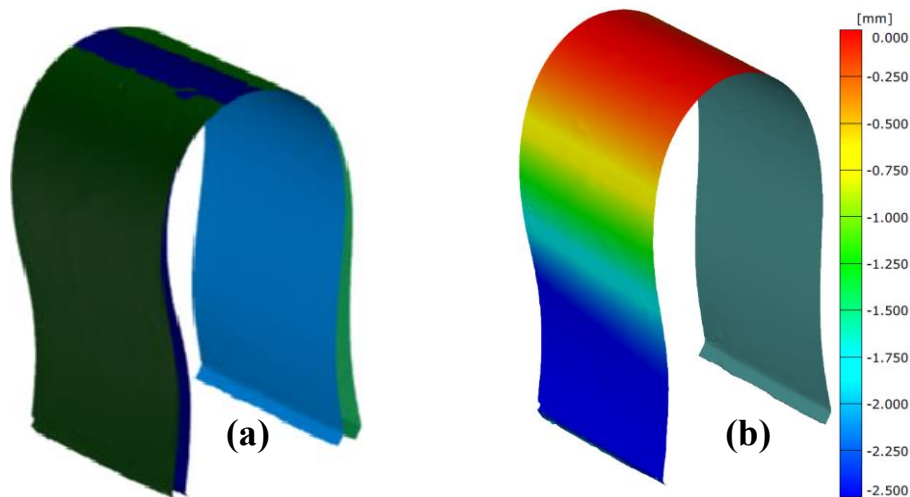


Figure 9: (a) 3D scan entre la géométrie déformée (bleu) et fixée (vert). (b) Carte d'écart de déplacement entre les deux géométries (units in mm)

### Essais de flexion 3 points

La figure 10 montre les courbes Force-déplacement de flexion des échantillons SMPC 3D testés à différentes températures. On peut remarquer que la valeur de l'effort diminue avec l'augmentation de la température de 30°C à 50°C, avec une force maximale qui décroît de 38 %.

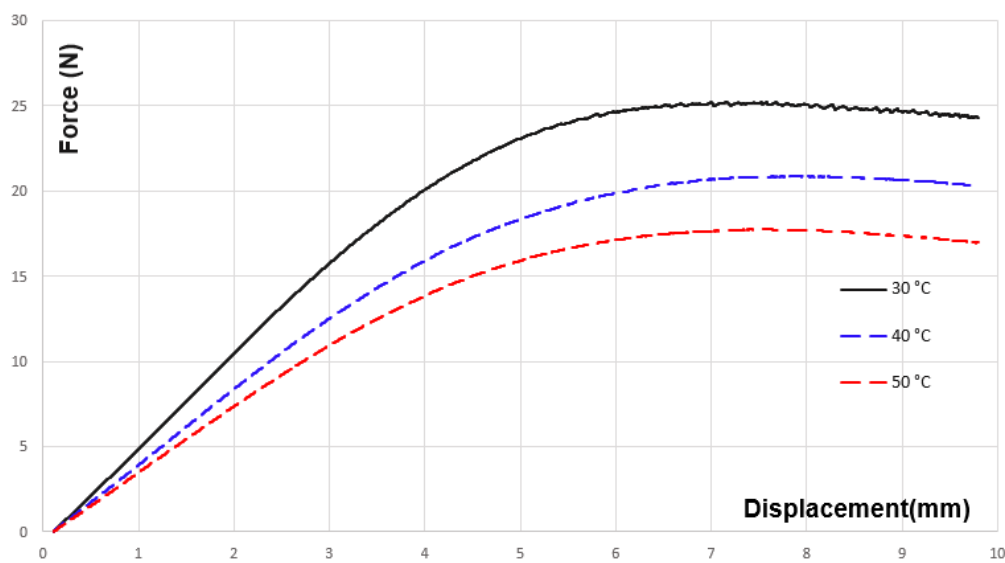


Figure 10: Force en fonction du déplacement à différentes températures du composite SMPCs

Le module de flexion moyen en fonction de la température est de  $2640 \pm 47$  MPa à 30°C, de  $2360 \pm 60$  MPa et  $1950 \pm 58$  MPa, à 40°C et 50°C respectivement. La contrainte flexionnelle maximum est de  $58,4 \pm 2,9$  MPa à 30°C,  $48,4 \pm 3,6$  MPa et  $42,6 \pm 0,6$  MPa, à 40°C et 50°C respectivement. Ce comportement était attendu car il est lié au comportement de la matrice polymère en fonction de la température, même si les températures d'essais restent inférieures à la température de transition vitreuse. Les observations MEB de ces échantillons n'ont pas permis de visualiser de dommages significatifs sur leurs surfaces.

### Essais de cisaillement inter-laminaire - ILSS

Normalement, un test ILSS figure 11 acceptable devrait montrer au point A une chute soudaine de force associée à une défaillance de l'interface. Ceci n'est pas observé pour les composites 3D, puisque la transition en ce point est continue. Ces composites ne présentent pas de rupture de l'interface inter couche, leur comportement est gouverné par la plasticité de la résine. En fonction

de la température, cette transition est de moins en moins observable jusqu'à ce qu'elle disparaisse pour la courbe à 80°C.

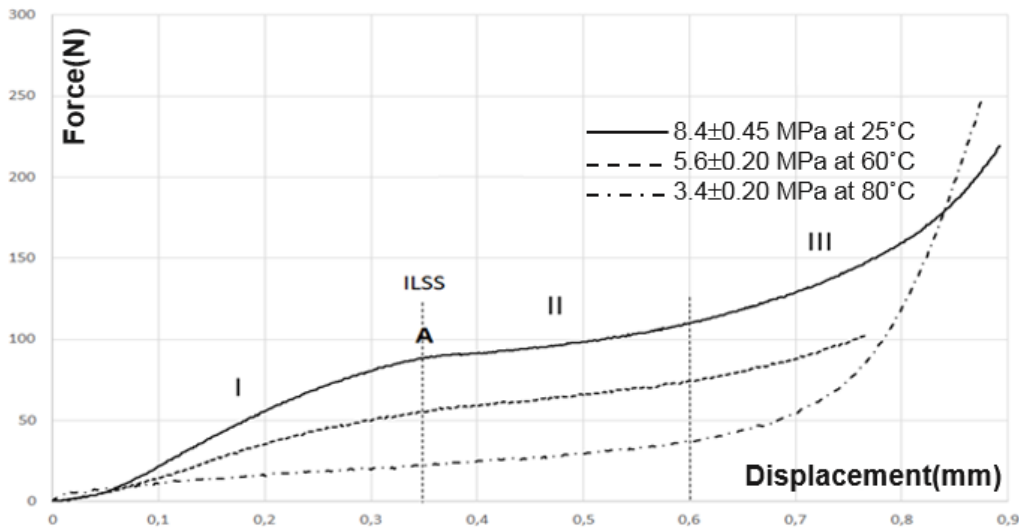


Figure 11: Courbe type d'un test ILSS en fonction de la température (25, 60 et 80°C)

L'ILSS est ensuite calculée à partir de la valeur de l'effort au point A. Pour 25°C l'ILSS moyen est de 8,4±0,45 MPa, suivi de 5,6±0,2 MPa et 3,4±0,2 MPa, aux températures respectives de 60°C et 80°C. On observe donc une diminution significative de la propriété de l'ILSS lorsque la température augmente de 25°C à 80°C.

Pour cet essai, l'ILSS doivent être interprété comme une capacité des SMPC 3D à être soumis à une forte courbure et donc à pouvoir subir une phase de compactage pendant le cycle d'éducation. L'absence de la première transition sur la courbe à 80°C montre qu'il est possible, même à des températures inférieures à  $T_g$ , de façonner le composite sans dommage macroscopique. Ceci a été confirmé par les observations MEB.

### Test complet sur composite autonome

Pour la première étape de chauffe (point A à B figure 12) qui précède celle de mise en forme le déplacement du SMPC 3D mesuré au niveau de l'appui central du montage de flexion 3 points est égal pour une température stabilisée de 92°C à 0,82 mm. Ce déplacement est lié à des asymétries des propriétés matériaux qui peuvent notamment être inhérente au processus de fabrication [27]. La seconde étape de mise en forme (à 92°C) se décompose en deux parties (B, a) et (a, C). On observe pour la seconde partie une diminution de l'effort induit par le glissement inhérent à la mise

en forme, entre l'échantillon et les appuis sur lequel il est posé. Pour cette seconde partie on remarque également une augmentation de la température qui peut provenir de la modification des échanges convectifs liés au fort changement de courbure de l'échantillon. Au point C, la forme imposée de forte courbure est obtenue sans apparition visible de délaminage ou de fissure à la surface de l'échantillon. L'étape de refroidissement (CD) se poursuit par un retour à la pré charge de 0.1 N, ceci pour permettre un retour élastique de la structure qui va être caractérisée par la différence entre la géométrie déformée et la géométrie fixée. Pour cet essai le retour élastique n'a pas été observé. Pour ce refroidissement, la courbe de l'effort montre une singularité (k,g,k') avec une remontée de cet effort (g, k'). Ce phénomène qui survient dans une plage de température comprise entre 90°C et 60 °C est lié à la température de transition vitreuse du polymère  $T_g$  et à la rigidification du réseau polymère au passage de cette température de transition.

La dernière étape de chauffe (DE) permet la recouvrance de la géométrie sous l'effort de pré charge de 0.1N et le poids propre de la structure. L'énergie élastique stockée est libérée, et la récupération de la forme initiale devient alors possible. On observe que cette récupération est quasi complète, le SMPC 3D autonome revient à sa forme initiale et montre ainsi sa capacité à recouvrir d'importante modification géométriques incluant notamment de fortes courbures.

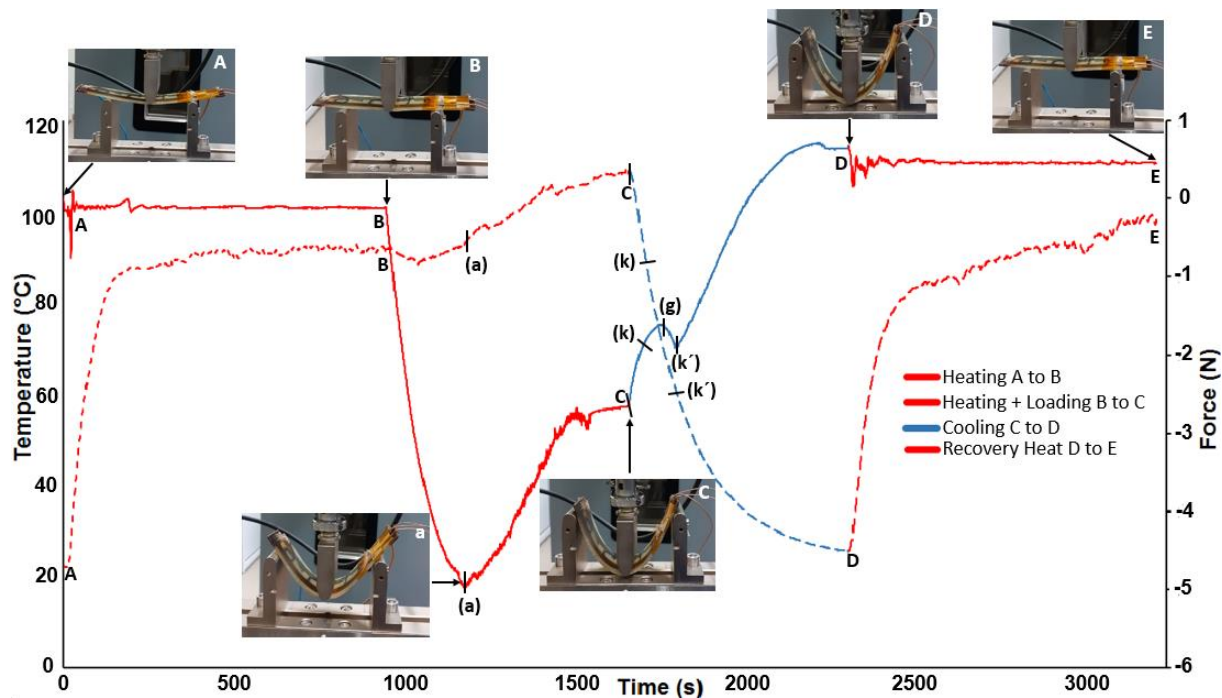


Figure 12: Courbes de chauffe et de charge pendant le cycle complet, éducation et recouvrance

## **Conclusion**

Au travers de plusieurs essais différents, le comportement de récupération de forme sans contraintes imposées (hormis son poids propre) du composite SMPC 3D a été systématiquement analysé. Les résultats obtenus ont montré que les SMPC 3D testés présentent une excellente récupération de forme sans dommages visibles, et ceci pour des géométries temporaires complexes dont l'obtention combine des effets de flexion et de torsion. La numérisation de la géométrie du SMPC 3D aux différentes étapes du cycle de mémoire de forme a permis d'identifier de manière précise les différences entre les différentes géométries : déformée et fixée, initiale et recouvrée. Ainsi les changements géométriques induit par le retour élastique de la structure après refroidissement et résiduel après recouvrance ont été quantifié.

Enfin le développement d'un test spécifique sur un SMPC autonome permet d'avoir un essai de caractérisation complet et précis qui peut servir de base à un travail de modélisation

## Table of Contents

Chapter 1: Introduction.....	31
1.1 General introduction.....	32
Chapter 2: Bibliography.....	36
2.1 Background .....	37
2.2 Intelligent materials.....	37
2.3 Shape memory materials (SMMs).....	39
2.4 Background of Shape memory polymers (SMPs).....	40
2.5 Architecture of SMPs .....	42
2.6 Stimulus method of SMPs.....	42
2.7 Structural Categorization of SMPs.....	43
2.8 Thermoplastic SMPs .....	45
2.9 Thermosetting SMPs.....	45
2.10 Epoxy as a SMP .....	46
2.11 Advantages of SMPs .....	48
2.12 Shape-memory Functionality of SMPs and their Composites .....	49
2.13 Different effects of SMPs.....	50
2.13.1 1-way SMEs/2-way SMEs.....	50
2.13.2 Multiple SME .....	52
2.14 SMP composites.....	53
2.14.1 Particle-filled SMPC.....	54
2.14.2 Fiber-reinforced SMPC .....	54
2.15 Effect of reinforcement on SM-ability of SMPC .....	54
2.16 Shape-memory effect in polymer composites .....	56
2.17 Characterization techniques for SMP and SMPC .....	57

2.17.1 Differential scanning calorimetry DSC .....	57
2.17.2 Interlaminar shear strength (ILSS) .....	57
2.17.3 Scanning electron microscopy (SEM) .....	57
2.18 The thermomechanical deformation process (TMDP) of SMPs.....	57
2.19 Applications of SMP and their composites.....	61
2.19.1 Bio-medical, Aerospace and industrial engineering Applications .....	61
2.19.2 Other Applications.....	64
2.20 Concluding Remarks .....	65
Chapter 3: Materials and Methods .....	66
3.1 Multilayer reinforcements for SMP composites .....	67
3.2 Multilayer weaving .....	67
3.3 Physical and mechanical properties of the produced fabrics .....	70
3.3.1 Bending behavior.....	70
3.3.2 Shear stiffness.....	71
3.3.3 Flexural modulus and rigidity.....	71
3.3.4 Breaking Force .....	72
3.4 Preform preparation.....	73
3.5 Resin for SMPC .....	75
3.5.1 Epoxy resin preparation.....	75
3.6 Thermosetting polymer and composite fabrication techniques.....	76
3.6.1 Compression molding.....	76
3.6.2 Mold preparation .....	76
3.7 Differential scanning calorimetry analysis (DSC) .....	78
3.8 Thermomechanical Characterization with different heating techniques.....	79
3.8.1 External heating system.....	79

3.8.2 Internal heating system.....	80
3.8.3 Shape deforming mechanism.....	80
3.9 Shape memory and recovery capability of SMP (external heating).....	81
3.9.1 Shape memory cycle of SMP .....	81
3.9.2 Shape recovery cycle of SMP.....	83
3.10 Shape memory and recovery capability of SN (external heating) .....	83
3.10.1 Shape memory cycle of SN .....	83
3.10.2 Investigation of shape fixity and shape recovery behavior of SMPC .....	84
3.10.3 Recovery cycle of SN.....	85
3.11 Thermomechanical characterization of SNC .....	85
3.12 Different shape memory and shape recovery capability of SMPC .....	86
3.12.1 Shape programming cycle .....	86
3.12.2 Shape recovery cycle .....	87
3.13 Flexure stiffness of SMPC .....	87
3.14 Interlaminar shear strength of SMPC.....	88
3.15 SEM analysis.....	90
3.16 Summary .....	90
Chapter 4: Results and discussion.....	91
4.1 Shape fixity and shape recovery capability of epoxy resin.....	92
4.1.1 Shape fixity displacement in pure epoxy resin.....	92
4.1.2 Shape recovery capability of pure epoxy resin.....	93
4.2 Investigation of flexure strength of SMPC .....	94
4.2.1 Flexure strength at different temperature .....	94
4.2.2 SEM analysis of SMPC after flexural modulus.....	95
4.3 Interlaminar shear strength (ILSS) characterization of SMPC .....	96



4.3.1 ILSS at different temperature .....	96
4.3.2 ILSS fracture pattern .....	98
4.4 Different shape memory and shape recovery capabilities of SMPC.....	100
4.4.1 Shapes memory capability of SMPC.....	100
4.4.2 Shapes recovery capability of SMPC .....	102
4.4.3 Effect of shape on recovery time .....	105
4.4.4 Surface characterization after shape recovery cycle.....	106
4.5 Quantitative measurements of shape fixity and shape recovery .....	107
4.6 Shape memory and shape recovery ability of hybrid carbon SMPC .....	111
4.6.1 Thermo-mechanical cycles .....	111
4.6.2 Different heating, loading and cooling cycles .....	114
4.6.3 Shape recovery speed and recovery displacement .....	116
4.7 Conclusion.....	117
General Conclusion.....	119
Future recommendations.....	122
Reference .....	124

## List of figure

Figure 7: recouvrance en fonction du temps. (a) M-shaped, (b) twisted and (c) spiral configuration .....	14
Figure 1: Illustration of the sensitive change of smart materials in ambient temperature [24] ....	38
Figure 2: Sophistication levels of intelligent (smart) structures (Modified from [52]) .....	39
Figure 3: Different types of shape memory materials within the world of material [41] .....	40
Figure 4: Schematic of polymer of networks during shape recovery [49] .....	42
Figure 5: Shape recovery (SR) of a pure SMP (top row), and a glass-fiber-reinforced SMP (bottom row) [49] .....	43
Figure 6: Schematic of structural categorization of SMPs (modified from [48]).....	44
Figure 7: Integrated insight into SMPs based on structure, stimulus, and SMF [82] .....	50
Figure 8: Describe the functioning of SMPs or SMCs (modified from [82]).....	51
Figure 9: (a) Schematic of triple-SM and SRC, (b) quadruple-SM and SRE of PFSA [91] .....	52
Figure 10: Quadruple-SR effect in polymer tri-layer-laminate [91].....	53
Figure 11: Thermomechanical deformation and recovery process of SMPs( modified from [105]) .....	58
Figure 12: 3D-thermomechanical behavior of SMPs [105].....	59
Figure 13: Schematic representation of the SME [107].....	61
Figure 14: Moisture-responsive functionality for Polyurethane SMP [108] .....	62
Figure 15: SMPC hinge: (a) Illustration of the hinge (1: curved SMPC shell; 2 and 3: hinge fixture) and (b) real scale hinge [109].....	62
Figure 16: Illustration of Z-shaped morphing wing [111] .....	63
Figure 17: Left wing morphing by joule heating [108] .....	63
Figure 18: (a) Shape memorized of the composite mast, (b) SR of the mast structure [112].....	64
Figure 19: SR of epoxy composite sheets from various folded permanent-shapes [113] .....	64
Figure 20: The weaving machine (left) and NCE loom system (right) .....	68
Figure 21: Graphical representation of the tested triple layered fabrics [116] .....	69
Figure 22: Bending rigidity [116].....	71
Figure 23: Bending Modulus [116].....	71
Figure 24: Illustration of Breaking force [116].....	72

Figure 25: Illustration of Breaking force [116].....	72
Figure 26: Nylon filament woven fabric SN perform.....	74
Figure 27: Illustration of carbon yarn insertion on one side SNC .....	74
Figure 28: Resin preparation for shape memory polymer and composite .....	76
Figure 29: Schematic drawing showing the used mold .....	76
Figure 30: Illustration of (a) resin plate and (b) composite plate production assembly .....	77
Figure 31: Illustration of produced specimens (a) SN and (b) SNC.....	78
Figure 32: DSC test results of the used epoxy based SMP.....	79
Figure 33: External heating source (Instron furnace) .....	79
Figure 34: Internal heating source (power supply) .....	80
Figure 35: Illustration of bending fixture to deform the specimens .....	81
Figure 36: (a) original shape, (b) deformed shape and (c) shape fixity in temporary shape .....	82
Figure 37: Measurement of activation displacement of temporary programed shape of epoxy resin (a) reference point, (b) activation displacement .....	82
Figure 38: Illustration of temporary programed shape of SN.....	83
Figure 39: Digitization process of the 3D shape of SMP composite provided by structured light and non-coded reference points .....	85
Figure 40: Illustration of apparatus used to characterize the shape memory and recovery cycle	86
Figure 41: Control heating Instron furnace.....	86
Figure 42: Illustration of shape recovery cycle .....	87
Figure 43: Experimental set up of three-point bending tests of SMP composite specimens in a thermal regulating chamber .....	88
Figure 44: Illustration of ILSS tests of SMP composite specimens in a thermal regulating chamber .....	89
Figure 45: Interval plot of shape memory programing cycle at different span lengths .....	93
Figure 46: Force versus displacement at different temperatures of triple layered SMP composite .....	95
Figure 47: SEM image after 3 Point bending experiments at different temperatures: (a) 25°C, (b) 40°C and (c) 50°C.....	96
Figure 48: Typical curve of ILSS test function on temperature (25, 60 and 80°C).....	98

Figure 49: SEM micrographs of layered composite specimens after short-beam three-point bending tests at different temperatures (a) 30°C (b) 60°C (c) 80°C.....	99
Figure 50: original shape of all composite specimens .....	101
Figure 51: Visual demonstration of temporary programmed simple shapes (a) U-shape, (b) S-shape and (c) loop-shape.....	102
Figure 52: Visual demonstration of temporary programmed complex shapes (a)-M-shape (b)-twisted-shape and (c)-spiral-shape.....	102
Figure 53: Series of photographs showing shape recovery as a function of time. (a) U-shaped, (b) S-shaped and (c) loop shape .....	103
Figure 54: Series of photographs showing shape recovery as a function of time. (a) M-shaped, (b) twisted and (c) spiral configuration .....	104
Figure 55: Illustrate the different composite shapes effect on recovery time.....	105
Figure 56: Illustrates the SEM image of the top surface appearance of (a) U-Shape, (b) S-shape and (c) loop shape .....	106
Figure 57: Illustrates the SEM image of the top surface appearance of (a) M-shape, (b) twisted-shape and (c) spiral-shape.....	107
Figure 58: Complete shape fixity and recovery mechanism.....	108
Figure 59: 3D models of the SMP composite during the shape memory cycle test, which are obtained by scanning their shapes. (a) Original shape, (b) deformed shape, (c) temporary shape and (d) recovered shape .....	109
Figure 60: Color deviation map computed as the perpendicular distance of each polygon point on the recovered shape to the original shape units in mm .....	109
Figure 61: (a) 3D scanned model of SMP composite demonstrates the difference between the temporary (green) and deformed (blue) shapes. (b) Color deviation map visualizes the geometric deviations between the two shapes (units in mm) .....	110
Figure 62: Illustration of experimental assembly used to characterize the morphing behavior of active layer .....	112
Figure 63: Illustration of complete mechanism of thermomechanical cycle of active layer .....	113
Figure 64: Complete recording of thermo-mechanical cycle of shape programming and shape recovery by 500N load sensor.....	114

Figure 65: Complete illustration of heating and loading, during shape programming and recovery cycle .....	115
Figure 66: Illustration of shape recovery speed vs temperature .....	116
Figure 67: Illustration of shape recovery displacement vs temperature .....	117

## List of Tables

Table 1: Machine specifications .....	68
Table 2: Specifications of the tested triple layered woven fabrics [116].....	70
Table 3: Illustration of preform.....	73
Table 4: Properties of epoxy resin .....	75
Table 5: Combination of the hardener .....	75
Table 6: Illustration of all specimens of different width.....	81
Table 7: Description of shape recovery capability of epoxy resin at different span lengths .....	93
Table 8: Description of experimental method and composite sample specifications .....	94
Table 9: Description of testing method and composite sample specifications .....	97
Table 10: Illustration of testing mechanism and specifications of composite specimen.....	101
Table 11: ANOVA for effect of composite shapes on recovery time.....	105
Table 12: Illustration of composite sample and experimental specifications .....	107
Table 13: Illustration of sample (composite + active layer) and experimental specifications...	111

## **Abstract**

Shape-memory polymers (SMPs) are polymeric stimuli-responsive materials that have the ability to return from a deformed state to their original shape induced by an external trigger, such as heat. Although these materials have become widely accepted as smart materials due to their advantages of large recovery capacity, they have essential limitations in certain applications due to their relatively low mechanical properties. The incorporation of reinforcements into SMPs will considerably enhance the mechanical properties. The objective of the current work is therefore to develop new SMP composites using three-dimensional woven reinforcements. A series of experiments including three-point bending and interlaminar shear tests are then performed on these SMP composites to investigate their mechanical responses at different temperatures. Moreover, shape fixity and shape recovery capability of epoxy resin is investigated. Furthermore, shape memory and shape recovery cycle experiments are carried out to evaluate the shape memory characteristics of these composites. These characteristics are then measured by using two different techniques (optical 3D scanner and three point bending test) to assess the accuracy of the shape fixity and shape recovery test. The results show that the developed SMP composites have very good shape recovery capability.

---

# **Chapter 1: Introduction**

---



## 1.1 General introduction

SMPs are those materials that can retain to their original shape after deformation in the presence of external stimulus. Although SMPs have become widely accepted as smart materials due to their outstanding advantages of large recovery capacity, low production cost, excellent molding ability and low density; they have essential limitations and great shortcomings in engineering applications.

Generally, the importance of composite materials is that several components complement each other, leading to synergies and thus improving or enriching the function of the matrix material. For SMPs, composites are made with two basic objectives, i.e., reinforcement and incorporate shape memory polymer as the matrix material. A SMP is reinforced principally to increase the driving force of the recovery process and to provide better carrying capacity, which correspond to high stiffness and high strength characteristics. Given the necessity for structures to be suitable for many practical applications that require particular functions, SMP composites are beginning to be studied. According to the types of reinforcements, SMP composites can be broadly divided into three classifications: nanofiber reinforced, particle/short fiber reinforced and continuous fiber reinforced composites. In this regard, several studies have been conducted to investigate the effect of different reinforcements on the shape memory behaviors of the composites. Typically, in SMP composites, the reinforcing ability of long-fiber is the greatest, followed by that of short fibers and particles. Particle or short-fiber reinforced SMP composites could not be used as a structural material due to their low stiffness and strength. On the contrary, a continuous fiber reinforced SMP composites represent outstanding mechanical properties [1]–[7].

The major drawback for extended use of SMPs in certain structural applications is their relatively delamination and low mechanical properties. Nevertheless, the inclusion of reinforcements into SMPs will significantly decrease the delamination problem while retaining intrinsic shape memory effects. Thus, the development of such SMP composites could provide a solution to the problem of low recovery stress of SMPs, making them stronger enough to produce larger recovery stresses as a result of increased the overall rigidity.

Recently, a new class of reinforcements has gained considerable attention, that is, 3D woven fabrics. The development of these fabrics arose from industry's need to reduce preforming steps,

to improve through-the-thickness mechanical properties such as interlaminar shear strength, to improve impact damage tolerance, and to enhance the delamination resistance which is particularly significant in the structural design process; all were problems associated with 2D textile fabrics [8]–[14]. According to the configurations and geometries of the 3D woven fabrics, they can be classified into four different categories, that is, the solid, hollow, shell, and nodal [15]. For the 3D solid fabrics, broadly, there are three types of 3D solid structures as follows: multilayer, orthogonal and angle interlocked. In particular, the multilayer woven fabrics are the 3D solid type fabrics that we are interested to incorporate them into SMP matrix in order to improve the mechanical properties of the produced 3D SMP composites while preserving inherent shape memory effects. The distinctive feature of these multilayer woven fabrics is that they have clearly defined fabric layers in the thickness of the fabric. Each layer is composed of a set of warp ends and a set of weft yarns. The connection of the layers is done by weaving either the existing yarns (self-stitching) or external sets of yarns (central stitching).

In spite of a wealth of development ideas involving shape memory behavior of 2D woven fabric composites have seen, the SMP composite of 3D woven fabrics is basically very limited or rather not existent. Therefore, the main objective advocated in this work is to fabricate outstanding 3D multilayer SMP composites, which may exhibit a promising application in the field of aerospace deployable structures. For this purpose, nine different multilayer stitched fabrics are produced with different weave structures, and different fabric thread densities using polyimide filaments. Then, a series of tests is carried out on these fabrics to evaluate their mechanical and physical properties. The layered fabric design that delivers high mechanical performance is next involved to manufacture the SMP composite samples, for which shape recovery capability is investigated. Fold-deploy and other shape memory cycle tests are performed to evaluate the shape memory characteristics. An optical 3D scanner based on fringe projection is further proposed to precisely acquire the geometry data and then perform inspection and deformation analysis on the formed SMP composite in terms of shape fixity and shape recovery behaviors.

In order to achieve the aforementioned objective of the research, two main steps are considered. Firstly, nine different 3D multilayer woven structures each having different weave in the intermediate layer and top and bottom plain all stitched together are produced using polyamide filament yarns both in warp and weft. These triple layered fabrics are developed on narrow

weaving machine equipped with multi beams and creel options. They are then tested at the dry state for air permeability, bending and shear properties. In the second step, the layered fabric that exhibits greater mechanical properties is incorporated to produce the SMP composite samples for which we examine the shape memory and shape recovery capability by using different characterization techniques. These 3D SMP composites are looked upon to create a better multiaxial structural performance, which would allow for improving the mechanical and functional properties and hence lead to enhance and broaden the applications of shape memory polymers. Particularly, isothermal 3-point bending stress strain experiments are carried out to obtain values of the flexural modulus and strength of the 3D SMP composite samples at temperatures less than the glass transition. Additionally, the interlaminar shear strength of these SMP composites are examined by 3-point bend of short beam method at temperature varying from 30°C to 80°C.

In this work, shape memory and recovery cycles are investigated by using different methods. Free and controlled recovery experiments are conducted to assess the shape recovery capability of the fabricated 3D SMP composites. First, SMP composite is conventionally processed to receive its original/permanent shape. The composite is then deformed at an elevated temperature and the intended temporary shape is fixed; this process is called SM programming. Finally, at elevated temperature a recovery transition from the temporary/deformed shape to permanent shape is restored.

Furthermore, different temporary shapes varying from simple to complex of 3D SMP composites are produced and investigated, including U-shaped, S-shaped, twisted, folded and spiral shapes. More specifically, sophisticated 3-point bending sensor and an optical 3D scanner based on fringe projection techniques are further employed to accurately, quantitatively describe the shape information and shape memory performance of the SMP composite. The shape memory performance is quantified in terms of the shape fixity and shape recovery. This is done by a fold deploy “U”-shape bending test through measuring the shape during 3D deployment process of the SMP composite.

The main contribution and novelty of the present work is therefore different from previous works by others, providing a series of thermal, mechanical, thermomechanical experiments of the considered multilayer SMP composites. This includes differential scanning calorimetry, 3-point

bending, interlaminar shear strength, and fold-deploy shape memory cycle tests, all together to evaluate the shape memory characteristics of the developed 3D SMP composites.

---

## **Chapter 2: Bibliography**

---

## 2.1 Background

Shape memory polymers (SMPs) are a class of active deformable materials that have dual-shape capability. They have drawn increasing attention during the last few decades because of their scientific and technological significance [29]. The shape-memory effect is a phenomenon and not an intrinsic property, meaning that polymers do not display this effect by themselves. The SMPs offer a unique ability to undergo a substantial shape deformation and subsequently recover the original permanent shape when exposed to external stimuli. These stimuli may be of various types such as heat (thermo-responsive), chemical (including water, chemo-responsive), light (photo-responsive), pH of the medium (pH-responsive), electrical current/voltage (electro-responsive), and magnetic field (magneto-responsive). Among them, thermo-responsive SMPs are still the most common and most attractive group because of its broad range of applications [22].

Initially, the very chapter presented the brief introduction of the smart materials in general. Later on, a comprehensive overview of shape memory polymers and its division into various heads (mainly thermoset and thermoplastic SMPs) is specified. Then, the chapter enlightened the various techniques that are essentially applied to characterize shape memory polymers. After that, the typical shape memory cycle (along with its characteristic parameters) that is used to conduct thermo-mechanical programming and recovery of the shape memory polymers is narrated. The various kinds of shape memory effects (one way, two way, triple-way and multi-way) that may occur in SMPs because of thermo-mechanical programming are also explained herein. Moreover, reinforcement wise categorization of SMP composites are also elaborated. Finally, this chapter briefly held the different significant applications of shape memory polymers and their respective composites.

## 2.2 Intelligent materials

Continuous development has been observed in the arena of intelligent/smart materials aiming at gaining high performance and versatility in functions for better engineering applications. These smart materials can be defined as, "the materials that can sense the environment and or their own state, make a judgement and change their functions according to a predetermined purpose"[23]. These smart materials can be distinguished from other smart systems due to their non-reliance on

intricate sense-response set up of a feedback system (Fig. 1). Instead they can be intrinsically sensitive to change in their ambient environment such as temperature, optical wavelength and PH values etc. [24].

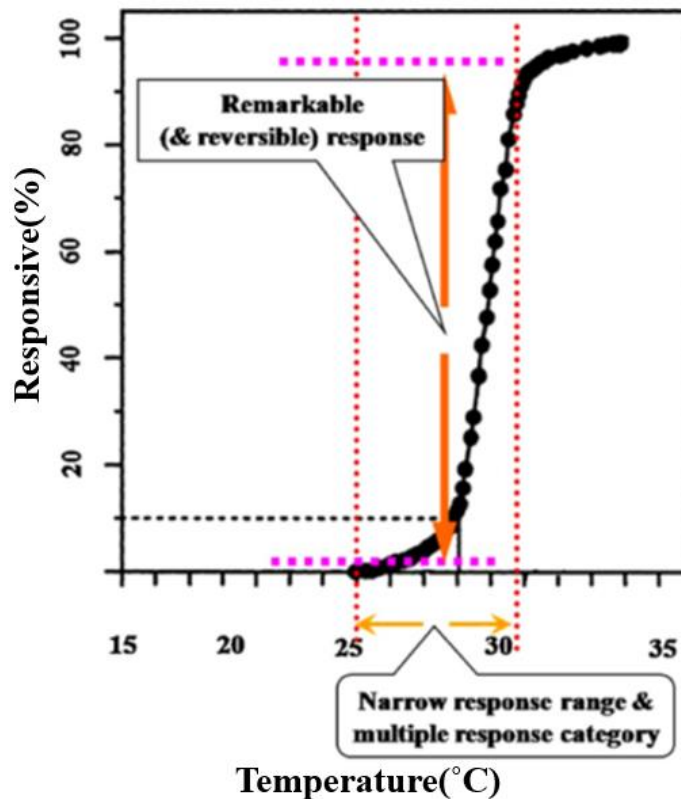
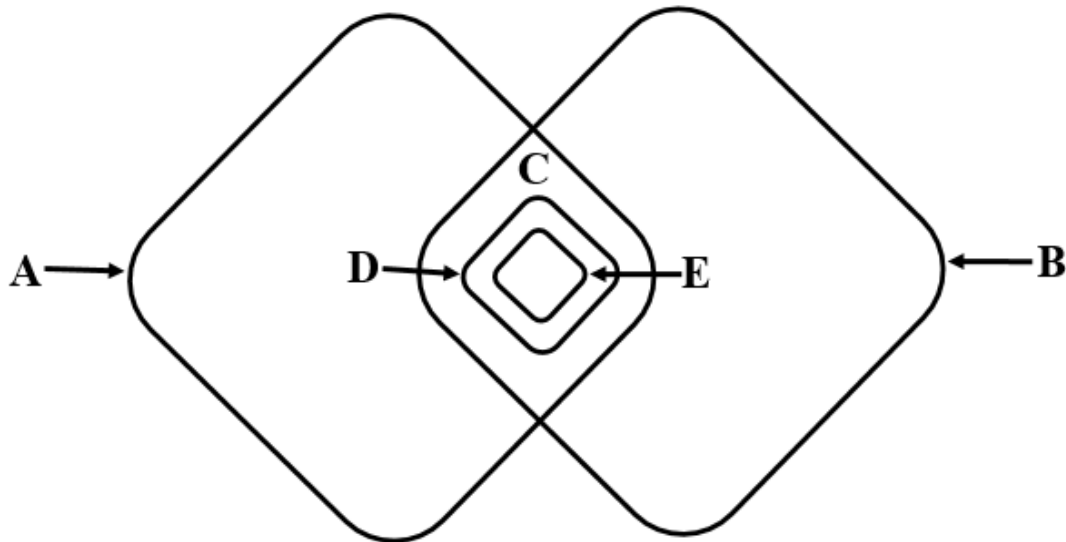


Figure 1: Illustration of the sensitive change of smart materials in ambient temperature [24]

Smart materials can be further used to develop various smart structures with different level of sophistication and characterization. These smart structures are usually divided in to five level. The sensory structures are being considered as the simplest of smart structures. As the name depicts, these are only able to sense the specific stimuli. The adaptive structures comes at the second level of smart structures as they have the specific actuators for responding to the specific stimuli. So these structures have the ability to sense and respond accordingly, unlike the first level structures. The next level is of controlled structures that have the ability to perform controlled functions with the help of installed actuators and sensors within these structures. Likewise, the fourth level is even more complicated in the context of performing controlled functions as well as structural functions and thus named as the active structures. After this comes the final and most advanced level where by highly integrated electronic logics are embedded within the structure and thus providing

artificial intelligence to these structural units. These structures at the last level of sophistication is named as intelligent structures. Here below in Figure 2. is the diagrammatic description of these levels of sophistication[25], [26].



**A: sensory structures B: Adaptive structures C: Controlled structure D: Active structure E: Intelligent structure**

Figure 2: Sophistication levels of intelligent (smart) structures (Modified from [52])

### 2.3 Shape memory materials (SMMs)

Amongst stimuli responsive materials (SRMs), there is a group of materials, which are capable of shape changing when introduced to the right stimulus. Depending on the type of shape changing, SRMs are further divided into two groups. That is, if the change occurred in shape (in the presence of right stimulus) is spontaneous and immediate then it will be called as shape change material (SCM). Electro-active polymer (EAP) and Piezoelectric material such as (PZT) are considered as two common examples of this category. While in the other group, the change that occurred in shape can be virtually kept forever until the right kind of stimulus is provided to attain the shape recovery of the material and it is thus typically named as Shape memory material (SMM). It is a noteworthy point to consider that all SMMs are basically characterized by shape memory effect (SME) which can be better defined as the ability of the material to regain its original shape at the application of right stimulus, after being intensely distorted [29].

Till now many types of SMMs have come to an existence. Out of which, shape memory alloys (SMA) and shape memory polymers (SMP) are the prominent ones in the current era. While the



mechanism behind the SMA in SME is the reversible martensitic transformation, the dual-segment/domain system is the mechanism for the SMP in SME [64].

Moreover, the most recent kind of SMM that is termed as shape memory hybrid(SMH) possess the exact mechanism as that of SMP. Not only this, also another type of SMM named as shape memory ceramic (SMC) is found to have the similar working principal of multi-phase system as in SMPs. Generally, it is believed that gels may be basically considered as SCM because of the swelling effect or electric charge generating therein,. However, some gels are found to have SME in them, for example, a changeable order disorder transition. Recently, a research demonstrated the activation of SMP by the using the swelling effect as present in gels [36]. Thus, the literature seems quite promising in providing the linkage between SMPs and other related types of SMMs.

It is a noteworthy point to consider that shape memory composite (SMc) is known as the composite having minimum of one SMM, (more prominently a SMP or SMA) as its constituent. Thus, it may help to clear the fact that SMc is not an autonomous subgroup of SMM. For instance, shape memory bulk metallic glass composite is basically comes under one form SMc's [40].The same has been demonstrated in Figure 3.

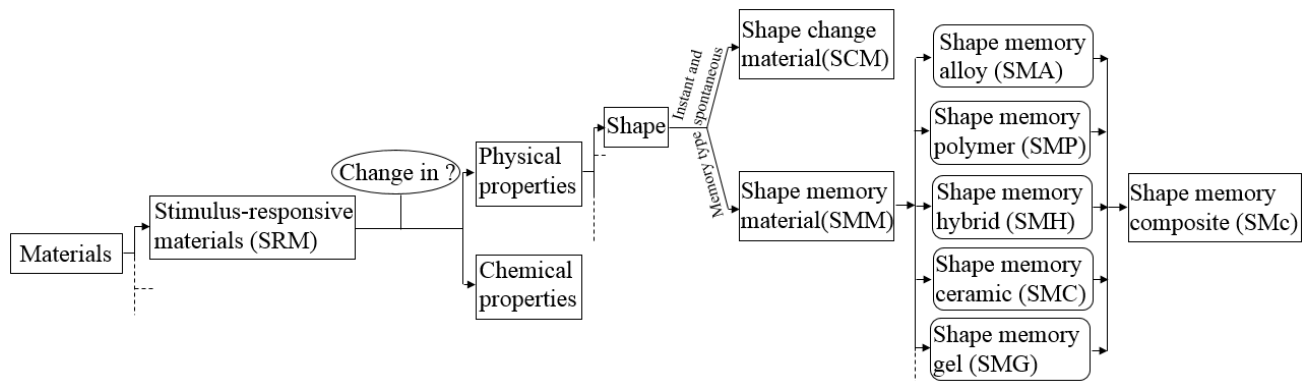


Figure 3: Different types of shape memory materials within the world of material [41]

## 2.4 Background of Shape memory polymers (SMPs)

Shape memory polymer has the ability to respond to specific stimuli and such responses are usually evident through various important macroscopic properties such as change in shape of respective polymer. It has been researched that the basic SMP's molecular architecture is consisted of an interconnected polymer network having underlying dynamic movement. The presence of a dual-Segments is crucial to the existence of a SMP; out of which one is highly elastic and flexible while

the other one with the ability to minimize its toughness when exposed to a specific stimulus. This second one is known to be the stimulus responsive domains or the specific molecular structures. Various stimuli such as heating, temperature, moisture or light has been researched for activation of shape recovery functionality in SMPs and their composites. Amongst various SMPs, which are responsive towards these stimuli, the thermos-responsive SMPs are deemed to be most common ones [42]–[44].

To explain further, SMPs which are prominently known for possessing SME, can be well traced back to as early as 1906, in case HSP (heat shrinkable polymer) is taken under the categorization of SMP. This discovery even seems even earlier than SMAs. Similarly, water shrinkable polymer (WSP) is another reference in the same context [45]. Not only this, Heat-shrink tubing consisted of polyethylene (PE) and ethylene-vinyl acetate (EVA), is being with used in the electrical engineering since long with an intention to protect conductors , joints and terminals. Although in the technical context, the title of first generation of real SMP is generally given to the polyorborene-based SMP. It was invented in Japan in 1984 by Nippon Zeon Co. This SMP and the other two discovered exactly after this, had been criticized for their limited process ability. These other two SMPs, the trans-isopolyprene-base and styrene-butadiene-based SMP were also developed in Japan at Kuraray Company and Asahi company respectively. However later on, a thermoplastic polyurethane (PU) SMP developed by Hayashi is known to have significant process ability, unlike the other three SMPs just highlighted. Due to its high process-ability it has been developed into wide range of products with various forms and transition temperatures and has its commercial availability in market [37].

From 1980s and onwards, there has been tremendous research on SMPs due to their wide-ranging novel characteristics. Till to date, there are more than 60 institutes or companies globally, where extensive experimentation and research work have been carried out regarding SMP. Recently, various kinds of polymers with SMEs have come to an existence. Considering the basic SME, some novel multi-functional SMPs or nano SMP composites are also anticipated. The other recent and successful example, developed by Cornerstone Research Group in USA, is the thermo-set polystyrene based . Overall, in the current era, the SMPs and their composites is being widely and rigorously explored for their unique characteristics and their applications in various fields [46].

## 2.5 Architecture of SMPs

SMP's are basically known to have dual-shape i.e. original shape and the deformed one. The molecular architecture of polymers actually facilitates such shape memory attribute [47]. To explain further, molecular structure of SMP is comprised of two basic elements that are stimuli responsive net points and molecular switches shown in Figure 4. Considering this regard, SMPs can be taken as copolymers having a hard segment and a soft segment thus acting as a fixed phase and reversible phase respectively. The function of the fixed phase is to prevent the outflow of neighboring polymer chains when the stress is applied. While the other phase, being responsible for polymer's elasticity experiences temporary deformation in the shape-memory cycle. This second reversible phase performs the function of a molecular switch thus stores the deformed shape below the transition temperature and later on allows the polymer to re gain its shape at or above the transition temperature (i.e. when the transition temperature is crossed) [48].

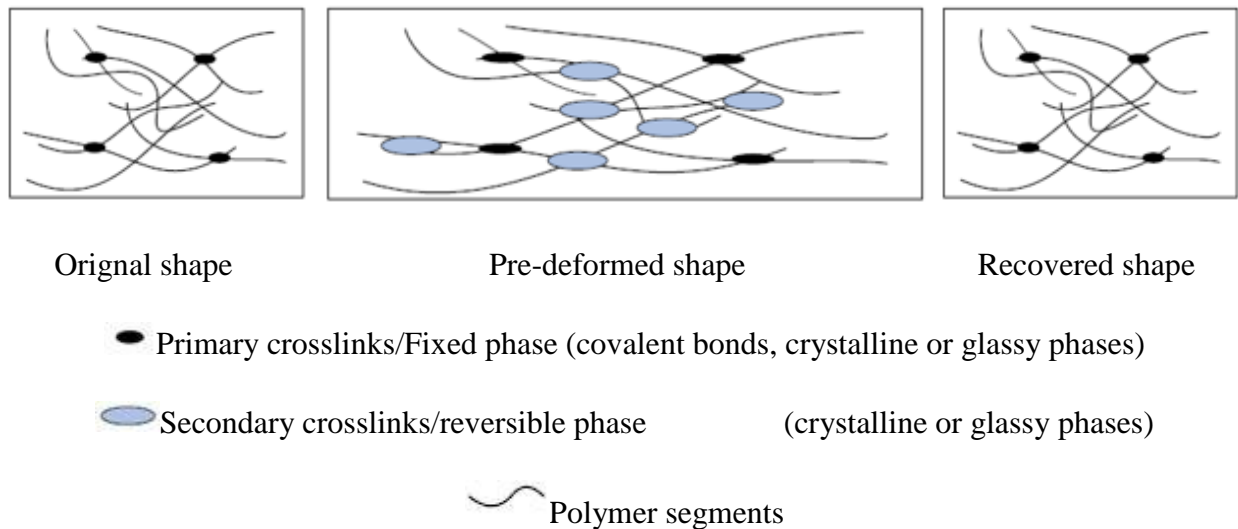


Figure 4: Schematic of polymer of networks during shape recovery [49]

## 2.6 Stimulus method of SMPs

SMPs have various actuation stimuli that can be generally categorized as joule heating, light, moisture and electricity e.tc. For instant, in thermos-responsive SMP's, the SME is directly activated by the application of heat stimuli. Such heat stimuli may be in the form of hot water or hot gas [50].

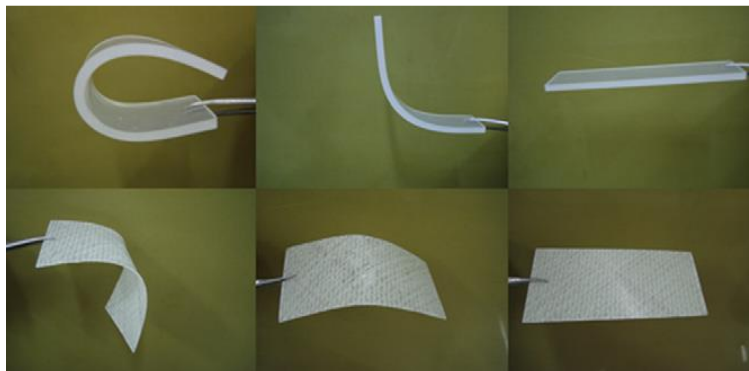


Figure 5: Shape recovery (SR) of a pure SMP (top row), and a glass-fiber-reinforced SMP (bottom row) [49]

Figure 5 demonstrates the thermally activated (i.e. hot gas) shape recovery cycle of a SMP in the top row while a glass fiber reinforced SMP in the bottom row. Based on the inconvenience regarding the usage of hot water or hot gas for the direct thermal activation of a SMP, these studies could not be explored further to the fullest. However, with regard to other stimuli such as light, magnetism and moisture, there is a possibility for incorporation of specially designed functional fillers to induce SME in the polymer. As far as, the water or solvent driven SMPs are considered; it is basically based on the diffusion of solvent particles in to the polymer that got immersed in water and later on act as a plasticizer thus reducing the transition temperature and eventually leading to the shape recovery of the polymer. This might be referred as indirect thermally induced actuation technique. Particularly, light induced SMPs are basically formed with the integration of reversible photo reactive molecular switches, embedded within the polymer. This may be differentiated from an indirect thermal-induced actuation method in a sense that here the stimulation is not linked to any temperature effects. Many other actuation methods of SMPs will be further deliberated in the coming sections [49].

## 2.7 Structural Categorization of SMPs

SMPs are basically known to be constituted of two main element namely molecular switches and net point. Net points are developed by intermolecular interaction and also with the help of covalent bonds between the molecules. Therefore, they may be either physical in nature or chemical. Further elaborating, there chemical or physical nature can be classified as thermosets and thermoplastics. Thermosets are basically chemically cross-linked SMPs that are made from appropriate cross linking chemistry; whereas thermoplastic are physically cross linked and known for their need of

constituting a polymer morphology with at least two isolated domains. Moreover, in SMPs the network chains may be in crystalline form or amorphous. Hence this depicts the transition temperature to be either melting temperature ( $T_m$ ) or the glass transition temperature ( $T_g$ ) [51]. In case the thermal transition is a glass transition, the micro Brownian motion of the network chains may be observed to get frozen below  $T_g$  and “switched” on at or above  $T_g$ , when reheated. On the contrary, if the thermal transition is the melting point, the switching domains get crystallized easily below  $T_m$  and later on re gain their prior shape after the temperature is raised or get above  $T_m$ . In a nutshell, the thermo-responsive SMPs may be categorized in four forms depending upon the nature of their permanent net points and the thermal transitions linked to the switching segments. These four categories are [29] :

- Physically Cross-linked thermoplastics with  $T_{trans} = T_g$
- Physically cross-linked thermoplastics with  $T_{trans} = T_g$
- Chemically cross-linked amorphous polymers ( $T_{trans} = T_g$ )
- Chemically cross-linked semi crystalline polymer networks ( $T_{trans} = T_m$ )

Researches state that in the recent years, there are more than twenty types of SMPs that have been synthesized and rigorously explored. The below Figure 6 demonstrates the classification hierarchy of prevailing polymer networks exhibiting the same SMEs [48].

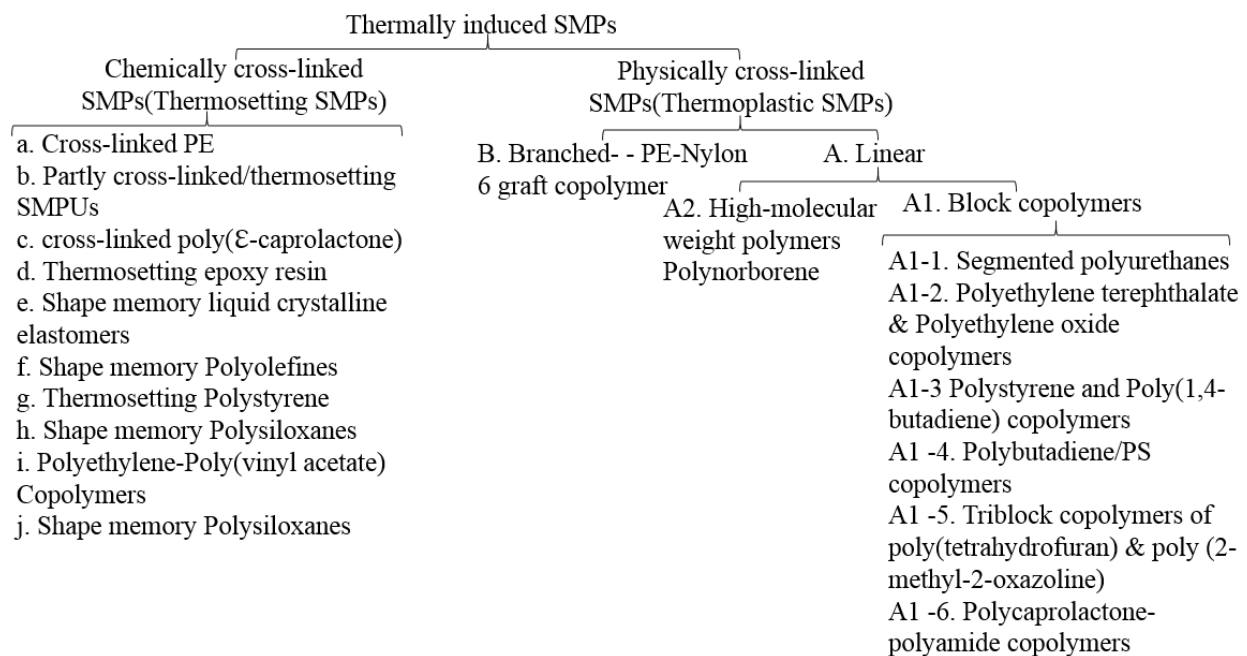


Figure 6: Schematic of structural categorization of SMPs (modified from [48])

## 2.8 Thermoplastic SMPs

In the physically cross-linked SMPs, the thermally activated SME is regulated by an underlying essential mechanism that is the synthesis of a phase detached morphology. In this process, one phase is responsible for the provision of physical cross links while the other phase holds accountable for acting as a molecular switch within the network. There further classification is possible and may be named as linear polymers branched polymers or a polymer complex [48].

Amongst the thermoplastic SMPs family, the one polyurethane SMP holds quite a prominent place due to its wide-ranging benefits. For instance, higher shape recoverability having maximum recoverable strain of greater than 400%, a greater range for shape recover temperature that is from 30 to 70C and the enhanced biocompatibility and processing ability [31].

## 2.9 Thermosetting SMPs

There are two ways for the formation of covalently bonded networks in case of chemically cross linked SMPs [56], [66]. For this purpose, initially during the process of polymerization, a polymer networks is produced by addition of a multi-functional cross-linker. The differing kind of monomers and content of cross likers may help to direct or adjust the mechanical, thermal and chemical attributes of the polymer system. The other way out for the synthesis of polymer network system is the succeeding cross-linking of the linear or branched polymer chains. The polymer backbones may vary from poly-olfines, polystyrene to polyurethanes and are crucial for the synthesis of polymer network. SMPs that are covalently bonded constitute chemically inter-linked structures which are responsible for their actual macroscopic shape determination. Such chemically inter-linked SMPs usually have network chain between their net points that plays the role of switching segments. Whereas, the shape memory switch is activated within the SMP with the help of thermal phase (transition) of the polymer section.

To add further, SMPs can be additionally categorized into two forms depending upon the thermal transition of the switching points.  $T_{trans}$  that is basically the transition temperature may be a glass transition (referred as  $T_g$ ) or a melting temperature (denoted as  $T_m$ ) [48]. Hence, in case the thermal transitional phase is related to the glass transition then the micro brownian motion within the polymer network chains may be seen frozen ultimately leading the temporary shape to get fixed at low-temperature. Due to this very transition, network chain areas become glassy in nature. SMPs

memorize this temporary shape and further accumulate the strain energy in their system. Afterwards, providing heat at or above  $T_g$  initiates the micro brownian motion and thus cause the opening of the switch. Glass transition usually holds a varied range of temperatures over which it may extend. On the other hand, if the thermal transition phase relates to the melting point, the switching point may crystallize at low temperature thus having a fixed shape and an accumulated strain energy. It then, regain the actual shape when the temperature level reached at or above  $T_m$ . In most cases of melting temperature, the transition usually appears to be prominent and quite Sharpe.

In comparative terms, chemical cross-linked polymers experience less creep than their physically cross-linked counter parts and that is why the permanent deformation during shape recovery cycle seems less in magnitude. Also, the thermal, chemical, mechanical and shape memory characteristics of the chemically cross-linked polymers are far better and improved than their physically cross-linked counter parts. Not only this, such characteristics are controllable if the certain things i.e. curing condition, cross link density and curing times are properly adjusted.

Thermoplastic polyurethane SMP as one of the significant thermoplastic SMP, holds a high shape recovery ratio of 90-95 % and with an elastic modulus of 0.5 and 2.5 GPa. Moreover, at contact with air, it exhibits unstable mechanical characteristics due to its sensitivity to moistness. On the other hand, epoxy SMP depicts better standing on the whole, with a shape recovery ratio in the range of 98-100%. Its elastic modulus is also improved one with a ratio of 2-4.5 GPa and it depicts more stability on exposure to space radiation and moisture.

The most researched SMPs are thermos-plastics SMPs (as Polyurethane SMP) having a functional usage at small level, for instance, in shape memory textiles and biomaterials. In contrast, thermosetting SMPs (as epoxy SMP) are mostly functional for structural purposes, for instance, vehicle actuator and space deployable materials [49].

## **2.10 Epoxy as a SMP**

The prominent position that epoxy shape memory polymer holds for the research purposes has already been elaborated in the earlier chapter. In the same regard, the utilization of Epoxy resin as SMP is frequently discussed in the literature. Epoxy is known to be researched for its shape

memory properties and other characteristics. For instance, thermo-mechanical cycling, level of environmental stability and other mechanical and electrical properties.

Few researchers utilized the nano-particles as reinforcement with an intention to explore its shape memory attributes. For instance, a group of researchers named Ken Gall et al. [67] utilized the combination of epoxy resin and SIC nano-particles for their experimentation purpose. The corresponding weight of SIC nano-particles used was 20% having an average diameter of 700nm. They mainly dealt with figuring out the internal stress storage that happens during the programming cycle and its releasing in the recovery cycle. Likewise, another group of researchers Xiaofan Luo et al. [68] performed experimentation on epoxy based SMP matrix. As reinforcement, they incorporated the non-woven carbon nano-fibers (CNFs) in this matrix. Their findings demonstrated the increased level of electrical conductivity, stress recovery and heat transfer in this resulting SMP composite.

Not only this, many researchers experimented the many other attributes of Epoxy through its thermos-mechanical cycling. For instance, Amber et al. [69] investigated the Veriflex-E and noted the occurring viscous effects in multi shape memory cycles. Veriflex-E is basically an epoxy based SMP resin and is thermally triggered. In this research they studied that how the increase in temperature effects the shape memory behavior in terms of deformation rate and vice versa. Ingrid A. Rousseau et al. [70] have prepared the epoxy SMP mixtures with three different di-amines as cross linkers. Diane M. Feldkamp et al. [71] have studied the range of deformability (rate of deformation) and high strength with intrinsically good thermal and chemical stability of epoxy based SMP networks. Similarly, Xuelian Wu et al. [72] developed three different kinds of epoxy based SMPs having different contents of linear epoxy monomer. After they studied the mechanical properties exhibited by this epoxy based SMP. Their results demonstrated the addition of higher linear monomer content is directly related to T<sub>g</sub>, shape recovery speed and its other mechanical attributes. To add further, another synthesized series of organic-montmorillonite (OMMT) modified shape memory epoxy (SMEP) composites is reported to be experimented in the literature. It is executed by Yuyan Liu et al. who demonstrated, that the incorporation of OMMT has the direct relation with toughness, tensile strength, transition temperature, and shape recovery speed of the composite. The only attribute that remained unaffected during this experimentation is shape recovery ratio Among few other related researches, one was done by V.A. Beloshenko et al. [73]



who investigated the electrical properties of carbon based epoxy composites. Another epoxy based SMP was synthesized by Deng et al. [74]. They further modified this composite using flexible epoxy. Their finding suggested that the incorporation of flexible epoxy decreased the  $T_g$  that ultimately enhanced the toughness properties of the resulting composite whereas the overall epoxy system remained unchanged in terms of shape memory properties.

For instance, Tandon et al. [75] have explored the use of styrene- and epoxy-based shape memory polymer resins for morphing applications and observed its durability and functionality in severe environmental conditions. Moreover, they also researched its some other attributes such as linear shape recovery, stored strain, rubbery and glassy state modulus and shape fixity. The damage that happened due to conditioned and continuous thermos-mechanical cycling is also recorded. Likewise, Yuyan Liu et al. [76] synthesized a series of epoxy based SM resins with the help of epoxy E-51 and different content of curing agent DDM (4,4-diaminodiphenyl methane). They have utilized the compressing molding technique and experimented these resins for space deployable structures. Their findings presented the superb performance of these SMP epoxies in terms of thermal, mechanical and shape recovery characteristics.

Also Tao Xie et al. [77] observed the change in  $T_g$  of epoxy based polymers by changing the system's cross link density and chain flexibility. Later on, results confirmed that all these cross-linked epoxy samples exhibit strong SMP attributes such as sharp  $T_g$ , remarkable shape fixity and shape recovery. Beloshenko et al. [73] also contributed in the same regard by using epoxy based polymer composites having an aggregated filler. Doing so, they intent to investigate any volume changes that may occur in the shape recovery cycle while the specimen undergoes SME. Similarly, the same group of researchers also reported the increase in volume in the specimen of thermally expanded graphite system. Additionally, Di Prima et al. have developed a model to predict the effect of relative density on elastic modulus [78].

## **2.11 Advantages of SMPs**

Initially in 1941 [79], the terminology of “shape-memory” was first presented by Vernon. Although the very significance of SMPs remained unexplored until 1960s. In 1960s SMPs regained the attention, when heat shrinkable tubes were prepared using cross-linked polyethylene

(PE) [80]. In 1990s, the efforts to make progress in SMPs got really heated-up and enormous development were made within short duration of five to ten years.

Due to rapid increase in the development and extensive research enquiries about SMPs, the characteristics of SMPs became more evident, especially in comparison to SMAs. Basically, SMPs have numerous benefits. For instance, they are responsive towards wide range of external stimuli such as heat, electricity to magnetic field and chemical. These stimuli may activate shape recover process and has the ability to co-exist at one point, thus resulting in the development of multi-sensitive materials. They also exhibit extremely supple and elastic programming that is, their underneath programming may be attained through various stimuli based on single-step processes and multi-step ones. In the context of structural designs, they possess versatile range and exhibit plenty of approaches for the development of net points and required switches.

In addition to this, SMPs exhibits highly adjustable characteristics that is, the properties of SMPs can be engineered and processed with quite ease. This can be achieved with the help of various composites, blending and synthesis techniques. Moreover, they are quite of use with regard to human tissues and for the purpose of biodegradability. To explain this, further, SMPs are actually developed from the soft materials that is responsible for their versatile functions that assists in the construction of help extremely ecological, biocompatible ad unique devices to interact with the human tissues thus facilitating the possibilities for intelligent medical and biological devices and apparatuses. Finally, due to exhibiting lightweight and large volume, SMPs have their significant applications in the development of aerospace items and aero-plane parts and devices. For instance, due to their lightweight, NASA and USA based Air force research laboratory give priority to use deployable devices of SMPs rather than SMAs ones [81].

## **2.12 Shape-memory Functionality of SMPs and their Composites**

The below Figure 7 demonstrates the various functionalities of SMPs. Due to ever increasing comprehension by scientists regarding SME mechanisms of SMPs occurred a tremendous growth in the techniques and procedures to attain versatility in shape-memory functions. Another factor in this context is the significant diversity in the kinds of SMP materials. Thus, due to extensive researches and need arouser, the approaches to design different SM functions have increased manifolds [82].

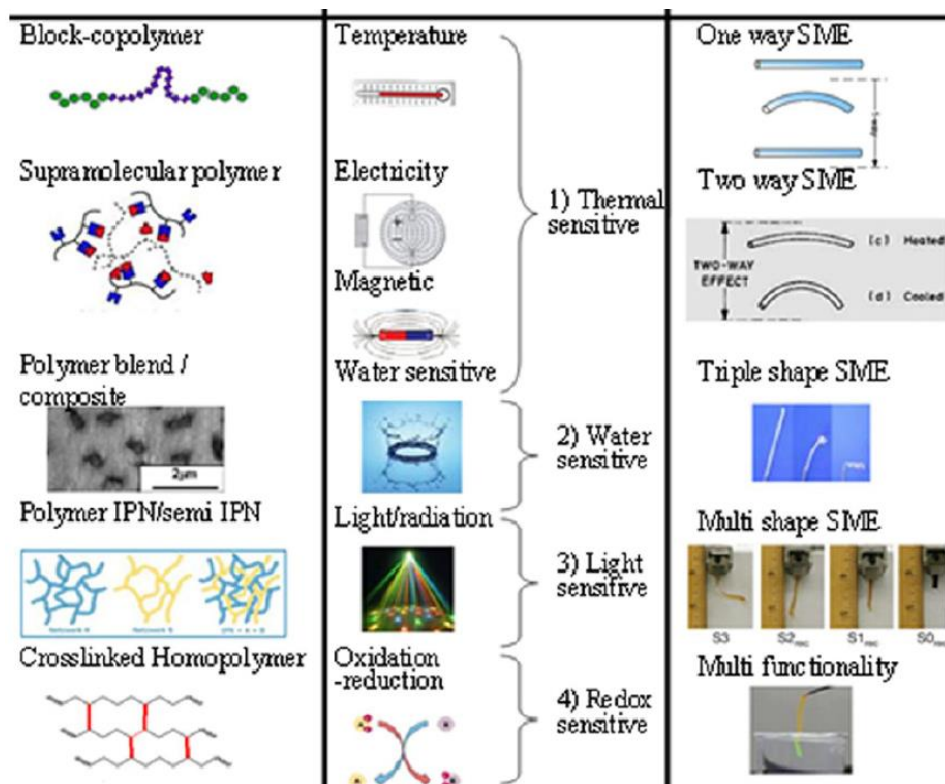


Figure 7: Integrated insight into SMPs based on structure, stimulus, and SMF [82]

Until now, various kinds of SMPs have come up to the screen, for instance, one-way SME, two ways, triple and multiple ways SMEs. Not only this, another type, temperature-memory effect has also widely researched. In addition, there is a possibility for attaining two or more various kinds of shape-memory functions at the same time in the same SMP material. For instance, a SMP network mainly composed of hydroxy-telechelic poly( $\omega$ -pentadecalactone) PPD and PCL, collectively known as PDCL network, has the ability to exhibit one, two and triple way SMEs when exposed to various programming [83].

## 2.13 Different effects of SMPs

### 2.13.1 1-way SMEs/2-way SMEs

Figure 8 illustrate the working principle of SMPs. During 1-way SME, the temporary shape is maintained when the stimulus is terminated, while for 2-way SME, once the stimulus is removed, the initial shape can be recovered from the temporary shape [82].

Previously it was believed that one-way SMEs are not capable enough to go with many applications of SMPs, mainly due to the simpler nature. However, with the development of the

increased number of the programming protocols as stated in the literature, the unique properties of one-way SMPs as flexibility and versatility became more and more evident. It is now believed that one-way SMPs are more application friendly than the two-way SMPs due to their complicate programming and sometimes not even require any programming at all. The original shapes of one-way SMPs are always predetermined during the development process. However, there is a possibility to vary the temporary shape depending upon the various shape-memory programming. Various kinds of evaluation techniques are existing for the purpose of characterizing one-way SMEs. for instance, cyclic tensile investigation, strain recovery process, bending tests, and shrinkage determination are among such methods. Different factors effecting the sharp-memory functions in SMPs with one-way SME have been sufficiently explored. One-way SME systems such as Shape memory poly-urethane (SMPU), Shape memory poly(urethane urea) (SMPUU) and Shape memory polyurethane (SMPU) ionomers have been used to determine various influencing factors in this regard. This actually includes the segment contents, thermo-mechanical cyclic conditions , processing conditions, molecular weight and crystallization of soft segments and maximum strain. An inclusive review regarding the shape memory characteristics of SMPUs with diverse assemblies has been presented by Ranta and Karger in 2008. It specifically highlighted the  $R_r$  and  $R_f$  of various SMPUs. It is also researched that segment content and molecular weight of soft segment are essentially important in determining the shape-memory characteristics such as shape recover stress, strain recovery rate  $R_r$  and strain fixity rate  $R_f$  The strain recovery rate describes the ability of the material to memorize its permanent shape, while the strain fixity rate describes the ability of switching segments to fix the mechanical deformation [90]. Not only this, acquiring a better one-way SME always demands a morphological assembly having isolated hard segments.

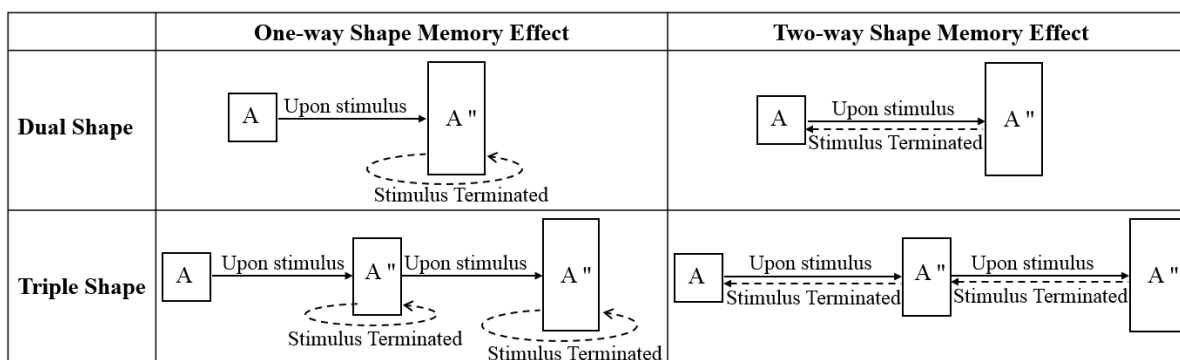


Figure 8: Describe the functioning of SMPs or SMCs (modified from [82])

### 2.13.2 Multiple SME

Later on in 2010, a group of researchers brilliantly developed the Quadruple SME using only one wide glass transition ranging from temperature 55 to 130°C. For this purpose, a commercial ionomer named perfluorosulphonic acid (PFSA) was used. Figure 9 demonstrates the quadruple-shape memory features of PFSA [91]. The same group of researchers explored the effect of varied thermomechanical stimulations at this PFSA's multiple SMEs. The findings suggested that during the development of multiple shape-memory cycles such thermo-mechanical stimulations widely effect the multiple shape-memory characteristics [94]. In the recent era, another new multiple SME system was explored by Xie et al., where by, they used a multi-composite SMPs originally developed from the combination of Fe<sub>3</sub>O<sub>4</sub>-SMP segment and a carbon nano-tube (CNT)-SMP segment separate through another  $T_g$  type SMP segment. Moreover, a quintuple - SME system is developed by Li et al., where by, they used a PMMA/PEG semi-IPN system having a wide glass transition ranging from (45 to 125°C). In the nutshell, these all investigations regarding triple SMEs and multiple SMEs will not only sufficiently fulfil the demands of complicate applications but also open the gateway towards further enriching the shape-memory properties of SMPs [82].

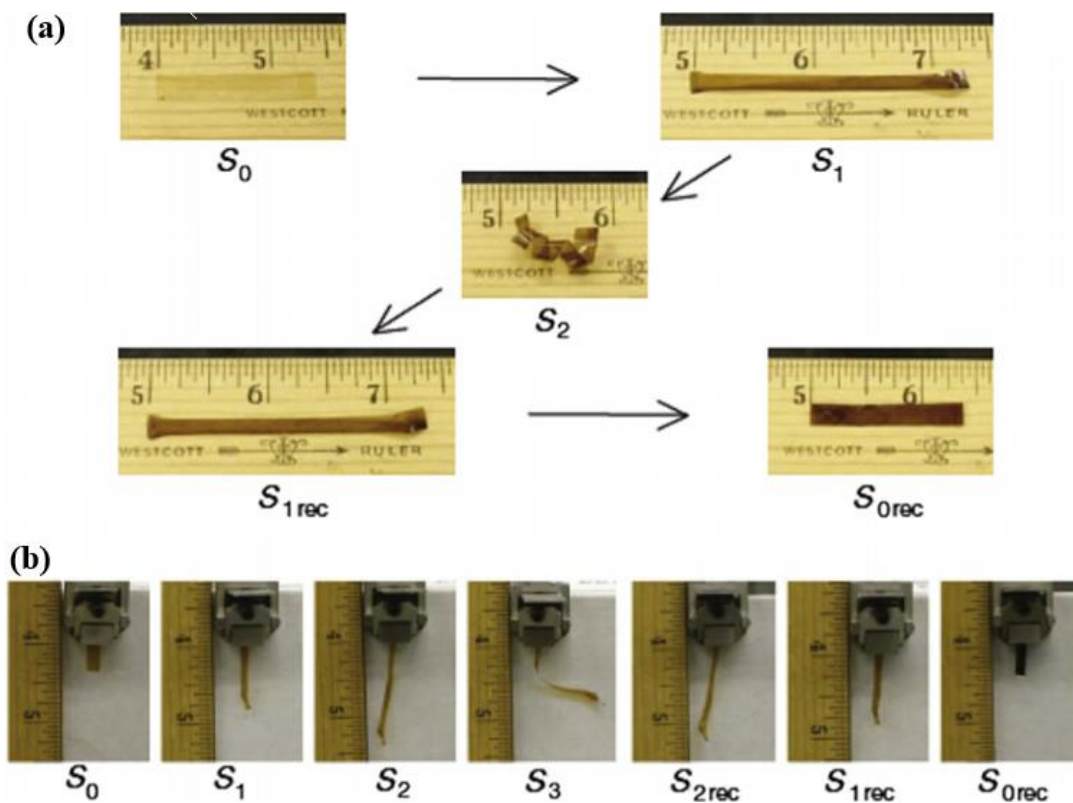


Figure 9: (a) Schematic of triple-SM and SRC, (b) quadruple-SM and SRE of PFSA [91]

To add further, another group of researchers named Podgorski et al. Developed polymer trilayer laminate. They illustrated the quadruple SME characteristic of the very structure. The structure underwent the same physical mechanism. The glass transition region of each layer is well separated. Therefore, doing so, three temporary shapes are programmed that are ultimately recovered upon heating. Quadruple shape-recovery performance of the trilayer laminate is illustrated below in Figure 10 [91].

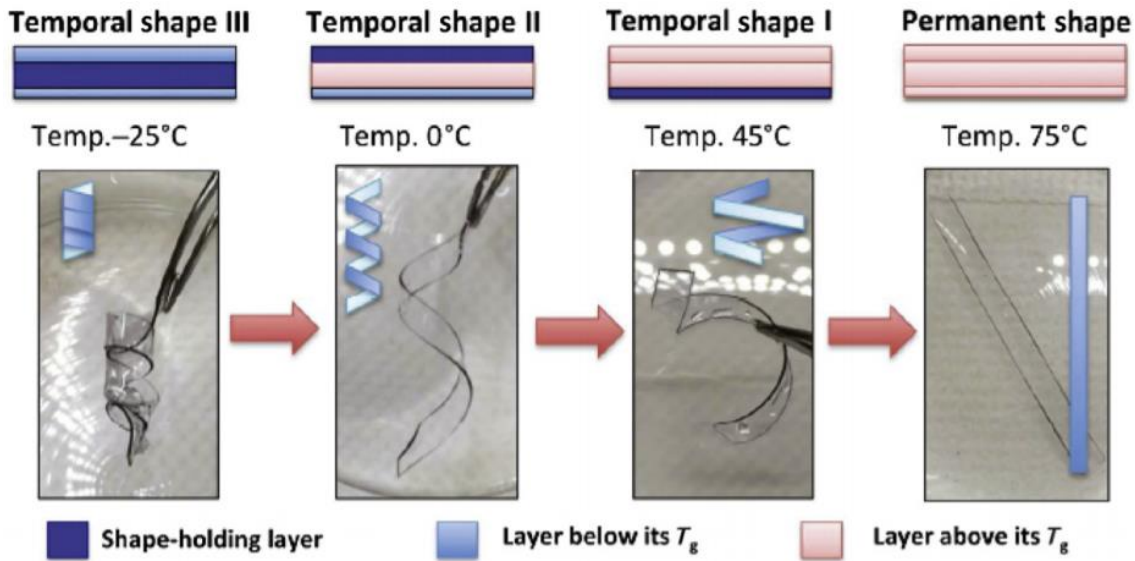


Figure 10: Quadruple-SR effect in polymer tri-layer-laminate [91]

## 2.14 SMP composites

SMPs has been strongly advocated for several Potential applications due to its easy programming, lower cost, less weight and efficient recoverable strain. Although, they do possess certain disadvantages which make them impossible to use for some applications. For instance, stress recovery rate of SMPs is low (I.e.  $3 \pm 2 \text{MPa}$ ) in contrast to their counterpart, SMA ( $0.5 + -0.25 \text{Gpa}$ ). The invention of SMPCs presented the remarkable alternative to this problem. They possess the higher recovery stress rates and thus can overcome this shortcoming of SMPs quite well. That is why, considerable amount of efforts have been put forwarded by the researchers on how to incorporate the use of composites in order to increase the natural low stiffness and less recovery stress in SMPs. SMPs are usually incorporated as a matrix material in such type of composition. The introduction of any type of reinforcement to the composite may help to enhance its strengths; hardness and actuation stress. Glass, nano-particles, Kevlar or finely chop threads of carbon are

few examples of reinforcement that may be used in composite structure. Likewise, there are few fillers, for instance, carbon black and carbon nano-tubes, which help to activate the composite material via heating effect through the provision of electric current to that material. Not only this, SMPC having magnetic particles have the possibility to get inductively activated if exposed to the changing magnetic field. Few prominent examples of magnetic particles are nickel zinc ferrate and iron oxide. This later explained method is advocated for presenting the benefits of wireless functioning[92]. Different type of reinforcements used for composites are described following.

#### **2.14.1 Particle-filled SMPC**

This type holds the SMPs that are fill through particles or short length fibers. Some examples of such particles that may be used for the filling purpose are carbon nano-fibers, carbon black,  $\text{Fe}_3\text{O}_4$  etc. where as short length fibers can be short carbon fibers etc. Such fillings enhances the elastic modulus or hardness of the polymer material which ultimately help to enhance the recovery stress of the composite structure. Although, it is noteworthy point, that such fillers perform as a function material only. For instance, electro-active SMPs may be attained through the incorporation of carbon black and choppy short carbon fibers [49].

#### **2.14.2 Fiber-reinforced SMPC**

They are also known as continuous reinforced SMPs. They are well known for exhibiting enhanced Mechanical characteristics, for instance, firmness, creep-resistant, strength and relaxation. Such enhanced characteristics make their use feasible in various deployable applications, for example, trusses, solar systems and antennas. In the same context, thermosetting SMP has the ability to act as multifunctional composites when endorsed with fiber reinforcement [49].

### **2.15 Effect of reinforcement on SM-ability of SMPC**

Generally, due to possession of low strength and stiffness ratios, SMPs experience elongated strain. However, as mentioned earlier, the incorporation of reinforcement fillers, for instance, nano fibers, fabric layers and carbon nano-tubes may remain helpful in enhancing the material's strength and stiffness. The SM-characteristics of shape-memory polymers also got affected by these reinforcements. The increased stiffness enhances the elastic modulus that ultimately results in increase of spring back displacement of the structure. This whole flow of events eventually reduces the overall fixity of the composite structure [93]. To add further, fiber volume fraction of the

reinforcement is an important factor that determines generally, the shape memory performance of the composite. That is, if the fiber volume fraction is greater in content then it will cause the fixity of the structure to reduce. Although, at the same time, the higher content of fiber volume fraction strongly activates the recovery cycle of the composite. This is because the elastic recovery of the reinforcement facilitates the composite's recovery. Consequently, the residual strain of the SMP composite with a higher fiber content becomes less in magnitude. This reduction in residual strains occurs because its one portion is already restored in the form of spring back recovery [94]. The literature is full with various studies that demonstrates how the SM characteristics of the composites are effected with changing reinforcements.

Another research explored the significance of SiC particles in the recovery process of composites. Ken Gall et al. explained that the ability of the composite structure to recover largely depends upon the existence of SiC particles. In fact, the incorporation of reinforcement reduces the recoverable strain and along with this it enhances the recovery process. Moreover, the stiffness and elastic modulus of the composite structure may be controlled through tailoring the volume fraction of SiC particles or by the use of alternate reinforcement type [95]. Similarly, the impact of carbon black usages in the composition of polyurethane nanocomposites is investigated by Sedat Gunes et al. The results demonstrated that with the addition of just 3 percent of CB a, the shape-memory characteristics deteriorates and by increasing up to 5 percent the SM features deteriorate completely because of brittleness of the added content [96]. In the same context, Subrata Mondal et al. Discovered that with the addition of 2.5 percent of carbon nano-tubes MWNT to the segmented polyurethane, increase the SM characteristics optimally. This is because of the fact that polymer structure gets enough hardness at this level of weight fraction [97].

Almost similar findings are presented by J M Cuevas et al., where by, they added the glass fiber reinforcement to the polyethylene composites structure. The findings suggested that the incorporation of reinforcement to the material enhances its stiffness which ultimately reduces the recoverable strain. After onwards, the impact of fiber volume fraction, fiber end position and fiber length on shape fixity were investigated by Masaaki Nishikawa et al. The findings suggested that these parameters strongly impact the composite's shape fixity feature. They further demonstrated that larger fraction of fiber volume and a larger fiber length cause general increase in the elasticity of the composites that eventually deteriorates the shape fixity of the structure. Likewise, fiber end



position imparts a strong affect both on the shape fixity or recovery ratio by influencing the overall hardness of the composite [98].

Another group of researchers, Takeru Ohki et al., suggested an ideal fiber weight fraction for a very low residual strain and that is between 10 and 20-weight %. Moreover, their findings also depicted that greater fiber fraction volume may result in improved recovery ratio of the composite. Although, it may be also be enhanced due to increased number of recovery cycles.

They also researched the relation between fiber weight fraction and recoverability for discontinuous fiber reinforced SMPCs. The hardness and recoverability parameters are dependent upon weight fraction of the discontinuous fiber. Furthermore, their findings suggested that with an incorporation of 50 percent of finely chop fibers, the hardness of the material may be enhanced by 4 times along with 2.5 times reduction in recoverable strain [94]. Similarly, Liang C et al., researched and explained that two important reinforcements namely, glass fiber and Kevlar, has the ability to enhance the hardness of the SMP resin and thus decreasing the recoverable strain [37]. Later on, Chun-Sheng Zhang et al. investigated the impact of carbon fabric reinforcement on the storage modulus and recovery of laminates. Their findings depicted that this reinforcement exhibits very larger elastic modulus than SMP sheet. At the same time, the SMP bases laminate are found to have much greater and stronger recovery ration than SMP sheet [99].

## **2.16 Shape-memory effect in polymer composites**

Up till now, very few researches have reported in the literature regarding 2-way SME and triple-SME in fiber reinforced SMPC. Whereas, for multi-SME no research has been found recently regarding the same context. 1W triple-SME in SMPC is initially reported by Xiaofan Luo et al. Via two-step programming. It is achieved through the addition of non-woven thermoplastic fibers into a  $T_g$  based SMP matrix to form a SMPC. As these fibers possess low melting temperature, this facilitates in attaining one transition whereas the second transition is obtained through the  $T_g$  of matrix. The two transitions then subsequently applied to get recovery of two temporary shapes, during the process [100].

Later on, 2W-SME in SMPC was explored by Hirohisa Tamagawa et al., whereby they developed a polymeric laminate by fixing a resin plate to the fiber-reinforced polymer plate with the help of

instant glue. The laminate structure experienced the bending due to difference of coefficients of thermal expansion between the resin and fiber-reinforced polymer plate [101].

## **2.17 Characterization techniques for SMP and SMPC**

### **2.17.1 Differential scanning calorimetry DSC**

The DSC measures the heat flow rate that occur to the sample and the reference sample during a controlled temperature programming. The thermal properties are a key feature of SMPs, especially glass transition temperature associated with the switching domains. DSC can be used to determine the thermal behavior of SMPs, especially glass transition temperature, specific heat, melting points, reaction Kinetics and percent crystallinity of the material [102].

### **2.17.2 Interlaminar shear strength (ILSS)**

The delamination properties of composites structure are evaluated by calculating their interlaminar shear strength (ILSS). The ILSS is determined by performing a three-point-bending test on a short-beam specimen. In literature it has been reported that, the ILSS of fibre reinforced polymer-composites could be improved by modification of the reinforcement or matrix [103].

### **2.17.3 Scanning electron microscopy (SEM)**

The basic mechanism of SEM consist of an electron cathode, which generate the electron beam as well as column's electromagnetic lenses swept over the surface of a sample. Primary electron generate the main signals of the electron beam, and the secondary electrons are specimen's bulk and the backscattered electrons and further-more X-rays. Moreover, the secondary electrons, which come from small layer on the sample surface and yield the excellent resolution that, can be realized by scanning electron microscope. Sample producing signals are made up when the electrons interact with the atoms. Interaction of the electron with the atoms generate the sample producing signals, which contain the information about the specimen's surface [104].

## **2.18 The thermomechanical deformation process (TMDP) of SMPs**

The thermomechanical deformation and recovery cycle of shape memory polymer SMPs has been characterized, following the procedure shown in Figure 11. Their different cycle are involved in the thermomechanical deformation process of SMPs, which are described in the following steps: (a) Apply heat above glass transition temperature  $T_g$  to SMP and deformed into intermediate shape

under external load: (b) cooled down the SPM to the room temperature or below glass transition temperature  $T_g$  and unloading : (c) Original shape recovered upon heating above glass transition temperature  $T_g$ , (d) finally, cooled down the original shape of SPM to the room temperature or below glass transition temperature [105].

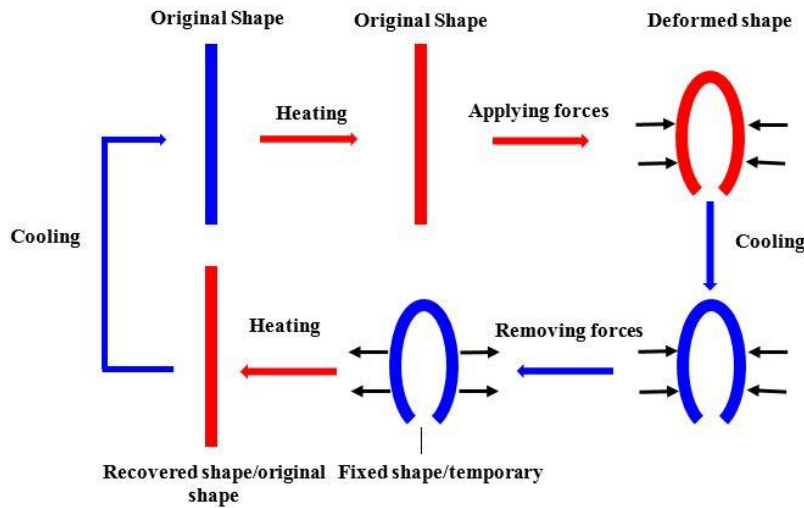


Figure 11: Thermomechanical deformation and recovery process of SMPs( modified from [105])

The thermomechanical behavior of SMPs is illustrated by 3D stress–strain–temperature diagram as shown in Figure 12. Thermomechanical behavior of SMPs can be described in the following four phases: (1) (Phase A→B) it is a high temperature deformation stage, in which SMPs shows the low elastic modulus, large fracture elongation. Moreover, obvious viscoelastic properties can be observed in some SMPs.(2) (Phase B→C) it is a constant strain cooling stage at low temperature in which gradually increases the elastic modulus of SMP. In order to maintain the constant strain, the required stress also increases gradually. (3) (Phase C→D) it is a low temperature unloading stage in which the stress is removed to zero, as well as the partial strain recovery and the maximum part of pre strain is stored in SMPs as a storage strain. (4) (Phase D→A) it is a shape recovery stage upon heating in which the stress is zero, also stored pre-strain decreases slowly with increasing-temperature until the SMP achieves its original shape [105]. SMP characteristics parameters during TMDP are described below.

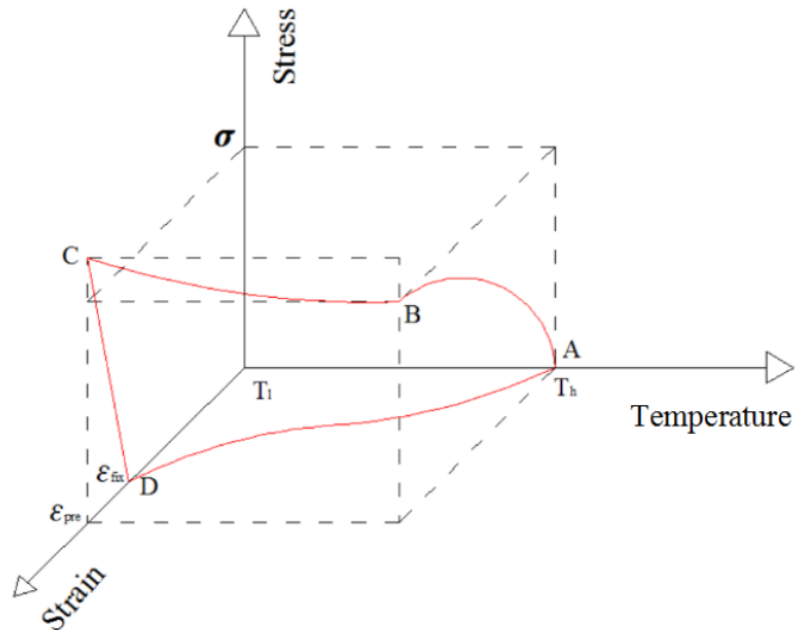


Figure 12: 3D-thermomechanical behavior of SMPs [105]

#### -Shape fixing components:

Such components are basically the chemically cross linked or physically entangled net points existing within an SMP network. Their function is to maintain the stability in the process of deformation and shape regaining.

#### -Shape switching components

Such components are polymer-based chain like structure existing within in the SMP network. It has the ability to divert from one state to another when exposed to change in temperature. This helps them to stay responsible for deformation and recovery related to temperature change.

#### - Shape deforming temperature

This is known as the temperature point where the polymer start to deforms up to specific strain and attains the temporary shape. That very temperature may be below, above or equal to  $T_g$  and plays a significant role in the overall performance of the SMP.

#### -Fixing temperature

Fixing temperature is basically the working temperature where the fixation of polymer's deformed temporary shape took place. As far as glassy SMPs are considered, this temperature is up to  $20^\circ\text{C}$

lower than that of  $T_g$ . Whereas, for the SMPs in the semi-crystal form, it is actually the crystallization temperature and is generally  $40^\circ\text{C}$  lower than  $T_g$ .

#### -Recovery Temperature

The temperature point where the recovery of permanent shape occurs is called recovery temperature. It is also known as transformation or switching temperature. It is normally  $20^\circ\text{C}$  greater than  $T_g$  of SMP.

#### -Shape fixity

It refers to the capability of SMP to maintain the given strain imposed in the material while it is being deformed after consequent removal of load and cooling process. It is denoted by RF and can be determined as the ratio of fixed displacement ( $d_f$ ) to the maximum displacement ( $d_{\max}$ )

#### -Shape recovery

It determines the capability of the SMP to restore the strain collected in the deformation process after consequent cooling and removal of load. There are two ways to express this, either as the ratio of fixed displacement to recovered displacement or as the ratio of recovered displacement to maximum displacement,  $d_{\max}$ .

#### -Recovery Speed

It is known as the percentage of recovery per unit time. It is affected by two main factors. One is the rate of recovery heating. While second is, considering the fixing to be performed at low temperature and the recovery at higher one.

#### -SM cycle life

It may be known as the repeatability and durability of the SMP characteristics along the subsequent cycles of SM.

#### -SM cycle time

It represents the amount of time needed by the SMP to get into temporary shape from its permanent shape and again restoring to permanent shape with a one SMP cycle. In other words, we may say that it is actually the time required for programming of temporary shape and the restoring of permanent shape.

## 2.19 Applications of SMP and their composites.

SMPs as being a unique form of smart materials, occupy a wide list of application fields ranging from space crafts to road vehicles. In the recent era, these are being recognized as essentially important type for their use in deployable components and various aerospace parts. SMPs may be employed for making booms, morphing skins, reflectors and trusses. Moreover, they also represent themselves as potential contributor in the field of smart textiles, automobile actuator, biomedicine etc. To add further, various patents regarding SMPs use have been recorded ,for instance, gripper, self healing composite system, adjustable automatic brackets in vehicle and intravascular delivery system [106].

### 2.19.1 Bio-medical, Aerospace and industrial engineering Applications

Bio-medicine and bio-inspiration are important are important research areas in the context of SMPs. For example, polyurethane SMP when get placed in human bodies serves as an outstanding biocompatible source and thus serves in the deployment of various medical instruments. In a recent era, a feasibility investigation is carried out regarding the making of SMP based polymer vascular stent (as demonstrated in Figure 13). This proposed stent will be used as a drug delivery system that will further ensure the decrease in restenosis and thrombosis. There is an expectation for enhanced biological tolerance by adopting biocompatible SMP based devices [107].

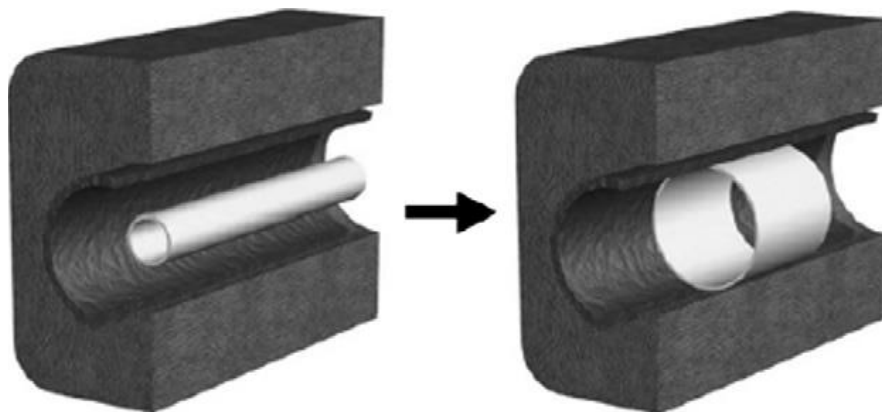


Figure 13: Schematic representation of the SME [107]

Stents holds an important place in the field of SMP's. Basically stents are comprised of tubes made from plastic or metal. These tubes are placed into the closed vessels of the human body, for instance, any artery or duct. After its placement, these stents are actuated through the stimulus of

heat or water as illustrated in the Figure 14. Regarding same concern, biodegradable stent holds an enormous and prominent position because of their advantageous property of getting dissolved in the human body. In other words, there remains no need to remove the stent after two examples of such biodegradable stents are PEG and PLA [108].

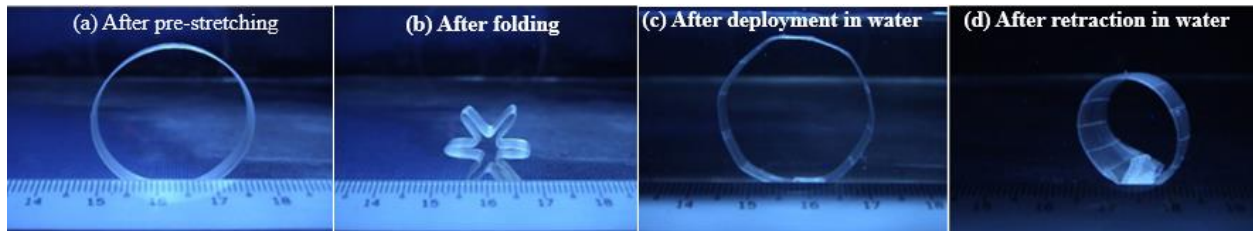


Figure 14: Moisture-responsive functionality for Polyurethane SMP [108]

The most common and conventional aerospace deployable devices include motor driven tools, mechanical hinge shown in Figure 15 etc. Such conventional devices are criticized for some inherited disadvantages, for instance, massive mechanisms, unnecessary impacts during deployment process and complicated assembly. On the comparison side, such intrinsic drawback may be overcome with the help of SMP fabrication over deployment devices [109].

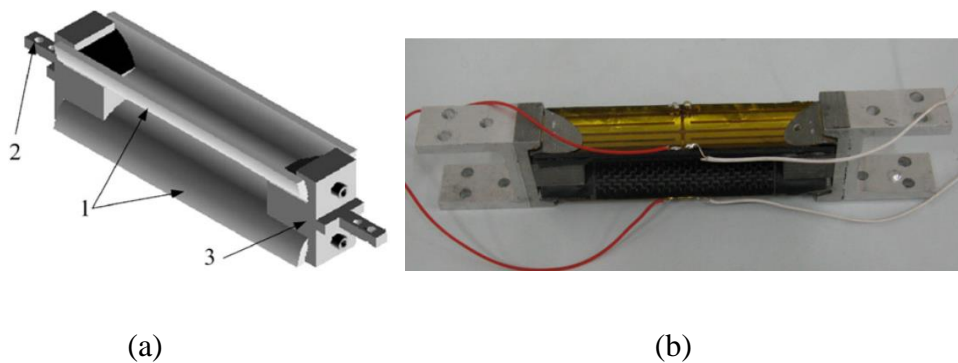


Figure 15: SMPC hinge: (a) Illustration of the hinge (1: curved SMPC shell; 2 and 3: hinge fixture) and (b) real scale hinge [109]

Aerospace and flight crafts are desired to be multifunctional for efficient cruising and highly flexible and quick action mode. The problem with the airplane movement is that its efficient perform may be destroyed at moving towards next sections of flight envelope. According to researchers, this problem may be resolved by radically changing the shape of flight vehicles during travel. By doing so, both the performance and flight envelope may get enhanced. It happens because of occurring tradeoffs among different shapes, for instance, SMPC's pre-deformed shape

and recovered shape [110]. It results in the maneuverability, good pace and less energy usages. In the same context, the Defense Advanced Research Project Agency (DARPA) is researching morphing technique to attain these radical shape fluctuations during air flight Figure 16 [111].



Figure 16: Illustration of Z-shaped morphing wing [111]

Another important application of SMPs is evident from its use in morphing of wings. In fact, in airplane all the basic characteristics such as maneuverability, rate of fuel consumption and flight conditions are mainly determined by shape of its wing. Usually, regular airplanes follows specific speed limits during their operation so there remain no risk or related issue. But for unmanned vehicles (UAVs) this morphing of wings becomes very critical due to certain versatile objectives attached to its operation. To say further, the flight conditions of any UAV is mainly controlled by morphology of its wing Figure 17 [108].

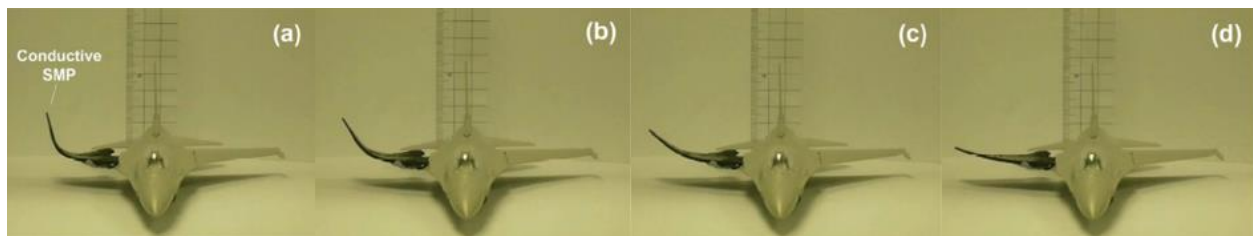


Figure 17: Left wing morphing by joule heating [108]

Foldable/origami structures having the capability of large deformation, which is largely, required for variety of space applications as well as industrial engineering, applications. In order to achieve the objective, the researcher has produced the different structures containing large deformability and self-folding capability property. The interlocking of two SMPC strips produces the mast structure for space antennas and each layer is made of carbon fiber fabric with the interlayer of SM epoxy Figure 18 [112]. Scientists also produced the complex shapes with continues glass fiber



reinforced thermoset epoxy resin composite by using unconventional method that offered the capability of shape changing due to the dynamic-ester bond Figure 19 [113].

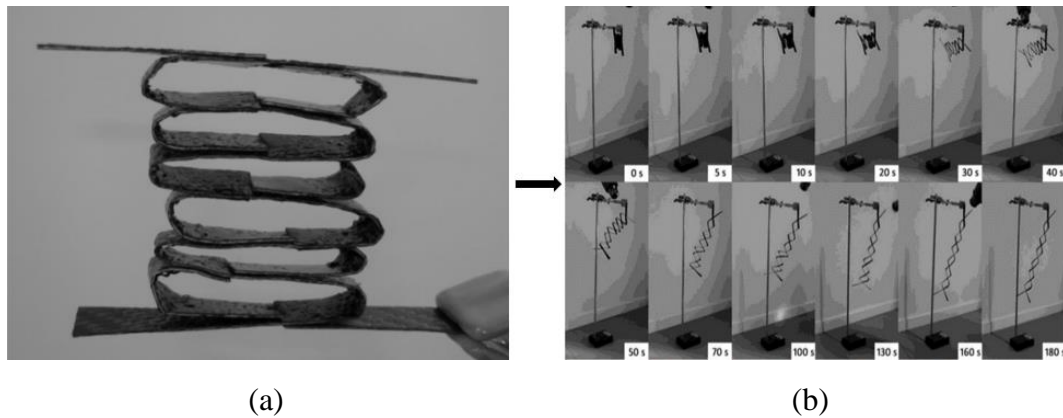


Figure 18: (a) Shape memorized of the composite mast, (b) SR of the mast structure [112]

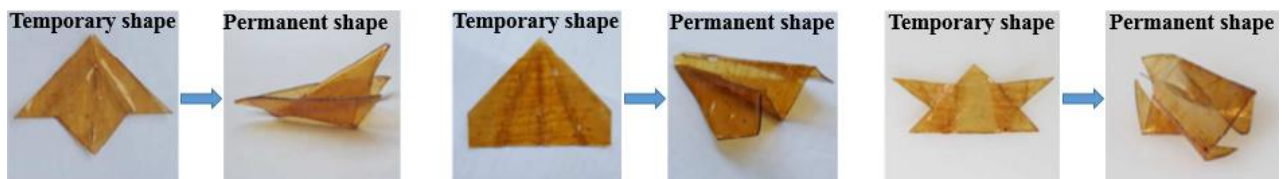


Figure 19: SR of epoxy composite sheets from various folded permanent-shapes [113]

### 2.19.2 Other Applications

There are various potential applications of SMPs [114]:

For instance, there is a possibility for SMP packaging for heat sensitive products. This may include sensor, drug, and food air delivery system. Its another use is in deployable structures such as, hubs, access denial barriers, automatically disassembled electronics and reusable SMP mandrel.

Moreover, SMPs also serves various applications in recreation items: For instance, camping material, lifesaving jackets, snow skis and boards. Along with this SMPs food, utensils may be another head in this context, such as meal boxes, plates and coffee mugs, storage boxes for hot/cold food items. Also SMP toys are very well known due to its advantage of simple reversible compaction, deployment and rigidization cycle (that is it decoys with high fidelity features).

To summarise, this review chapter has systematically discussed various aspects of SMPs, including the background, fundamentals, fabrication, SMP composites and the corresponding potential applications across a variety of fields.

## **2.20 Concluding Remarks**

This review chapter has systematically discussed various aspects of SMPs, including the background, fundamentals, fabrication, SMP composites and the corresponding potential applications across a variety of fields.

In the upcoming chapter the material and methods are going to be discussed in order to achieve the said purposes of this research. Firstly, nine different 3D multilayer woven structures each having different weave in the intermediate layer and top and bottom plain all stitched together are produced using polyamide filament yarns both in warp and weft. These triple layered fabrics are developed on narrow weaving machine equipped with multi beams and creel options. They are then tested at the dry state for air permeability, bending and shear properties. In the second step, the layered fabric that exhibits greater mechanical properties is incorporated to produce the SMP composite samples for which this research examine the mechanical characterization as well as shape memory and shape recovery capability of SMPC by using different characterization techniques.

---

## **Chapter 3: Materials and Methods**

---

A composite is an engineered material that is a substance comprised of two or more materials, insoluble in one another, that are combined together to produce a helpful engineering material comprising of certain properties, not possessed by its constituent parts [115]. If any reinforcement is reinforced with a polymer resin which exhibiting shape memory properties, then it is known as a shape memory polymer composite.

### **3.1 Multilayer reinforcements for SMP composites**

This paragraph summarizes the work of Moussa Alloui [116] who focused on the development and characterization of 3D interlock reinforcements, which have been used for the manufacture of 3D shape memory composites.

The different multilayer reinforcements with different weaves and densities were produced using high performance polyimide filament yarns in both directions, namely, warp and weft. In their dry states, these 3D reinforcements are tested and examined bending, shear and breaking strength properties to gain better understanding of their structural properties before they can be incorporated into the SMP epoxy for the eventual manufacture of the targeted SMP composites.

### **3.2 Multilayer weaving**

Multilayer weaving is a multilinear technique, the principle of which is to interlace two sets of threads namely the warp and weft threads in lengthwise and crosswise respectively to form a multilayer fabric. In the multilayer weave, each layer is formed of a series of independent warp yarns and a series of weft yarns. The warp threads are wound on an independent beam; for example, to weave a triple layer fabric, three beams are required.

To produce the multilayer fabrics that we are seeking to study, we use the weaving loom MÜLLER machine with NCE model as shown in Figure 20 and specifications of preparation are given in the Table 1. This loom is intended for multilayer weaving; it has 12 blades and allows weaving on a narrow width of 32 cm.



Figure 20: The weaving machine (left) and NCE loom system (right)

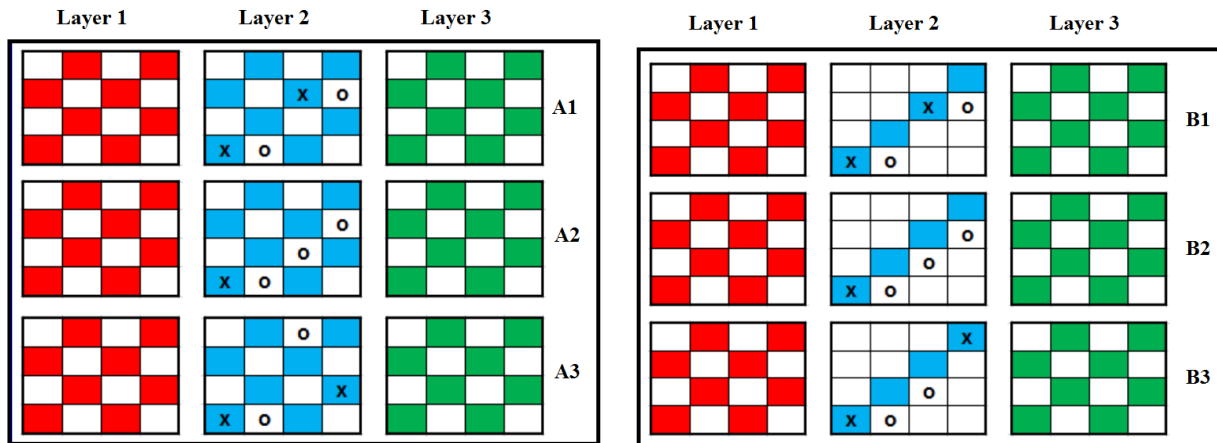
Table 1: Machine specifications

Sr. #	Parameter	
1.	Machine make, model and type	MULLER NC10
2.	Machine working width (cm)	33
3.	Reed count (dents/cm)	19
4.	Speed of machine	650 rpm
5.	Shedding type	Dobby
6.	Weft insertion type	Rapier
7.	Creel capacity or beam capacity	792ends

The multi-layer fabrics that have been produced and tested [116], are composed of three superimposed fabrics linked together by ascensions and descensions of the warp of the intermediate layer on the wefts of the upper and lower layers, so as to obtain a single fabric. These layers are woven simultaneously and are each formed of a warp and a weft. So we have three warp layers at the entrance of the machine and a weft inserted successively in the face layer, the middle then that of the back layer.

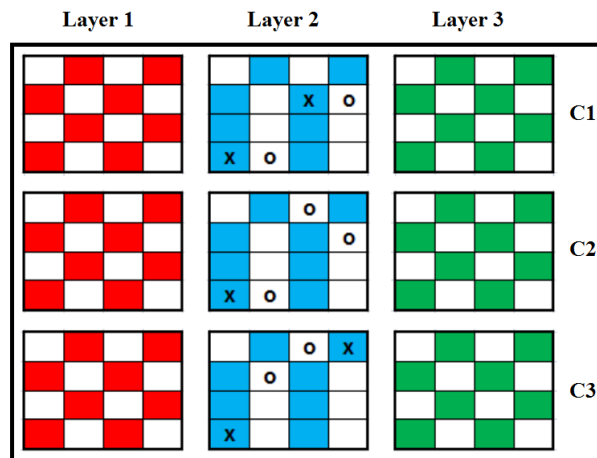
Nine different multilayer preforms have been woven. To this end, three weaves (A, B and C), three bindings (L1, L2 and L3) and three thread counts (16, 20 and 24) are chosen to produce nine different triple-layered fabrics through performing different combinations. Knowing that the fabric A with binding L1 is designated by A1, and the fabric A with the binding L2 is designated by A2, and so on. Figure 21 illustrates the application of stitching to binding distinct layers together to form integrated 3D multi-layer weaves. In Figure 21, three sets of multilayer woven fabrics (3-layers) are produced by combination of three weaves, plain, 1/3 twill and 3/1 warp rib. In category A, the weaves in all three layers are plain, while in B and C category the weaves on face and back

are plain and in the middle are 1/3 twill and 3/1 warp rib, respectively. In these fabrics, we shall distinguish two types of stitches, the first is called an upper stitch which is symbolized by (X) where the center warp lift over the upper layer weft, and the second is called a lower stitch which is represented by means of the symbol (O) produced when the center warp is under the lower layer weft (see Figure 21).



(a) Plain weave in all layers

(b) Plain weave in the face and back layer and 1/3 twill in the middle



(c) Plain weave in the face and back layer and 3/1 warp rib in the middle

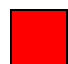


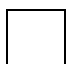
   warp over weft     weft over warp

Figure 21: Graphical representation of the tested triple layered fabrics [116]

### 3.3 Physical and mechanical properties of the produced fabrics

Polyamide yarns PA 6.6 are used to produce the multilayer reinforcements. The warp and weft yarns are multi filaments (128 yarns) of 940 dtex. The specifications of the tested triple layered fabrics are given in Table 2.

Table 2: Specifications of the tested triple layered woven fabrics [116]

Sample	Weave	Yarn linear density (dtex)		Warp density		Weft density per cm
		Warp	Weft	Ends/cm/layer	Ends /cm /3layers	
A1 16	Plain weave in all layers	940	940	8	24	16
A2 20		940	940	8	24	20
A3 24		940	940	8	24	24
B1 20	Face and back plain weave & middle 1/3 twill	940	940	8	24	20
B2 24		940	940	8	24	24
B3 16		940	940	8	24	16
C1 24	Face and back Plain weave & middle 3/1 warp rib	940	940	8	24	24
C2 16		940	940	8	24	16
C3 20		940	940	8	24	20

To evaluate the mechanical and physical properties of the fabrics presented in Table 2, including the crimp, areal density, permeability, bending and shear strength properties, a series of test have been realized. All nine woven multilayer reinforced was tested for bending rigidity, shear stiffness and breaking force to choose the best reinforcement for SMP.

#### 3.3.1 Bending Rigidity

The purpose of this test is to experimentally determine the bending behavior of the developed multilayered structures. This test could evaluate the ability of the fabric to withstand deformation when subjected to a bending load. The cantilever test method was used according to standard test method ASTM D1388. The results of bending rigidity is shown in the Figure 22. It is evident that the sample A<sub>3</sub> 24 produced with plain weave in all three layer exhibited better bending rigidity among the nine samples.

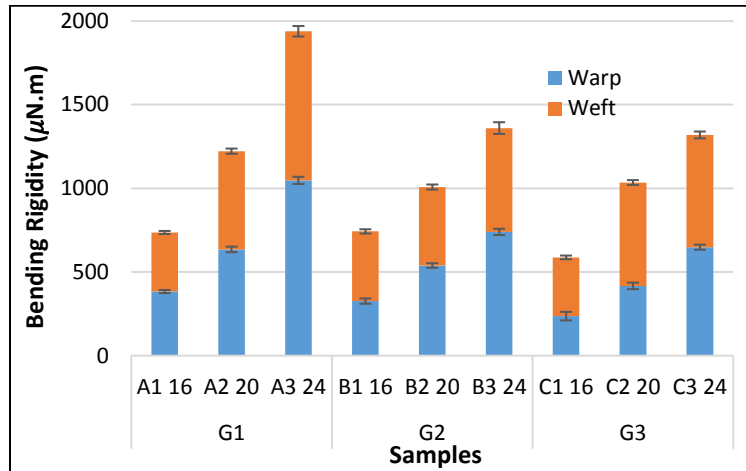


Figure 22: Bending rigidity [116]

### 3.3.2 Bending modulus

The bending modulus is illustrated in Figure 23. The results show that the bending modulus increase with the filling density. All the sample in group G<sub>3</sub> exhibited higher bending modulus and rigidity as shown in Figure 22 and 23 because of the plain weave in all three layers of the specimens. Moreover, it is noteworthy that the woven fabric of the type A3 24, which has a plain weave in the middle and higher weft density exhibits higher bending modulus and bending rigidity compared to other fabric samples.

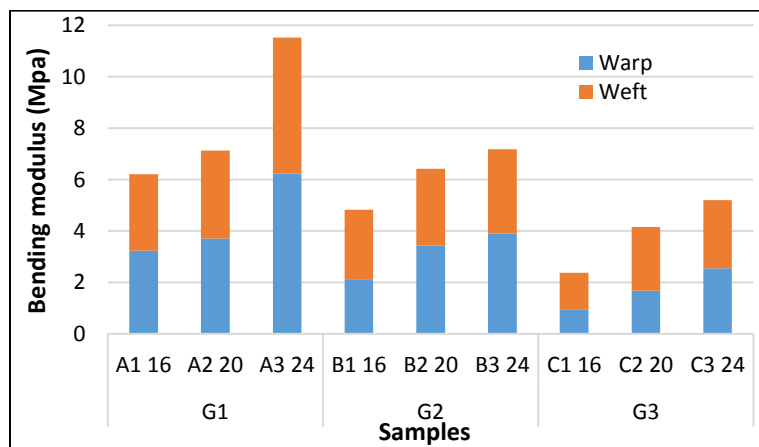


Figure 23: Bending Modulus [116]

### 3.3.3 Shear stiffness

Practically, textile fabrics are subjected to a wide variety of complex deformations, so the shearing behavior is one of the most important mechanical properties that contributes to the performance



and appearance of woven fabrics. The shear property enables fabric to undergo complex deformations and to conform to the shape of the body. Shearing influences drapability, flexibility and formability of the fabric. Thus, shear properties are essential not only for fabrics but also for textile composites. The Kawabata evaluation system (KES-FB1) is used to determine the shear properties of the developed layered fabrics. The results are recorded in Figure 24. It is evident from the figure that the again sample A3 24 possess higher shear stiffness when compared with other samples.

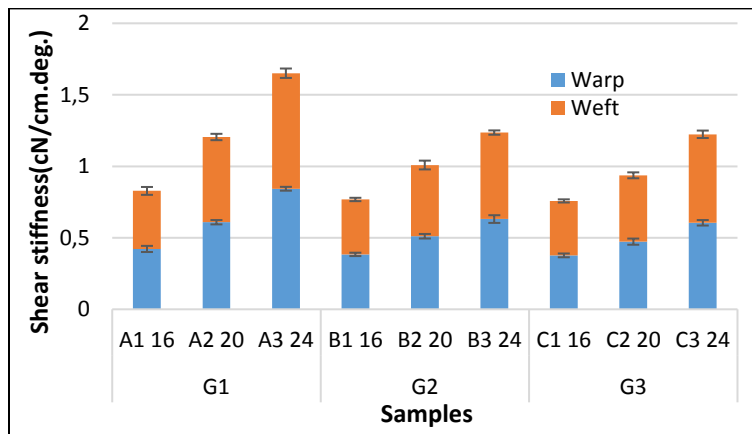


Figure 24: Illustration of Breaking force [116]

### 3.3.4 Breaking Force

The breaking force of all the nine samples was measured. The result are shown in the Figure 25. It is again evident that multilayer sample A3 24 possess a slight higher breaking force as compared with the other specimens.

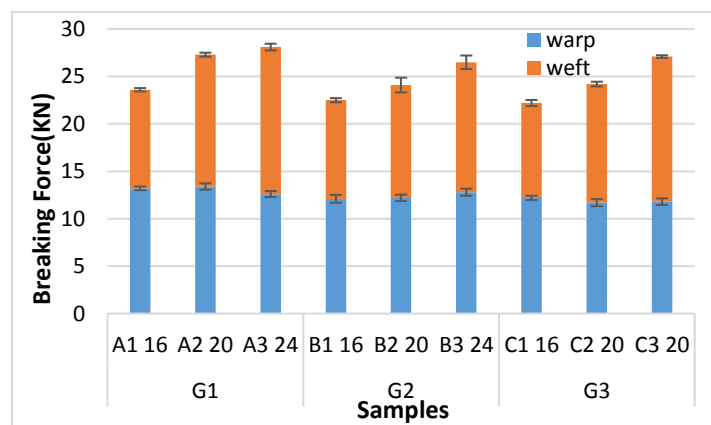


Figure 25: Illustration of Breaking force [116]

So far, all what related to the physical and mechanical properties of the constituents of the SMP composite materials either for the matrix or reinforcements are deeply investigated and discussed. Based on the performed characterizations on the layered reinforcements, we find that the design of triple layer fabric of type A3 24 which has a plain weave pattern in all layers and high filling densities in warp and weft directions, possesses overall good physical and mechanical performances compared to other layered fabric types. Therefore, in the next section, the designated fabric (A3 24) will be employed in manufacturing the SMP composite samples for which its functionality in terms of shape memory behavior is analyzed. Furthermore, experiments will be performed to evaluate the thermomechanical properties of these composites by three-point bending and interlaminar shear strength test.

### 3.4 Preform preparation

The multilayer woven fabric is modified into two different types of preform by introducing carbon filament yarns and without carbon filament yarn (see Table 3). The preform details is given in the following table.

Table 3: Illustration of preform

Sr. #	Sample code	Preform type
1	SN	100 % nylon filament woven
2	SNC	Hybrid preform with carbon strip/2cm

The SN preform has been prepared by cutting Nylon filament woven fabric to the size equal to the mold plate i.e. 170mm × 170mm shown in Figure 26. Hybrid preform introduced with carbon layer (SNC) have also been prepared.

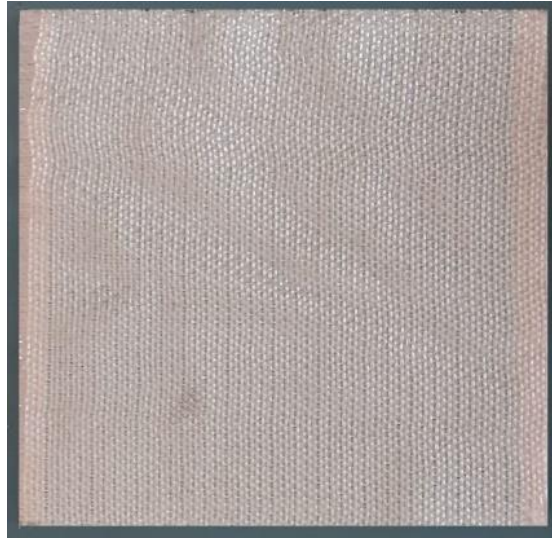


Figure 26: Nylon filament woven fabric SN perform

The SNC preforms have been prepared by cutting the two adhesive copper foil tapes and eight carbon tows (yarns) of the same lengths equal to the length of the Nylon filament woven fabric i.e. 17 cm. These adhesive copper foil tapes has been pasted on the woven fabric. Then, eight carbon tows (yarns) have been placed in parallel on the surface of Nylon fabric in a way in which two tows (yarns) have the same distance between them. After that, the both ends of all eight carbon tows (yarns) have been glued on adhesive copper tape by the help of conductive epoxy resin. Thus, the SNC is prepared shown in Figure 27.



Figure 27: Illustration of carbon yarn insertion on one side SNC

### 3.5 Resin for SMPC

As a matrix, for shape memory composites (SMCs) various types of thermoset (e.g. Vinyl ester, Polyester resin, polyurethane) and thermoplastic (e.g. Polyethylene, Polypropylene, polystyrene etc.) resins can be used. However, in present work, Epoxy resin is concerned as a matrix material because of its excellent shape memory property.

#### 3.5.1 Epoxy resin preparation

Epoxy resin is widely used as a matrix material for different applications generally in the field of aerospace and impact resistance. It can be found from the literature, that, the epoxy-resin is widely used material as a shape memory polymer. In the light of remarkable shape memory property, electrical property and stability in the environment etc., the epoxy based matrix material is an excellent choice. Furthermore, epoxy resin exhibit good heat resistance and mechanical properties that possibly contributes to the best composite impact resistance [117], [118]. For present research, selected epoxy resin properties are given in Table 4.

Table 4: Properties of epoxy resin

Viscosity	Density	Gel time
1200 - 1400 [mPa s]at 25°C	1.1 - 1.2 [g/cm <sup>3</sup> ]	7 - 11 minute at 100°C

A warm curing epoxy Bisphenol A (epichlorhydrin) epoxy resin (number average molecular weight < 700), Araldite® LY1564 system with amine hardener Aradur® 3486 and Aradur® 3487 from Huntsman® Swiss based company is selected as a matrix to manufacture the 3d-reinforced composite structure. The resin and hardeners are manually well mixed in vessel as recommended ratio (shown in Table 5) provided by manufacturer. After that, negative pressure is applied by vacuum pump through pipe (Fig. 28) in order to take out the air bubbles from the container.

Table 5: Combination of the hardener

Araldite® LY1564	100
Aradur® 3486	25.5
Aradur® 3487	8.5

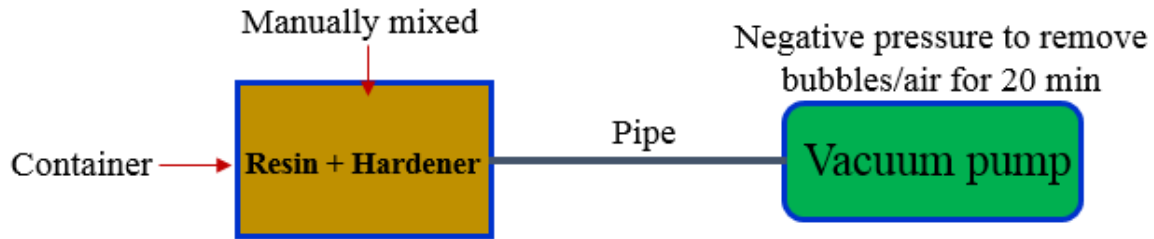


Figure 28: Resin preparation for shape memory polymer and composite

### 3.6 Thermosetting polymer and composite fabrication techniques

#### 3.6.1 Compression molding

Different methods are used for thermosetting composite fabrication. The preference of fabrication method for a specific composite part depends on the material, design of part, and the end use.

#### 3.6.2 Mold preparation

In order to obtain the controlled thickness and proper placement of reinforcement, a special stainless steel mold ( $170\text{mm} \times 170\text{mm} \times 2\text{mm}$ ) prototype is prepared at lab scale shown in Figure 29. Mold has two parts lower part and upper part. Both parts of the mold have eight bars that can be opened by the help of screw to remove the composite structure. Firstly, the mold releasing gel is applied to the both lower and upper parts of the mold, which protect the mold from stickiness of resin. In this way, the prepared composite plates can be removed easily.

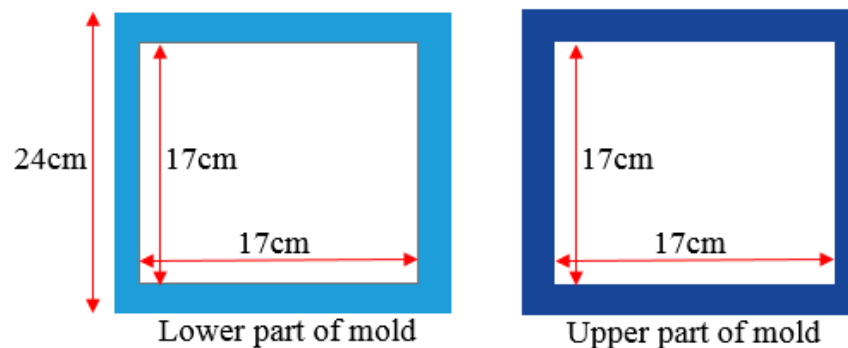


Figure 29: Schematic drawing showing the used mold

Simple epoxy resin (without reinforcement) SMP and 3d-reinforced composite specimens ( $170\text{mm} \times 170\text{mm} \times 1.4\text{mm}$ ) has been manufactured in order to investigate the shape memory properties.

To produce the SMP plate (Fig. 30 (a)), resin is poured on the lower part of mold and then closed by upper part of mold. Finally curing of SMP is occurred in two steps in 1<sup>st</sup> step the mold is left at ambient temperature for 24h and then for post curing mold placed in the furnace at 100°C for 4h (recommended by the manufacturer). All preform are already prepared as described earlier. SN preform is placed on the female part of mold. Than the bubbles are removed from the resin by using vacuum pump. The matrix (Epoxy resin + hardener) is poured by hand layup technique into the reinforcement placed on female mold. So now, female mold is closed by male part of the mold and both parts are then sealed with sealant tape. After that, negative pressure is applied by vacuum pump through pipe to the prepreg (Fig. 30 (b)) in order to take out the air and bubbles from the mold assembly. Furthermore, the primary curing is performed at ambient temperature  $T_a$  for 24h and for further polymerization; the composite plate (with mold assembly) is then again post cured in furnace at 100°C for 4h. All shape memory polymer composite plates SN and SNC (Fig. 31) are demolded and specimens are then cut into the required dimension.

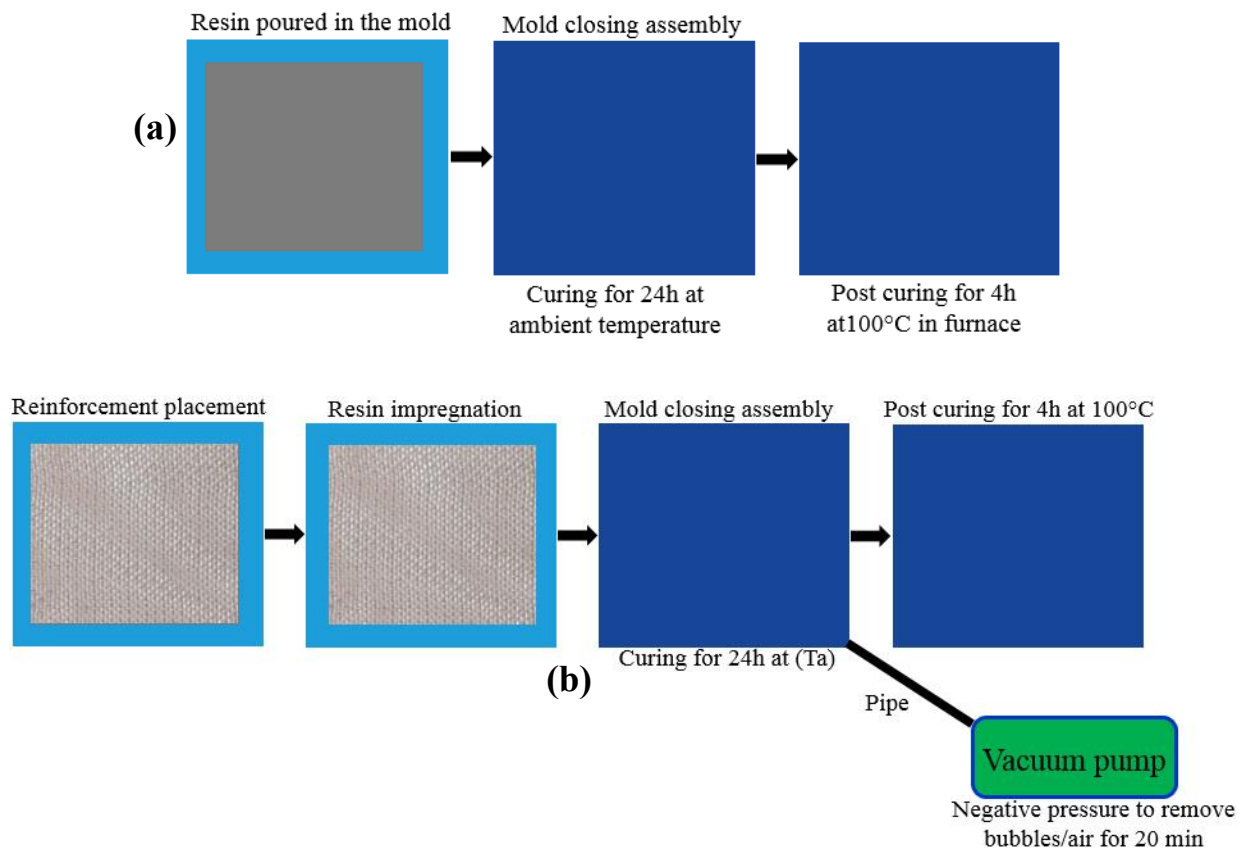


Figure 30: Illustration of (a) resin plate and (b) composite plate production assembly

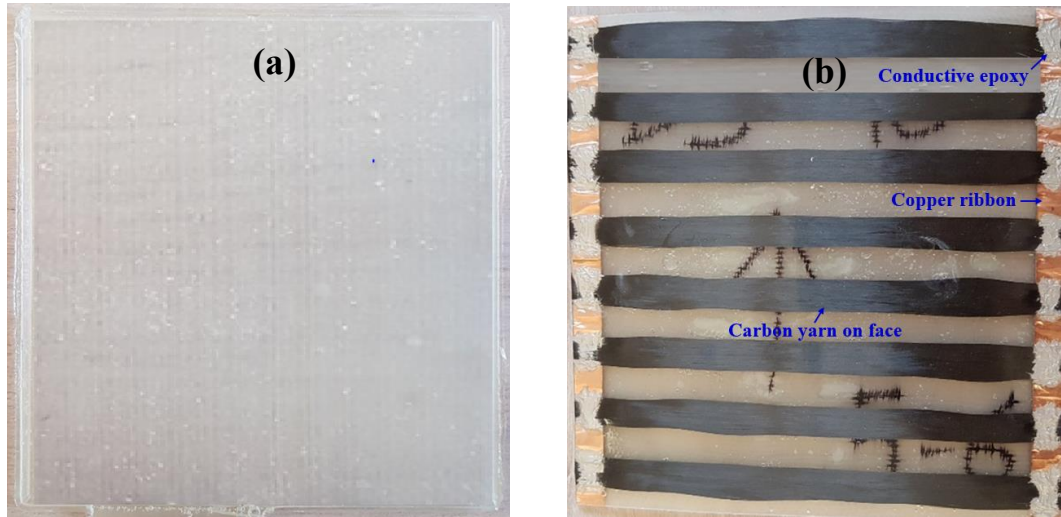


Figure 31: Illustration of produced specimens (a) SN and (b) SNC

### 3.7 Differential scanning calorimetry analysis (DSC)

Differential scanning calorimetry is carried out here to define the characteristic temperatures of the epoxy based SMP samples, including the temperatures of glass transition and melting. The DSC is a thermo-analytical technique that used to determine the critical glass transition temperature ( $T_g$ ) during the transition process, which is often defined as the median point of the glass transition range in the heating ramp. In this work, DSC measurements are conducted using DSC Q200 of TA instruments at a cooling and heating rate of  $10^\circ\text{C min}^{-1}$ . The test temperature range is from  $-20^\circ\text{C}$  to  $250^\circ\text{C}$ . The sample mass is about 5.153 mg, and protection gas is nitrogen at 50.0 ml/min. The result of the DSC experiment of the epoxy based SMP illustrates the heat flow (W/g) versus temperature (Fig. 32). This graph provides direct information about the glass transition temperature of the used matrix that is typically measured as the midpoint on the DSC curve (point of inflection); it is found to be  $86^\circ\text{C}$ . Moreover, from the DSC curve, there is an obvious peak value at a temperature of  $115^\circ\text{C}$ , which indicates that there is a state transition inside SM epoxy at that temperature. Transformation occurs in the heating process, which shows  $115^\circ\text{C}$  is the crystallization melting temperature of the used epoxy. In fact, the crystallization process is analyzed by cyclic DSC measurements with the following temperature profile (heating and cooling rate  $10^\circ\text{C/min}$ ): initially when the temperature reached  $-20^\circ\text{C}$ , there would be a thermostatic process lasting for 3 min. Then heating from  $-20^\circ\text{C}$  to  $250^\circ\text{C}$ , holding for 1 min, cooling to  $-20^\circ\text{C}$ , holding for 3 min, heating to  $250^\circ\text{C}$ , holding for 1 min, and cooling to  $-20^\circ\text{C}$ .

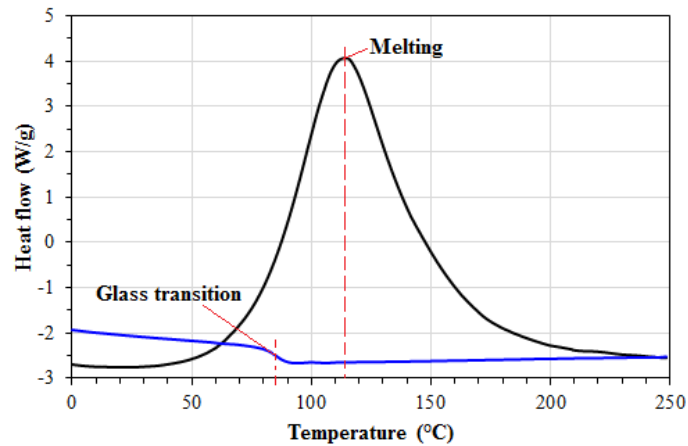


Figure 32: DSC test results of the used epoxy based SMP

### 3.8 Thermomechanical Characterization with different heating techniques

#### 3.8.1 External heating system

Different shape memory cycles have been carried out to investigate the shape memory effect in composite samples, first is the temporary shape programming cycle or initial fixity, and then the recovery cycle of already programmed shape. These programming and recovery cycles are elaborated ahead. In order to perform the shape memory cycles heat as a stimulus is used. Shape memory programming and recovery cycle are then carried out on Instron furnace Figure 33.

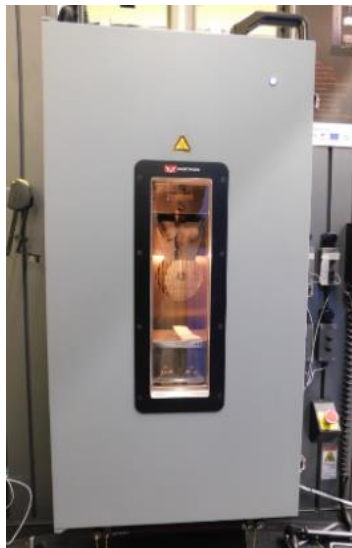


Figure 33: External heating source (Instron furnace)



### 3.8.2 Internal heating system

In addition, the both programming and recovery cycles are carried out on internal heat generation through power supply (Fig. 34). As far as heat generation is concerned, it is made done with the help of carbon yarns. These yarns are actually embedded within the composite and worked as an active layer. Due to the application of electric current as produced from the electric generator, the composite undergone deformation. This deformation mainly occurred because of joule's effect that took place inside the composite.



Figure 34: Internal heating source (power supply)

### 3.8.3 Shape deforming mechanism

Present research work, deals with the development of 3D-reinforced SMPC by using epoxy resin as a matrix. Therefore, firstly, the shape memory ability of epoxy resin is characterized, in order to develop the 3D-reinforced composite system with impressive shape memory ability by using this epoxy resin. In addition, one of the aim of this research work is to obtain the large deformation in present composite system. For this purpose, a special mechanism is adopted to obtain the maximum activation displacement by deforming the shape memory polymer into a U-shape. Because, if, epoxy resin exhibits the high shape memory property, then, possibly the impressive shape memory property can also be achieved by this new 3D-reinforced composite system.

Bending fixture shown in Figure 35 is used to place the specimen on it, which make it possible to alter the distance between two spans. Therefore, the adjustable free length span ( $D$ ) is selected to

decrease from (120mm to 100mm and 80mm), which gives the large shape fixing curvature ( $\epsilon_f$ ). However, it is clear from the equation 1 that  $\epsilon_f$  is inverse proportional to the D and direct proportion to A, so that by decreasing the D large activation displacement (A) can be obtained.

$$\epsilon_f = \frac{A}{D} * 100 \quad 1$$

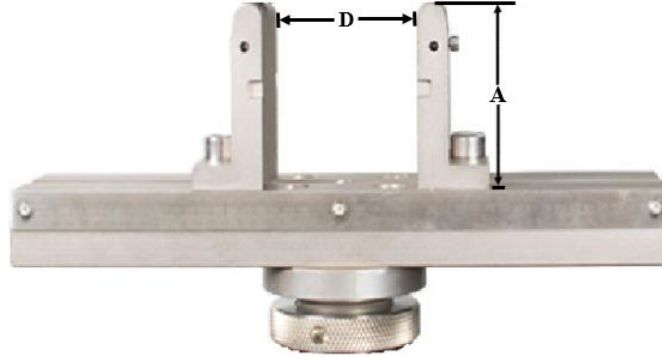


Figure 35: Illustration of bending fixture to deform the specimens

### 3.9 Shape memory and recovery capability of SMP (external heating)

#### 3.9.1 Shape memory cycle of SMP

To investigate the shape memory behavior of epoxy resins, all specimens of different dimensions (three for each) shown in Table 6 are selected to deform into a simple U-shape. Deformation temperature  $T_d$  ( $T_d = T_g + 5^\circ\text{C}$ ) is taken in order to deform the shape of samples during manual mechanical loading also the shape recovery temperature  $T_r$  is the same as deforming temperature  $T_d$ . After that, to fix the temporary programmed shape of specimen is then cool down to the ambient temperature  $T_a$ . The same programming and recovery cycle is performed on each specimen for three time. Original/permanent shape of epoxy resin plate is shown in Figure 36 (a). After performing the programming cycle the obtained deformed U-shape can be seen from the Figure 36 (b) and finally the obtained deformed shape of epoxy resin is fixed in temporary shape (Fig. 36 (c)) at room temperature by releasing it from the bending fixture.

Table 6: Illustration of all specimens of different width

Sample code	Sample with(mm)
A <sub>10</sub>	10
A <sub>20</sub>	20
A <sub>40</sub>	40

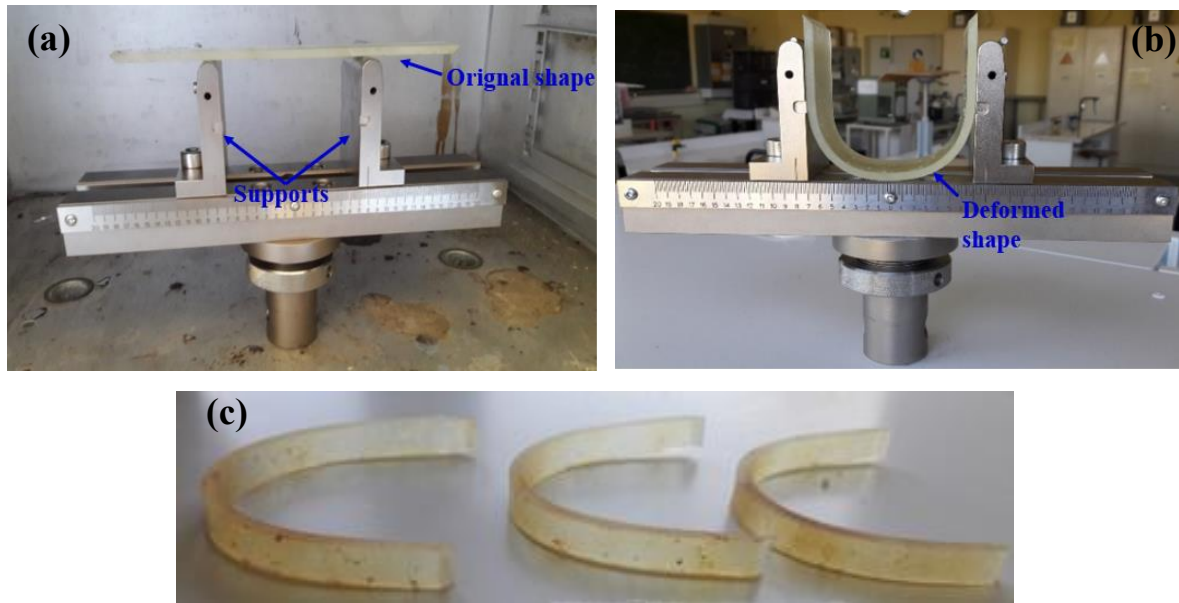


Figure 36: (a) original shape, (b) deformed shape and (c) shape fixity in temporary shape SMP are successfully deformed into temporary programmed U-shape. Large activation displacement obtained from this shape memory epoxy system is measured by digital Vernier height gauge shown in Figure 37. Firstly, set the tip down on a table in order to obtain the zero on the main scale screen after that, move the scale in vertical direction until to get the height of deformed SMP. So finally, the reading appear on the screen digital scale is note down.

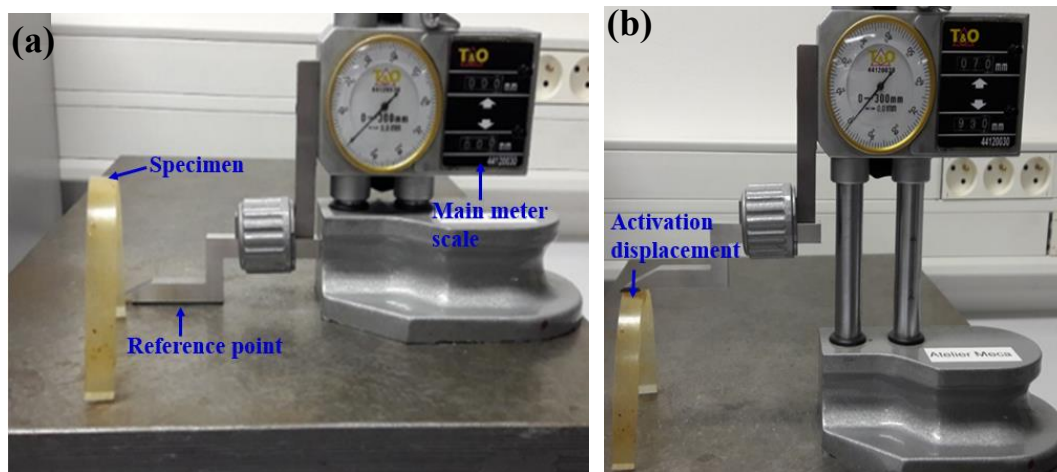


Figure 37: Measurement of activation displacement of temporary programmed shape of epoxy resin (a) reference point, (b) activation displacement

### 3.9.2 Shape recovery cycle of SMP

To investigate the recovery capability of epoxy resin specimens, the samples are then carried out in furnace. During recovery step the recovery temperature  $T_r$  is selected as same as  $T_d$ . All specimens are observed to recover their original permanent shapes successfully in the presence of external stimulus (heat) without any external loading.

From this experimental study, the impressive shape memory and shape recovery ability is found in epoxy resin. Hence, this epoxy resin is decided to use as a matrix for 3D-reinforced composite structure. However, the same manufacturing procedure is used to prepare the composite structure as epoxy resin plates are produced. Moreover, this manufacturing procedure is already described earlier (section; SMP and SMPC manufacturing).

### 3.10 Shape memory and recovery capability of SN (external heating)

#### 3.10.1 Shape memory cycle of SN

To investigate the shape memory behavior of SMPC, three specimens are deform into a simple U-shape.  $T_d$  ( $T_d = T_g + 5^\circ\text{C}$  i.e.  $91^\circ\text{C}$ ) is taken in order to deform the shape of samples during manual mechanical loading also the shape recovery temperature  $T_r$  is the same as deforming temperature  $T_d$ . After that, to fix the temporary programed shape of specimen is then cool down to the ambient temperature  $T_a$ . The same programing and recovery cycle is performed for three time. Original/permanent shape of epoxy resin beam is shown in Figure 38 (a). After performing the programming cycle the obtained temporary U-shape can be seen from the Figure 38 (b).

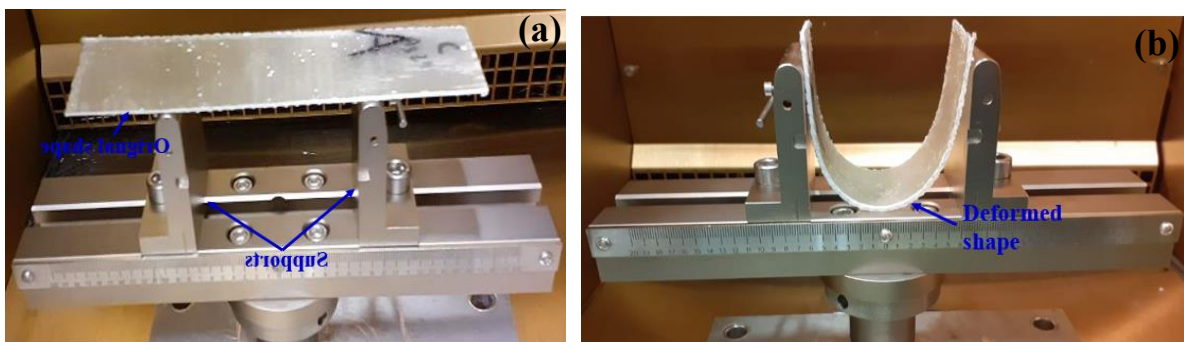


Figure 38: Illustration of temporary programed shape of SN

### 3.10.2 Investigation of shape fixity and shape recovery behavior of SMPC

The most significant parameters for quantifying shape memory properties are the shape recovery and the shape fixity. The shape recovery quantifies the ability of the SMP composite material to recover its original shape whereas the shape fixity quantifies the ability of the material to fix the temporary shape. These two parameters are used as measures of inherent shape memory performance. A new 3D characterization technique is therefore needed to adequately and quantitatively describe the shape memory properties. Here, an optical 3D scanner based on fringe projection technique for 3D surface profile is used to quantitatively evaluate the shape fixity and shape recovery of the developed multilayer SMP composite samples.

Optical 3D scanners are now more frequently used to get 3D measurements of any physical object. These digitization systems are based on obtaining of surface coordinate points by scanning the surface illuminated by structured light. The spatial coordinates of points forming the surface of the scanned object are determined based on triangulation principle. The digital model of the object is obtained through polygonizing the cloud of points. In this research, experimental 3D shape measurements to quantitatively describe the 3D deployment behavior of a SMP composite sample of dimension  $170\text{mm} \times 42\text{mm} \times 1.4\text{mm}$  are performed using GOM ATOS Core MV135 equipment with a measuring volume of  $135\text{mm} \times 100\text{mm} \times 100\text{mm}$  and camera resolution of  $2448 \times 2050$  pixels (see Figure 39).

Before making the measurements, it is essential to clean up the sample surface. In addition, in order to increase the precision of assembly of the individual scans from various measuring positions, non-coded reference points are applied on to the surface of the sample. An anti-reflective coating is also sprayed on the surface to prevent light reflections during scanning. The composite sample is then placed on a table and is scanned from different positions.

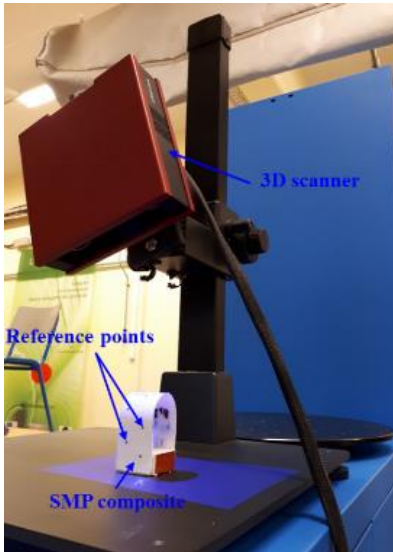


Figure 39: Digitization process of the 3D shape of SMP composite provided by structured light and non-coded reference points

### 3.10.3 Recovery cycle of SN

To investigate the recovery capability of SMPC, the specimens are then carried out in furnace. During recovery step the recovery temperature  $T_r$  is selected as same as  $T_d$ . All specimens are observed to recover their original permanent shapes successfully in the presence of external stimulus (heat) without any external loading.

### 3.11 Thermomechanical characterization of SNC

Composite specimen is cut into 170mm×32mm×1.8mm, and then thermo-mechanical characterization (Fig. 40) based on 3-point bending test is performed on tensile tester machine (Instron 250kN). The composite sample is placed on 2-supporting spans, which are 90 mm apart. A load cell of 500N (accuracy of 0.01N) is employed to measure the precise forces. For the temperature measurement, thermocouples of type K are used. As all the composite plates used in this work have an active layer of eight carbon yarns, so, for each test, one thermocouple is put on the carbon yarn whereas the second thermocouple is put in between the two carbon yarns. Both the thermocouples are put on the upper side of the composite plate. The temperature for the thermocouple on the carbon yarn is always greater than the second one. These thermocouples are connected to DAQ system, which works with the LabVIEW software. Hence, different temperatures are visible in LabVIEW software which can be exported to Excel sheets.



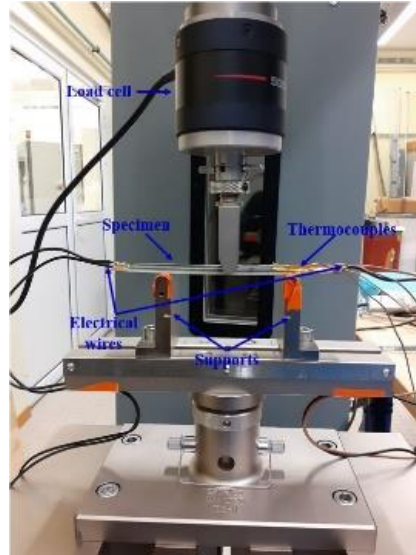


Figure 40: Illustration of apparatus used to characterize the shape memory and recovery cycle

### 3.12 Different shape memory and shape recovery capability of SMPC

#### 3.12.1 Shape programming cycle

To characterize the shape memory, fixity and recovery behavior of 3D reinforced composite plate. Firstly, the composite specimen of the same dimensions ( $17\text{cm} \times 14\text{mm} \times 1.4\text{mm}$ ) are decided to deform into a different simple shapes like loop, U-shape and S-shape and then in second phase again composite specimen is deformed into very complex shapes like M-shape, twist shape and spiral shape at elevated temperature ( $T_d = T_g + 5^\circ\text{C}$  i.e.  $91^\circ\text{C}$ ) in furnace (Fig.41). In order to fix the specimens into temporary programmed shapes are then cool down to ambient temperature.



Figure 41: Control heating Instron furnace

### 3.12.2 Shape recovery cycle

To investigate the recovery capability (Fig. 42) of shape memory composite specimens, the samples are then carried out in Instron furnace (as described earlier). During recovery step the recovery temperature  $T_r$  is selected as same as  $T_d$  i.e.  $91^\circ\text{C}$ . All shape memory composite specimens are observed to recover their original permanent shapes successfully in the presence of external stimulus (heat).

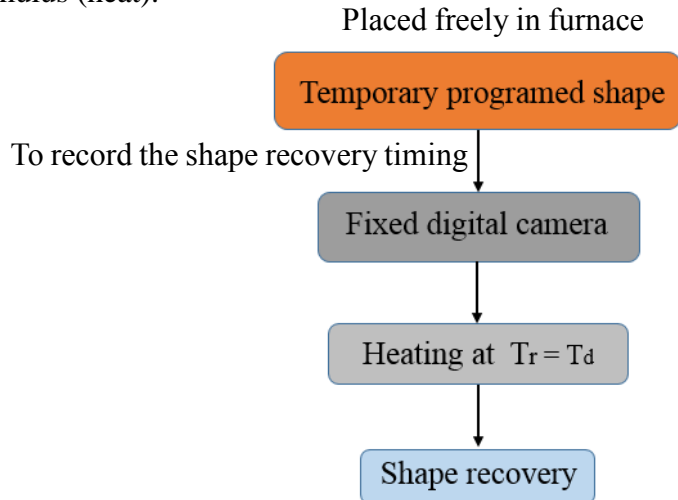


Figure 42: Illustration of shape recovery cycle

### 3.13 Flexural stiffness of SMPC

It is essential to examine the variation of flexural stiffness and strength of the developed triple layer SMP composite under different temperatures to investigate the bending performance. The experiments at different temperatures are performed according to ISO 14125:1998 on five specimens, the dimensions of which are with thickness of 1.4 mm, width of 14.7 mm and length of 70 mm. The experiments are performed using Instron universal testing machine 5985 with a three-point bending rig in a temperature controlled chamber as shown in Figure 43. The machine is equipped with a 500 N load cell. The indenter and the two support rollers all have cylindrical surfaces with diameters of 10 mm and 4 mm, respectively. The support span is 56 mm, with a span-to-thickness ratio of 40:1. The isothermal bending tests are carried out by heating the specimens to target temperatures of  $30^\circ\text{C}$ ,  $40^\circ\text{C}$  and  $50^\circ\text{C}$  at a heating rate of  $5^\circ\text{C}/\text{min}$ . The specimens are then left at the target temperature for at least 10 min to allow the system to reach its thermal equilibrium. The bending tests are then carried out at 1 mm/min and the tests are stopped when the displacement of point in the central span reached the maximum value of 10 mm. During



the bending test process, the values of applied load and deflection are recorded. From these values, the flexural stress  $\sigma_f$  and flexural strain  $\varepsilon_f$  of the composite samples can be sequentially calculated by the following formulas:

$$\sigma_f = \frac{3FL}{2bh^2}; \quad \varepsilon_f = \frac{6Dh}{L^2}$$

where  $F$  is the load,  $L$  is the support span,  $b$  and  $h$  are respectively the width and thickness of the tested specimen,  $h$  is the thickness of specimen,  $D$  is the maximum deflection of the center of the specimen. Besides, the flexural modulus, a measure of the stiffness during the first or initial step of the bending process, can be calculated from the initial slope of the load–deflection curve using the following equation:

$$E_f = \frac{mL^3}{4bh^3}$$

With  $m$  the initial slope of the load–deflection curve



Figure 43: Experimental set up of three-point bending tests of SMP composite specimens in a thermal regulating chamber

### 3.14 Interlaminar shear strength of SMPC

The thermomechanical properties of the fabricated multilayer SMP composites are evaluated by calculating their interlaminar shear strength (ILSS) at different temperatures. The ILSS is determined by performing a three-point bending test on a short-beam specimen (Fig. 44). Short

beam shear (SBS) test is performed on a minimum of three samples to obtain their interlaminar shear strength, which is a measurement of reinforcement-matrix binding strength. In general, in this test, failure occurs due to a combination of interlaminar shear cracking, buckling, local contact crushing or flexural failure, and fiber rupture of the specimens. Following the NF EN ISO 14130 standard, the short beam shear test is conducted on universal testing machine Instron attached with an environmental chamber under 250 KN load cell with a cross head speed of about 1 mm/min. As required by the test method, the specimen width, length and span are adjusted according to the specimen thickness. Therefore, specimens are cut in the following ratios: length = 10 × thickness and width = 5 × thickness leading to a sample size of 14mm×7mm×1.4mm. The span to thickness ratio in the SBS is set to five. As a result of this test, a load displacement curve is obtained from which the apparent ILSS value is calculated using the relation derived from the classical beam theory:

$$\tau_s = \frac{3P}{4bh}$$

Where  $\tau_s$  is the short beam interlaminar shear strength, P is the maximum load; b and h are respectively the specimen width and thickness.

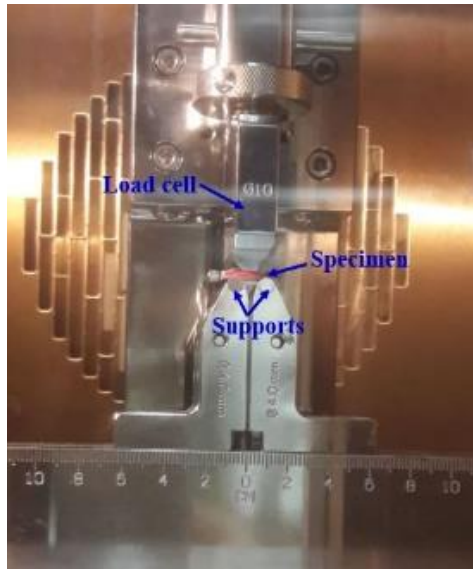


Figure 44: Illustration of ILSS tests of SMP composite specimens in a thermal regulating chamber

### **3.15 SEM analysis**

Scanning electron microscopy (SEM) is used to scan the surface of sample in order to investigate the surface topography. In present research work, JEOL JSM-IT100 scanning electron microscope (SEM) at 15 kV accelerating voltage is used. SEM analyze is conducted to analyze the fracture appeared on the surfaces of the 3D-multilayered composite specimen after the investigation of flexural modulus and interlaminar share strength ILSS.

### **3.16 Summary**

3D multilayer woven fabric is developed in order to produce the multilayer reinforced shape memory polymer composite as well as shape memory polymer plate is prepared by using epoxy resin. Then, a series of tests are conducted on this shape memory polymer composite to evaluate the mechanical properties Shape memory, shape fixity and shape recovery properties of said composite and polymer plate are investigated by using different characterization techniques.

---

## **Chapter 4: Results and discussion**

---

The property investigated for shape memory composites that are manufactured and studied in this work is actually its ability to self-deploy a structure following a thermal activation (self-folding structure). This is performed at a temperature equal to that which allowed their initial compaction (conventionally  $T_g + 20$  to  $30$  ° C),  $T_g$  being the glass transition temperature of the matrix. The first part of this chapter deals with the capacity for this matrix to be shaped (education phase) and then to recover its initial geometry. The second part relates to the characterization of the properties in bending of composite only (3D reinforcement and matrix): bending test 3 points below and ILSS. For different geometries, the shaping properties of the composite are then explored. The last part of this chapter deals with the characterization of the active composite structure integrating a heating system (carbon wires). The full cycle of education and recovery is studied.

The glass transition temperature ( $T_g$ ) of the matrix is  $86^\circ\text{C}$  (Fig. 32 chap. 3), the interval of this transition is equal to  $[80^\circ\text{C}, 90^\circ\text{C}]$ . For these different tests, the temperatures used to characterize the behavior of the 3D composite are chosen either below this interval to determine the properties of the composite in its operating range (i.e. after deployment), or in this interval and beyond to study the properties formatting and recovery.

## **4.1 Shape fixity and shape recovery capability of epoxy resin**

### **4.1.1 Shape fixity displacement in pure epoxy resin**

In order to investigate the shape memory capability of epoxy resins, all specimens of different dimensions (Table 6) are deformed manually into a simple U-shape (Fig. 36) at selected temperature  $T_d$  ( $T_d = T_g + 5^\circ\text{C}$ ). After that, to fix the temporary programmed shape of specimen is then cooled down to the ambient temperature  $T_a$ .

It is evident from the Figure 45 that, at high span length of 120mm shape fixity displacement obtained is 60mm and at 100mm span length the shape fixity displacement is almost 70mm in all specimens. However, at less span length 80mm shape memory resin specimens show very high shape fixity displacement (i.e. almost 75mm). Therefore, it is clear from the graphical representation that the activation displacement increases with decreasing the span length. Because on decreasing the span length, more compact temporary shape is obtained which provides large activation displacement. Only breakage observed in the specimen having the width of 40mm at 80mm span length, which led to Shape memory-programming failure. It is because the width of

sample is more and intention is to obtain more compact shape. Several breakage causes are possible, like bubble existence inside the structure during production or possibly during large deformation the SMP structure exhibits high level of forces inside the structure, which leads to the breakage.

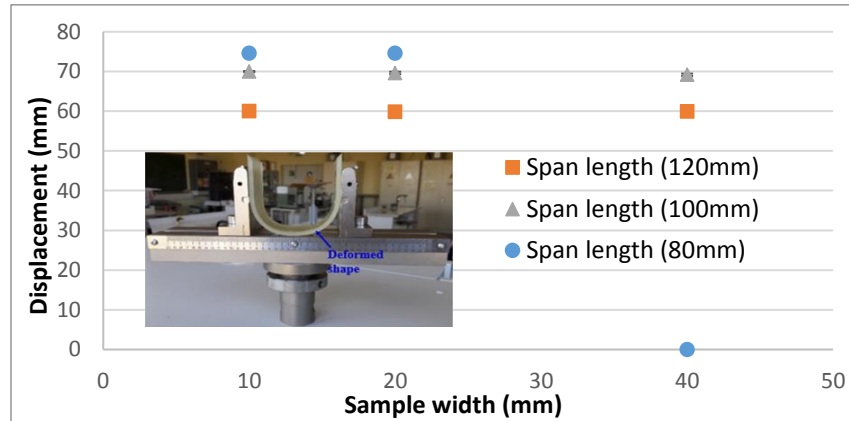


Figure 45: Interval plot of shape memory programming cycle at different span lengths

#### 4.1.2 Shape recovery capability of pure epoxy resin

Shape recovery is all about the amount of residual stresses, which are induced in the actuators during programming cycle. Moreover, high activation rate could be achieved from any shape memory polymer by inducing more residual stresses into the sample. After successful achievement of high activation displacement, shape recovery capability of different samples are also investigated. The same temperature is used for shape recovery and shape programming cycle. Table 7 illustrates that all samples shows 100% shape recovery and gain their original permanent shape at span length of 90mm and 70mm. Moreover, the samples (A<sub>10</sub> and A<sub>20</sub>) are deformed at 50mm span length also shows their 100% shape recovery capability. However, the sample A<sub>40</sub> do not take part in shape recovery competition due to the breakage, which happened during shape memory programming cycle as described earlier.

Table 7: Description of shape recovery capability of epoxy resin at different span lengths

Sample code	R <sub>r</sub> (%) at D=120mm	R <sub>r</sub> (%) at D=100mm	R <sub>r</sub> (%) at D=80mm
A <sub>10</sub>	100	100	100
A <sub>20</sub>	100	100	100
A <sub>40</sub>	100	100	Breakage

The obtained results authenticate the use of this resin for the production of 3D composites. It is also worthy to note that the shaping of this sample can be obtained for a temperature  $T_g + 5^\circ\text{C}$  which is the upper limit of the interval while characterizing the glass transition of the resin.

## 4.2 Investigation of flexure strength of SMPC

### 4.2.1 Flexure strength at different temperature

For structural applications, it is necessary to analyze the variation of strength and flexural stiffness of the developed multilayer SMP composite under different temperatures to investigate the bending performance. The experimental protocol used to investigate the flexural stiffness of 3D reinforced composite structure is shown in Table 8.

Table 8: Description of experimental method and composite sample specifications

Width (mm)	14.7		
Length (mm)	70		
Thickness (mm)	$1.4 \pm 0.1$		
Test type	3 point bending		
ISO	14125:1998		
Sport span (mm)	56		
Nb of sample tested	5		
Temperature range ( $^\circ\text{C}$ )	30	40	50
Thermal equilibrium time	10min		
Bending speed	1mm/min		

Figure 46 shows the flexural force-displacement relationships of the tested composite specimens under different temperatures. It can be noticed that the maximum value of force of these curves decreases with increasing the temperature from  $30^\circ\text{C}$  to  $50^\circ\text{C}$ . For the same type of composite sample, the maximum force is reduced by about 38 % when the temperature raised from  $30^\circ\text{C}$  to  $50^\circ\text{C}$ .

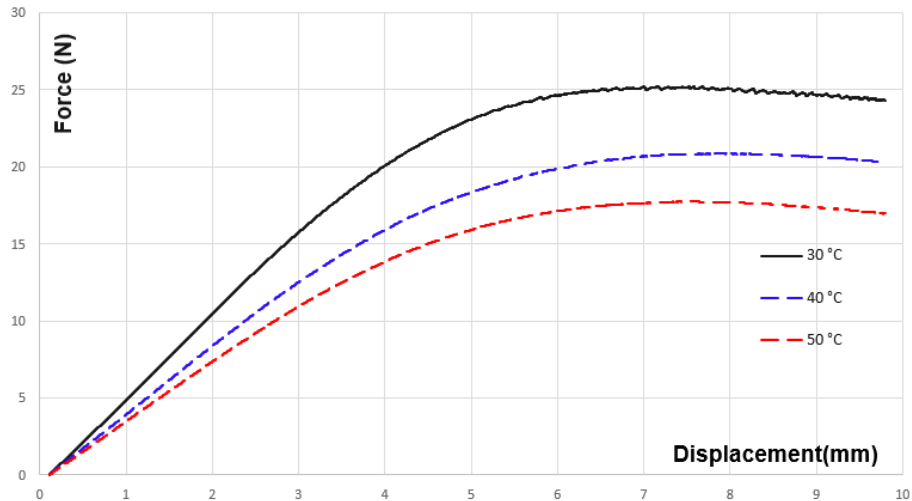


Figure 46: Force versus displacement at different temperatures of triple layered SMP composite. Furthermore, from the three-point bending results based on temperatures; the average flexural modulus is found to be  $2640 \pm 47$  MPa at  $30^\circ\text{C}$ , followed by  $2360 \pm 60$  MPa and  $1950 \pm 58$  MPa, at  $40^\circ\text{C}$  and  $50^\circ\text{C}$  respectively. Another interesting characteristic which can also be interpreted out of the results is the flexural strength. The average flexural strength is found to be  $58.4 \pm 2.9$  MPa at  $30^\circ\text{C}$ , followed by  $48.4 \pm 3.6$  MPa and  $42.6 \pm 0.6$  MPa, at  $40^\circ\text{C}$  and  $50^\circ\text{C}$  respectively. Both flexural modulus and strength of the SMP composite samples decline obviously with the increase of temperature. Such reductions are expected, since at low temperature the bonding between matrix and reinforcement is high, while at high temperatures the matrix softens and the bonding strength decreases, with a resulting in an overall reduction of the composite mechanical properties.

#### 4.2.2 SEM analysis of SMPC after flexural modulus

Failure mode in flexural is analyzed by Scanning electron microscope (SEM) at different temperatures  $25^\circ\text{C}$ ,  $40^\circ\text{C}$  and  $50^\circ\text{C}$  (Fig. 47). At both  $25^\circ\text{C}$  and  $40^\circ\text{C}$  temperature the epoxy-polyimide composite laminates have shown the flexural failure of the matrix. As can be seen from SEM results that at ambient temperature ( $25^\circ\text{C}$ ) Figure 47 (a) more cracks appear on the sample's surface while less observed at  $40^\circ\text{C}$  Figure 47 (b). In fact, at  $50^\circ\text{C}$  Figure 47 (c) cracks are not observed; this can be explained by the fact that from  $50^\circ\text{C}$  the specimen becomes soft so that the specimen does not resist more against the stress applied during 3-point bending test, hence, no fracture produced in the composite beam.



Here also, the increased temperature played an obvious role in order to improve the failure-mode of the composite specimens. Moreover, temperature works as a healing agent. In addition, at ambient temperatures (25°C) and at 40°C, when the crack propagates through the composite structure, crack-tip do not break the strong 3D-reinforcement fabric structure. The strong 3D-reinforcement structure possibly resists the crack propagation as well as increase the interfacial bonding between matrix and reinforcement.

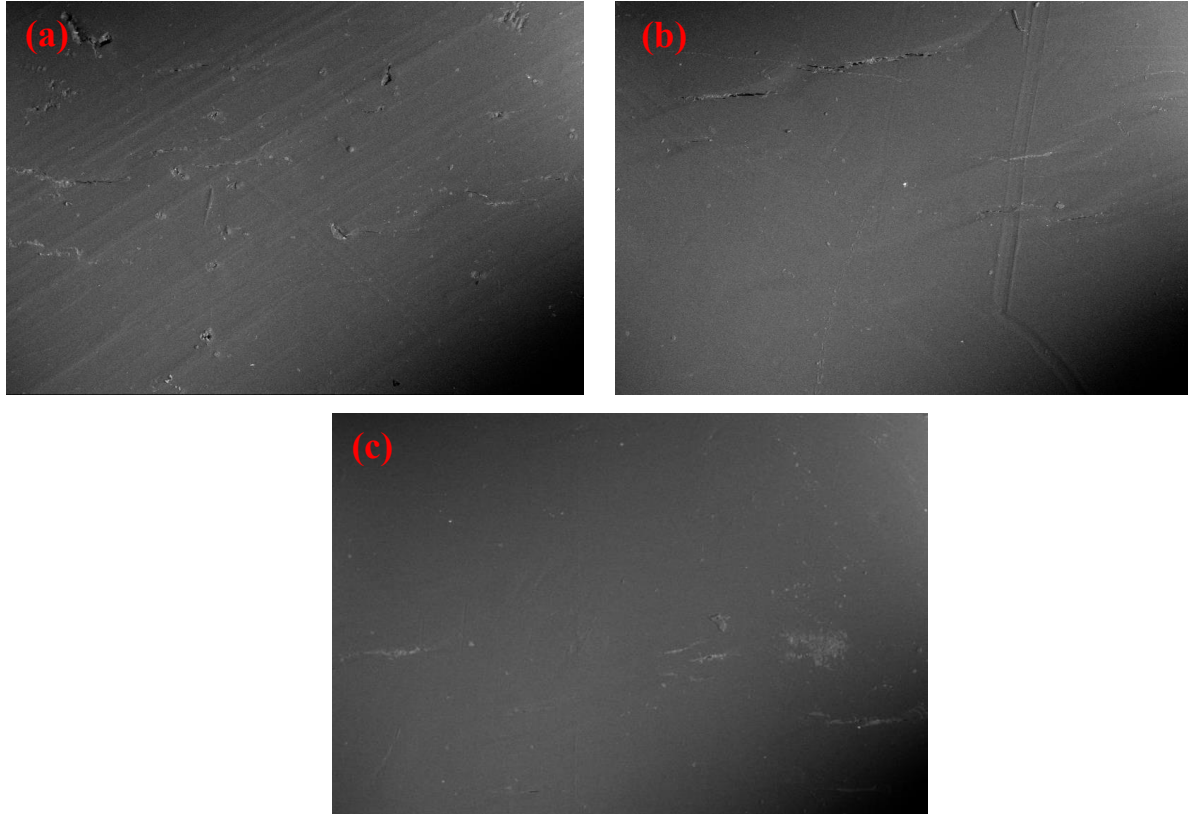


Figure 47: SEM image after 3 Point bending experiments at different temperatures: (a) 25°C, (b) 40°C and (c) 50°C

### 4.3 Interlaminar shear strength (ILSS) characterization of SMPC

#### 4.3.1 ILSS at different temperature

The ILSS is determined by performing a three-point-bending test on a short-beam specimen. Short beam shear (SBS) test is performed on a minimum of three samples to obtain their ILSS, which provides the reinforcement-matrix binding strength. The complete experimental mechanism that is used to investigate the ILSS property of 3D reinforced composite structure can be seen from Table 9.

Table 9: Description of testing method and composite sample specifications

Test type	3 point bending		
Thickness (mm)	$1.4 \pm 0.1$		
Width (mm)	$5 \times \text{thickness} = 7$		
Length (mm)	$10 \times \text{thickness} = 14$		
Test type	3 point bending		
ISO	14130		
Nb of sample tested	3		
Span sport (mm)	$5 \times \text{thickness} = 7$		
Temperature range (°C)	25	60	80
Thermal equilibrium time	10min		
Bending speed	1mm/min		

The isothermal SBS tests are carried out by heating the specimens to target temperatures (25°C, 60°C and 80°C) The load-displacement curves obtained for the sample at 25°C is a typical curve of ILLS test (Fig. 48). This curve is made of three parts, the first is nearly elastic (I) and leads to a small load drop (point A) which is classically associated with ply interface failure under shear stress (acceptable rupture for ILSS) and the related value of force is used for the computation of the ILSS stress. The second part (II) is a transition stage during which several phenomena may occur: interface rupture (acceptable rupture), plasticity (unacceptable rupture). Finally, the last stage is a stiffening stage, because the sample is in compression between the close supports.

Normally, an acceptable ILSS test should show at point A a sudden fall in force that is associated with interface failure. This is not observed for 3D composites, since the transition at the point is continuous. These composites do not show interface failure, their behavior is driven by the plasticity of the resin. As a function of temperature, this transition is less and less observable until it disappears for the 80°C curve.

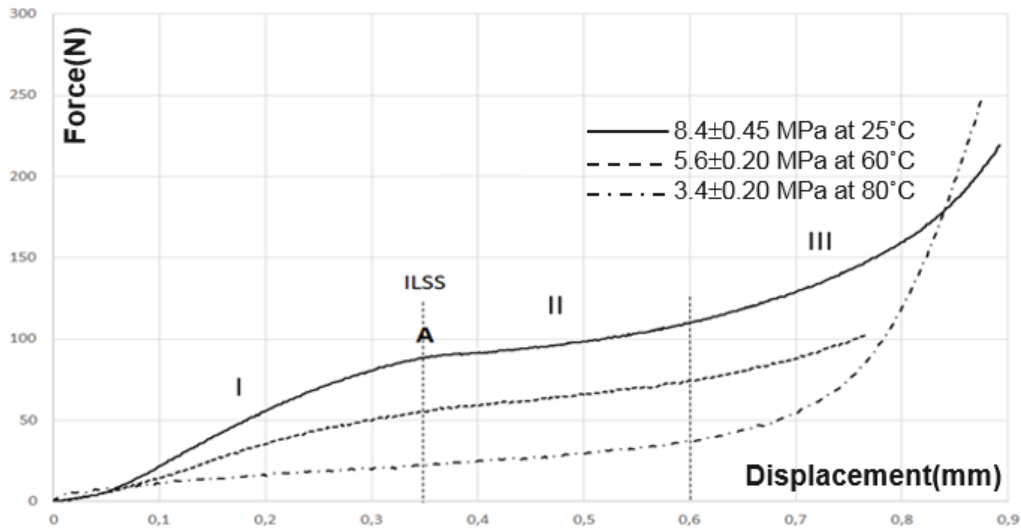


Figure 48: Typical curve of ILSS test function on temperature (25, 60 and 80°C)

From the load histories, the apparent ILSS is calculated using the previous equation (4). An average ILSS value is found from three tests at each temperature. In case of low temperature (25°C), the average ILSS is  $8.4 \pm 0.45$  MPa, followed by  $5.6 \pm 0.2$  MPa and  $3.4 \pm 0.2$  MPa, at temperatures of 60°C and 80°C respectively. Thus a significant decrease in the ILSS property is observed with increasing temperature from 25°C to 80°C.

For these tests, these ILSS values are to be understood as an ability for 3D composites to be subjected to strong curvature and thus be able to undergo the compaction phase during the education cycle. The absence of the first transition on the curve at 80°C shows that it is possible even at temperatures below  $T_g$  to shape the composite without macroscopic damage.

#### 4.3.2 ILSS fracture pattern

After short beam shear tests, the fracture appeared on the top and bottom surfaces of the specimens are examined by SEM at 15 kV accelerating voltage. Note that no visible damages are found through the cross-sections of the test specimens. The damages are induced only on the top surfaces of the specimens. Figure 49 (a), (b), and (c) illustrate the SEM images of fracture pattern observed in the top surface at different temperatures 30°C, 60°C and 80°C respectively. The main type of damage mode here is the localized damage beneath the punch. The localized damage is caused by the excessive stress concentration beneath the central punch resulting in crushing of the matrix. Essentially, a bending force is acting on the surface under the central loading zone. Thus, this zone is subjected to compression and the samples may undergo localized buckling leading to matrix

cracking. From Figure 49, it can be seen that the failure mode is a transverse crack in the matrix. In Figure 49 (a), a big crack can be observed at low temperature 30°C. Notably, matrix breakage is obvious, due to the severe localized compression. However, at high temperatures 60°C and 80°C, the cracks found in specimens are small as demonstrated in Figure 49 (b) and (c), respectively. The decrement in failure mode is in fact noteworthy at high temperature of 80°C (Fig. 49 (c)). Increased temperature played an obvious role in reducing the induced damage in the test specimens. Additionally, when the crack propagates through the specimen, the fracture resistance of the composite is noticeable due to the triple layered reinforcement. The failure occurs only in the matrix and not in the reinforcement-matrix interface. The strong 3D-reinforcement structure possibly resists the crack propagation as well as increases the interfacial bonding between matrix and reinforcements.

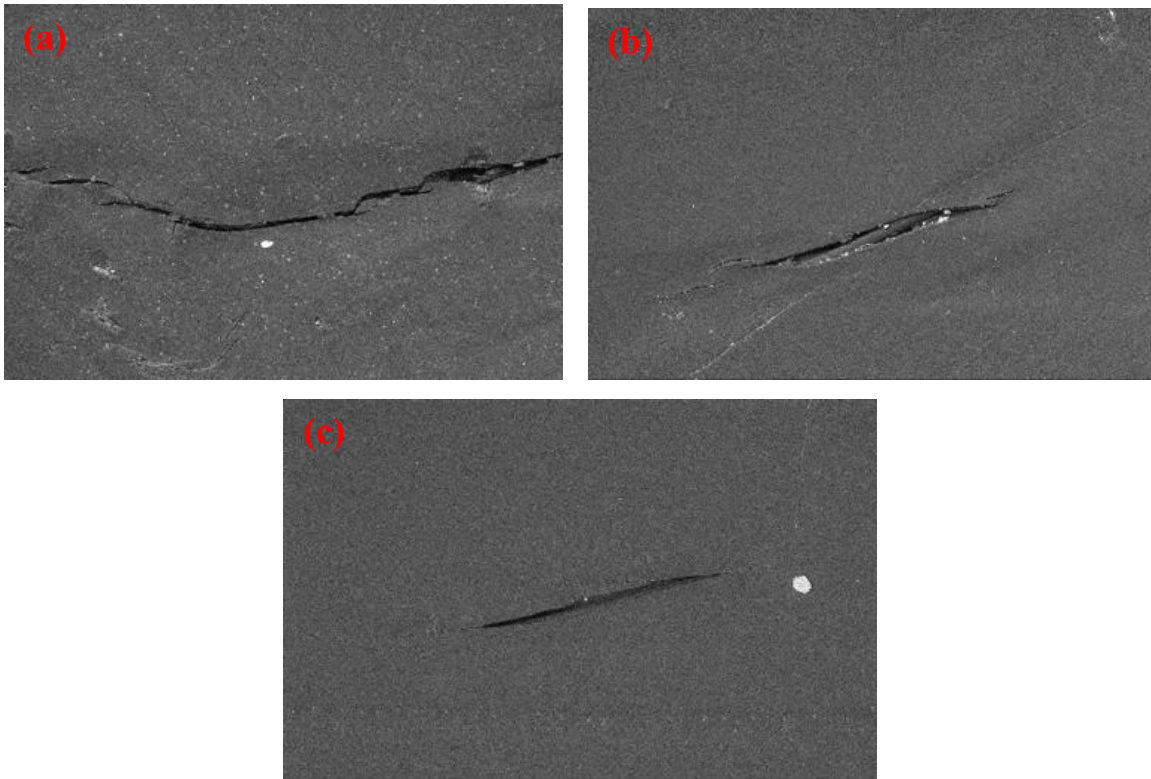


Figure 49: SEM micrographs of layered composite specimens after short-beam three-point bending tests at different temperatures (a) 30°C (b) 60°C (c) 80°C

This ILSS test is used to show the ability for this 3D composite to locally admit large radius of curvature. It is observed that the use of a multilayer reinforcement makes it possible to have no inter-laminar rupture. The composite thus keeps its cohesion in thickness and the ruptures

observed are actually the matrix ruptures on the sample surface and diminish when the temperature increases.

#### **4.4 Different shape memory and shape recovery capabilities of SMPC**

##### **4.4.1 Shapes memory capability of SMPC**

Shape memory recovery is the discriminating quality of SMP composites which distinguishes them from other conventional polymers. Hence, it is of utmost importance to characterize the fabricated SMP composites for their shape recovery characteristics. There are two operational modes of recoveries that are usually performed to study the recovery of the induced shape memory property: constrained and unconstrained recovery conditions. Constrained recovery involves the measurement of the stress produced in the SMP when recovery is activated while the temporary deformation is constrained. This style of recovery would be useful when considering applications wherein the SMPs are used as actuators. Unconstrained free recovery is a mode of recovery in which the external stresses are removed and the recovery of the SMP is allowed to take place under zero constraint. Deployable applications are considered to be examples of free recovery conditions. In this work, experiments in unconstrained free condition have been carried out to fully characterize the shape-memory response of the developed triple layer SMP composites.

For this purpose, the original flat shape of the SMP composite is obtained when the material is initially prepared through molding. We characterize the shape memory properties of the composite specimens by an unusual method, so-called the fold-deploy shape memory test for the purpose of application on space deployable structures. The complete experimental specifications that are used to investigate the shape memory and recovery behavior of 3D reinforced composite structure can be seen from Table 10. Towards that end, the deformed temporary shape is achieved in different configurations, including U-shaped, S-shaped, M-shaped, loop, twisted and spiral shapes from its original form. Take bending or U-shaped as an example: first, a SMP composite specimen is bent manually at an elevated temperature. Then, the sample is placed inside a bath with cold water for a few seconds to ensure that the sample temperature decreased below the network relaxation temperature and therefore fix its temporary bending shape. The constrained bending force is then removed to obtain the temporary shape, which is self- maintained unless the temperature may get

elevated again. Lastly, the specimen is heated to its deformation temperature allowing it to recover its original shape.

Table 10: Illustration of testing mechanism and specifications of composite specimen

Test type	Manual deformation
Specimen type	3D reinforced composite
Thickness (mm)	$1.4 \pm 0.1$
width (mm)	14
Length (mm)	170
No of sample tested	3
Thermal equilibrium time (min)	20
Deformation temperature ( $^{\circ}\text{C}$ )	$T_d = T_g + 5^{\circ}\text{C} \pm 1$ ( $91^{\circ}\text{C}$ )
Shape fixity temperature ( $^{\circ}\text{C}$ )	Ambient temperature ( $T_a$ )

Shape memory programming and recovery cycle experiments are accomplished using temperature-controlled chamber Instron model 3119-616. The temperature of the specimens is allowed to equilibrate with the chamber for 15 min prior to starting the shape memory programming. The specimens are deformed into different shapes varying from simple to complex. Simple shapes of U-shaped, S-shaped and loop (Fig. 51) are initially achieved in order to demonstrate the shape memory behavior of the composite. After successfully attaining the shape memory effect, the specimens are carried out against the more deformed patterns of M-shaped, twisted and spiral (Fig. 52) in order to make folded configurations that could be used for space applications. All specimens are successfully deformed into temporary shape no fracture observed during programming cycle.



Figure 50: original shape of all composite specimens



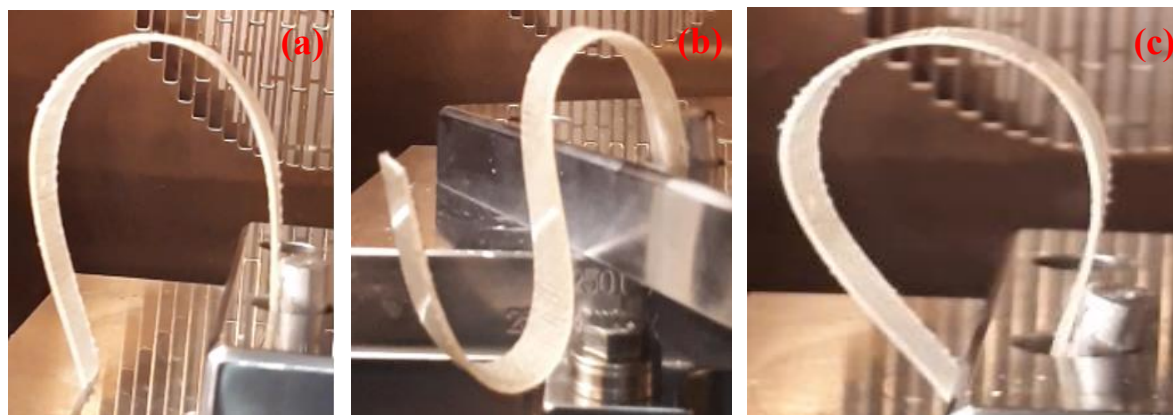


Figure 51: Visual demonstration of temporary programmed simple shapes (a) U-shape, (b) S-shape and (c) loop-shape

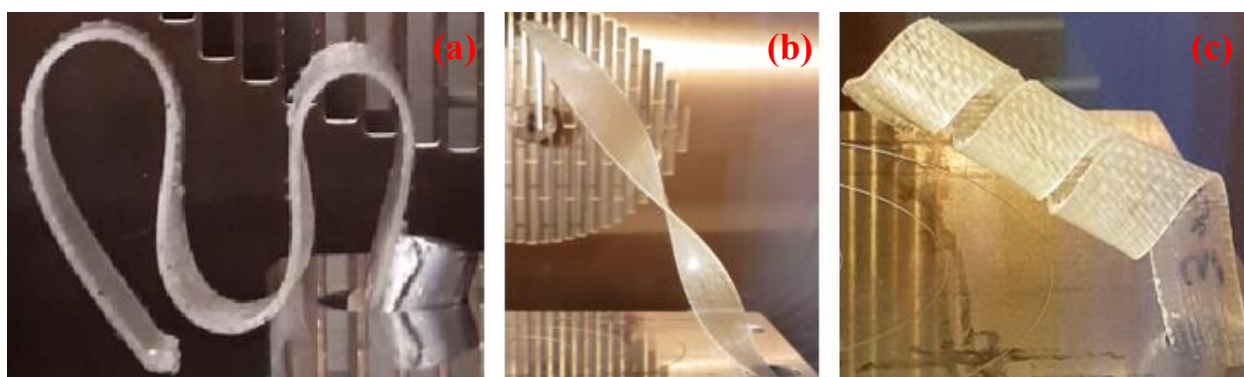


Figure 52: Visual demonstration of temporary programmed complex shapes (a)-M-shape (b)-twisted-shape and (c)-spiral-shape

#### 4.4.2 Shapes recovery capability of SMPC

These temporary shapes are obtained upon cooling down the specimens to the ambient temperature and unloading. In unconstrained condition, the recovery-process of the specimens is analyzed by heating them to a recovery temperature, to allow the free recovery. Recovery tests are performed in the preheated environmental chamber set at a temperature of 100°C by holding one end of the specimens with a fixed length of 5 mm. Later on, the recoverability is measured as shown in Figure 53 and 54. A video camera is used to record the shape recovery process. According to the recorded images, the shape recovery time is witnessed for all deformed shapes. Details of the recovery stage for the U-shaped, S-shaped and loop are reported in Figure 53. Figure 53 (a) illustrates the shape recovery time of the U-shaped specimen at the shape recovery temperature of 100°C. In this case, a very good shape recovery is achieved and a time of 25s was necessary for a full recovery. For

the S-shaped, the specimen readily recovers to nearly its original shape in 26s (Fig. 53 (b)). In the case of the loop configuration, the time variation of its shape recovery is exposed in Figure 53 (c); the shape is recovered to nearly its original shape during the recovery time of 29s.

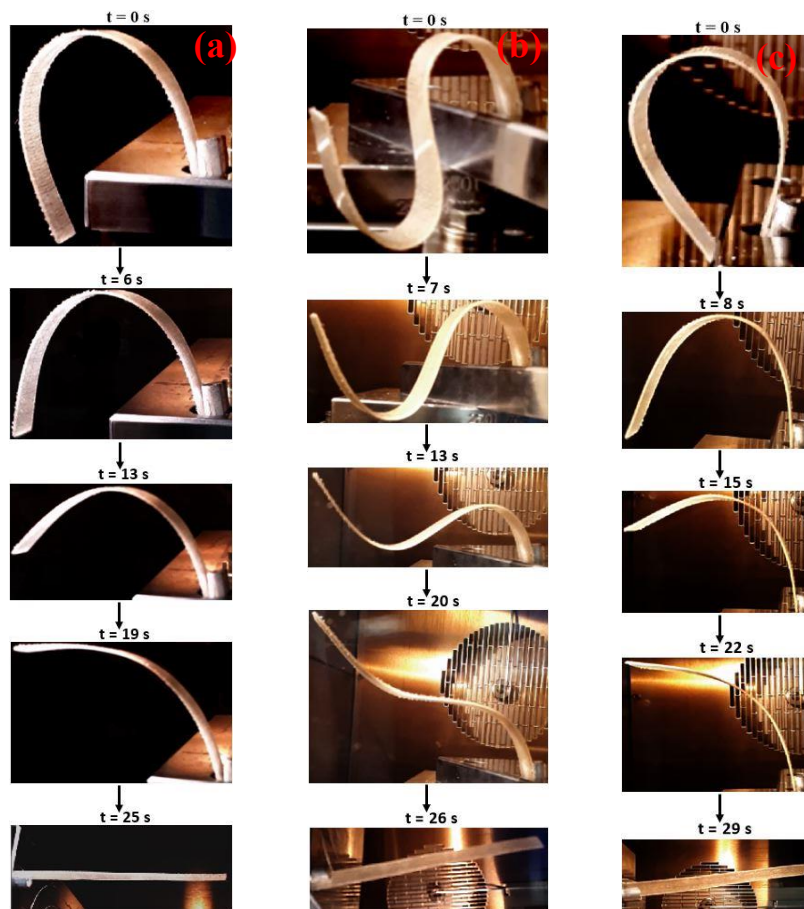


Figure 53: Series of photographs showing shape recovery as a function of time. (a) U-shaped, (b) S-shaped and (c) loop shape

We turn now to investigate the effect of shape complexity on the recoverability of the developed composite. The designs of large deformed shapes of which three configurations are demonstrated, the M- folded, twisted and spiral configurations, are displayed in Figure 54. Figure 54 (a) shows the characteristics during the recovery process of the M-folded pattern. It takes about 31s to recover the original shape. The twisted and spiral patterns attained the deformations along their longitudinal axes, unlike the other conventional shapes whose deformations are along their lengths. Their deploying sequences are shown respectively in Figure 54 (b) and (c). After 34s and 49s the recovery is practically completed for the twisted and spiral configuration, respectively.



For the twisted shape, the sample is rotated around the longitudinal axis thereby leading to a torsion deformation of the specimen. Although torsion is presently applied as an alternative deformation mode that is different from the commonly used method such as bending or compression, the testing protocol used here follows a similar thermomechanical cycle as that used in traditional shape memory effect testing.

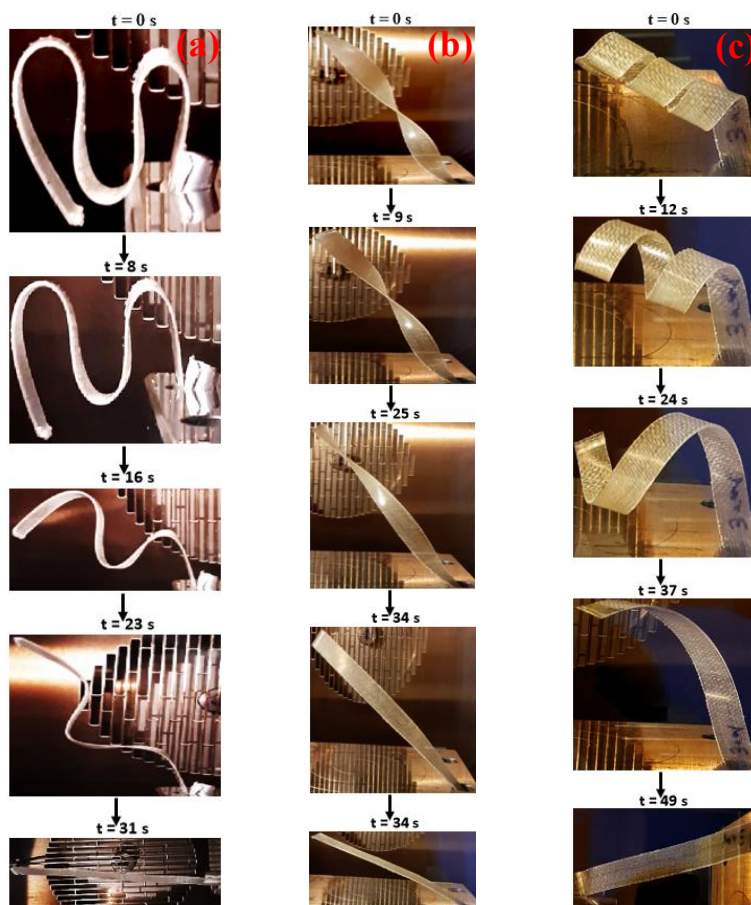


Figure 54: Series of photographs showing shape recovery as a function of time. (a) M-shaped, (b) twisted and (c) spiral configuration

In general, satisfied shape memory performances in terms of the shape recovery capability and shape recovery time are observed through the shape memory recovery tests. All composite samples recover to nearly their original permanent shapes within less than 1 min. The shape recovery time increases for complex shapes of the specimens with a little longer time is used to finish deformation recovery of the spiral specimen. The recovery rate is faster when the applied deformation is lower and the recovery time is going shorter with simpler pattern.

#### 4.4.3 Effect of shape on recovery time

In this part, the effect of shapes on recovery time is analyzed by using ANOVA technique. In order to obtain the recovery time of different shapes, eighteen composite beams are used in which three test, one on each composite beam is conducted. In ANOVA, P-value less than 0.05 describe the confidence level of significance, so here in Table 11 the value of p is found  $0.000 < 0.05$  which shows that the effect of shapes on recovery time is significant. Both ANOVA Table 11 and Figure 55 represents that composite shape has significant effect on recovery time. The composite is deformed into 6 different shapes (u-shape, loop shape, s-shape, spiral and m-shape) and it is evident from the Figure 55 that the spiral shape followed by twisted shape exhibited higher recovery time as compared with all other shapes.

Table 11: ANOVA for effect of composite shapes on recovery time

Source	DF	Adjusted SS	Adj MS	F-Value	P-Value
Sample (among groups)	6	1201.50	200.250	209.79	0.000
Error (with in groups)	11	10.50	0.955		
Total	17	1212.00			

Source: Source of variation; DF: Degree of freedom; Adj SS: Adjusted sum of squares; Adj MS: Adjusted mean squares; F-value =  $\frac{\text{Mean of sum of squares among groups}}{\text{Mean of sum of squares with in groups}}$ ; confidence level or significance level = P-value =  $1 - 0.95 = 0.05$ .

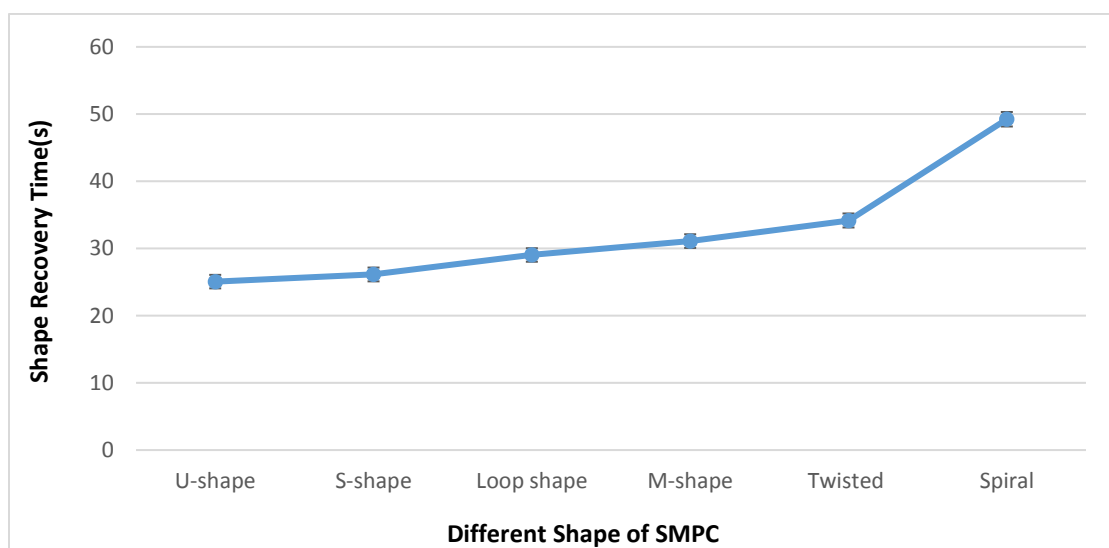


Figure 55: Illustrate the different composite shapes effect on recovery time

#### 4.4.4 Surface characterization after shape recovery cycle

Scanning electron microscopy (SEM) analysis has provided the information about surface topography of this composite system. As described earlier, all samples recover their original shape completely at elevated temperature. After shape recovery analysis, the top surface appearance of all composite specimens are investigated by using SEM. SEM image illustrate the top-surface appearance of all specimens shown in Figure 56, which are deformed into simple shapes like U-Shape, S-shape and loop shape. The surface area of all specimens has found clean. The surface area of all samples are exposed to compression due to external force. But here, temperature played an obvious role in order to prevent the surface of specimens from fracture. Figure 57 illustrate the SEM analysis of complex shapes M-shape, twisted-shape and spiral-shape. Here also, the fracture are not observed on the surface of all specimens. However, the surface area of all complex shapes has undergo the large compression as compared to the simple shapes. In addition, during both situations temperature played an obvious role of a self-healing agent.

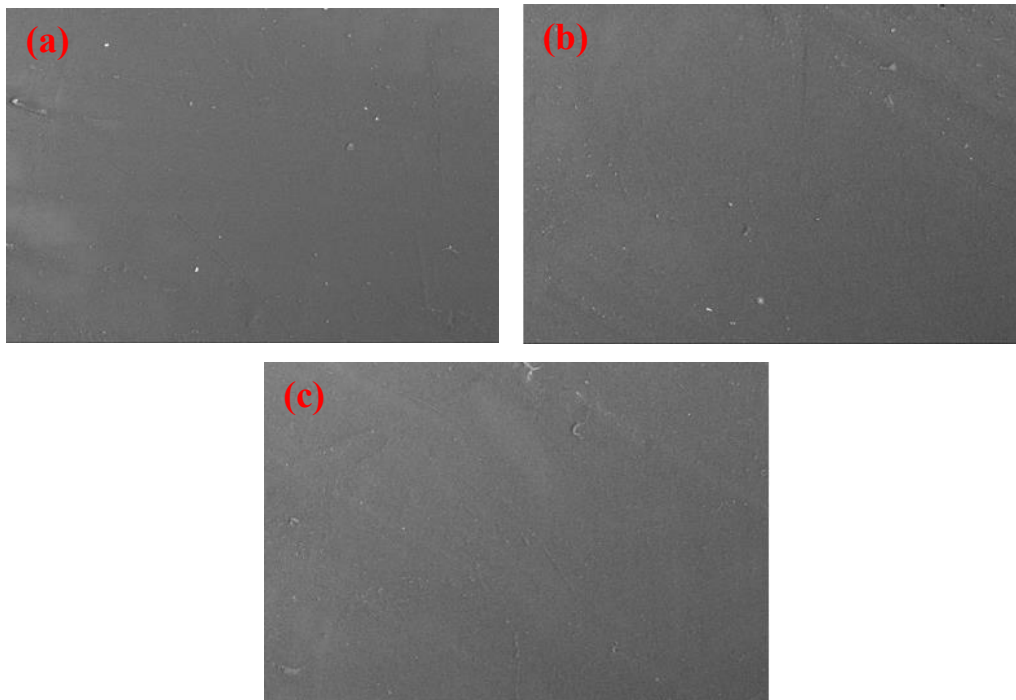


Figure 56: Illustrates the SEM image of the top surface appearance of (a) U-Shape, (b) S-shape and (c) loop shape

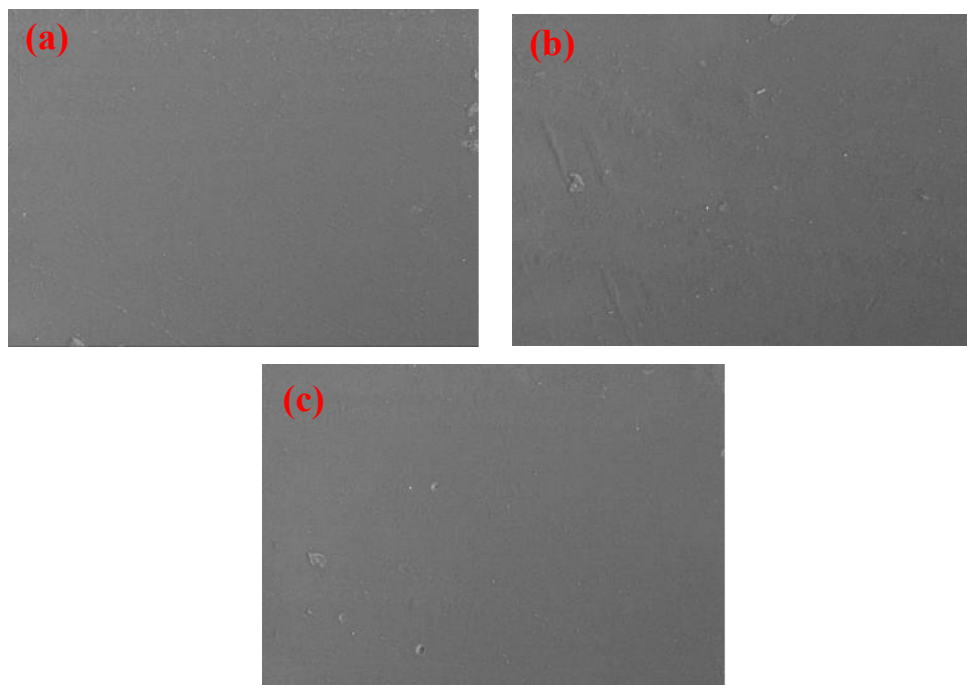


Figure 57: Illustrates the SEM image of the top surface appearance of (a) M-shape, (b) twisted-shape and (c) spiral-shape

#### 4.5 Quantitative measurements of shape fixity and shape recovery

In this part the shape fixity and shape recovery capability of a composite sample (matrix + 3-layer reinforcement) is quantitatively measured by using advanced optical 3D non-contact scanner. The specifications of specimen and experimental protocol that are used to investigate the shape fixity and recovery behavior of 3D reinforced composite structure can be seen from Table 12.

Table 12: Illustration of composite sample and experimental specifications

Test type	Manual deformation
No of sample tested	3
Thermal equilibrium time (min)	20
Deformation temperature (°C)	$T_d = T_g + 5^\circ\text{C} \pm 1$ (91°C)
Shape fixity temperature (°C)	Ambient temperature ( $T_a$ )
Recovery temperature (°C)	$T_r$
No of sample tested	3
Thickness (mm)	1.4±0.1
width (mm)	42
Length (mm)	170

Initially, the composite sample is put inside the furnace. After this, it is made deformed into a U shape at an increased temperature and cooled in chilled water. Then temporary shape is made fixed with the help of scotch. Later on, this attained sample composite is placed on the desk for scanning purpose. This temporary U-shaped sample composite is scanned for various positions once before the removal of the scotch and one after the removal. The experimental mechanism is demonstrated in Figure 58. Following this a 3D digital models in STL format are produced through subsequent polygonization and via obtained clouds of points.

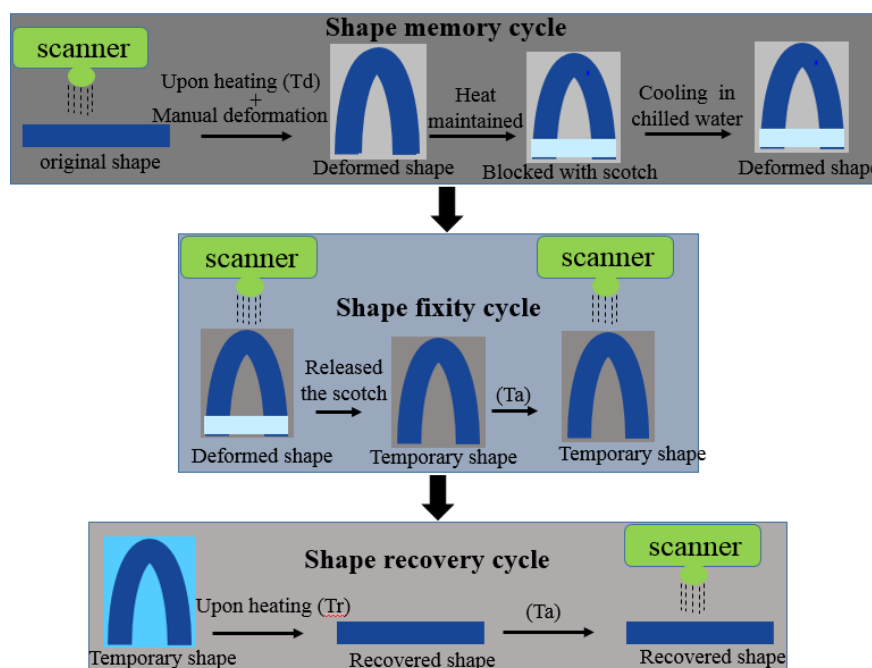


Figure 58: Complete shape fixity and recovery mechanism

The 3D shapes of the sample during the course of the four states that are: original, deformed, temporary and recovered shapes as obtained from the scanned data are presented in Figure 59. In the next stage, the recovery efficiency is measured through a comparison between permanent shape and recovered shape. Doing this, the closeness of the dimensions are evaluated comparison wise as for recovered sample and the one at the start of the shape memory cycle. The final deformation or geometric deviations can be visualized by color deviation map as displayed in Figure 60.

It is evident from the above figure that the alterations of the recovered shape to the original shape are quite mild. Numerically speaking, these are ranging from  $-1.25$  to  $+0.30$  mm. It depicts

the quantitative representation of the one important characteristic of present SMP composite and that is to attain full recovery upon reheating.

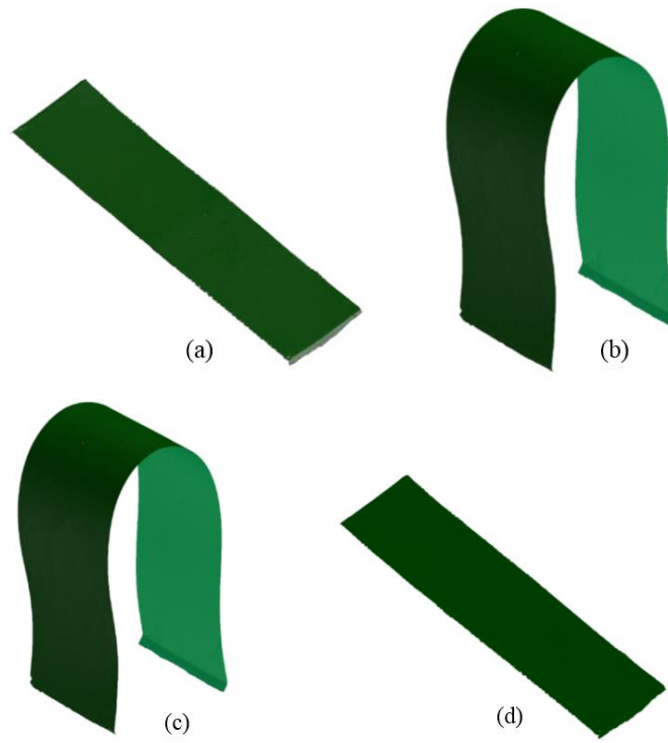


Figure 59: 3D models of the SMP composite during the shape memory cycle test, which are obtained by scanning their shapes. (a) Original shape, (b) deformed shape, (c) temporary shape and (d) recovered shape

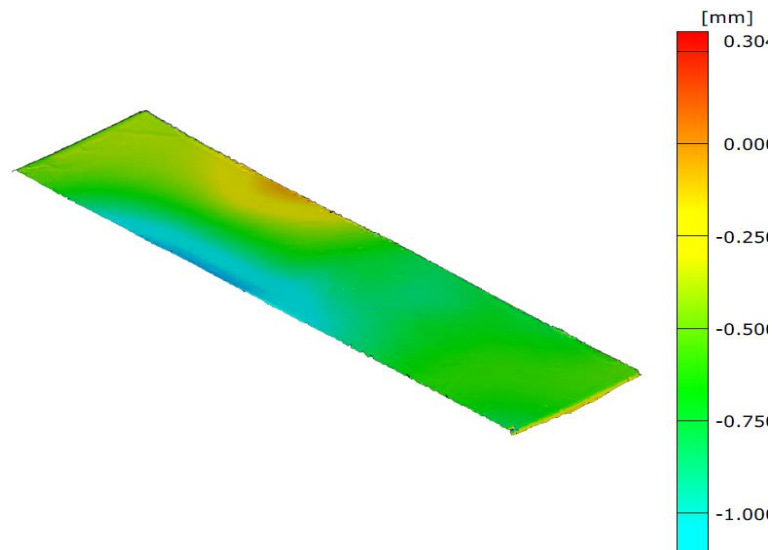


Figure 60: Color deviation map computed as the perpendicular distance of each polygon point on the recovered shape to the original shape units in mm

Like wise, in order to measure the shape fixity attribute of this SMP composite, a comparative evaluation may be performed between the deformed shape model (after applying deformation at elevated temperature) and temporary shape model (after cooling and unloading). Following this, a Color map of deviations is thus generated as an output representing the dimensional and shape deviations between the two shape states. Figure 61 (a) presents the comparative representation of the green coloured fixed shape and the blue coloured deformed shape of the sample under observation .The full field deviations between the two data sets are next computed and displayed in different colors in Figure 61 (b) to appraise the material's ability to hold the shape after it has been deformed. This figure clearly depicts the range of deviated values that is between 0 to -2.50 mm. The deviation value as equal to zero in the upper region depicts that the temporary shape remarkably maintained its dimensions. On the other hand, going down the length of lower region, the small deviation may be observed as equal to 2.50 mm. This is actually due to the cylindrical geometry of sample at the bottom. This is, thus explaining that the temporary shape may not completely hold stable after removal of the force under low temperature. The difference between the temporary and deformed shape can be attributed to the elastic deformation mechanism, which is evident in areas prone to greatest deformations. In a nutshell, these results as attained under the programmed thermomechanical cycle illustrates that the present multilayer SMP composite exhibits high shape fixity during cooling and unloading, and is able to achieve almost full recovery upon reheating.

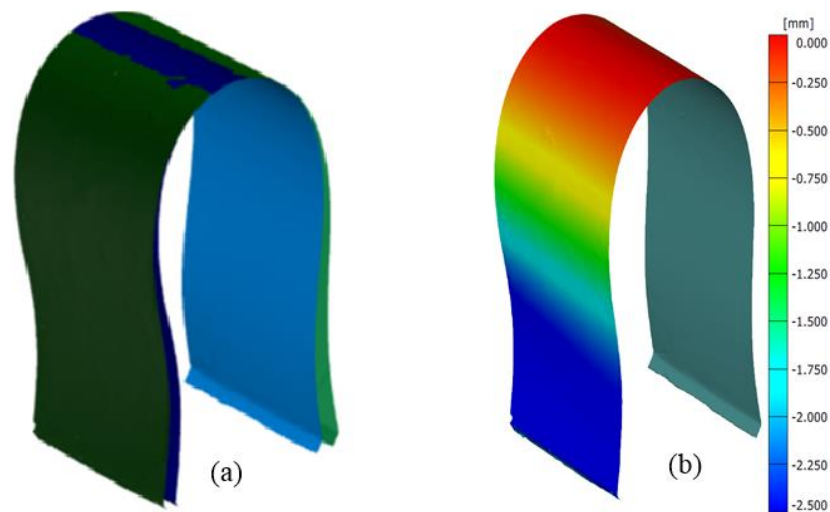


Figure 61: (a) 3D scanned model of SMP composite demonstrates the difference between the temporary (green) and deformed (blue) shapes. (b) Color deviation map visualizes the geometric deviations between the two shapes (units in mm)

Uptill now, the thermomechanical bending characteristics of the fabricated multilayer SMP composite sample is evaluated. Moreover, with the help of thermomechanical cycle test, some further SMP characteristics are investigated. Along with this, quantitative characterization of 3D deployment behavior is performed using 3D scanning technique. It is hereby represented that the developed multilayer SMP composite can be willingly reshaped by deforming it at an elevated temperature and then cooling in the deformed state. Upon reheating, the composite almost fully returns towards the original cured shape without delaminating or degrading the material.

## 4.6 Shape memory and shape recovery ability of hybrid carbon SMPC

### 4.6.1 Thermo-mechanical cycles

In this section, the morphing behavior of sample (matrix + 3-layer reinforcement + active layer) is characterized by using 3-point bending test. The specifications of specimen and experimental protocol that are used to investigate the shape fixity and recovery behavior of structure can be seen from Table 13.

Table 13: Illustration of sample (composite + active layer) and experimental specifications

Test type	3 point bending
No of sample tested	3
Deformation temperature (°C)	$T_d = T_g + 5^\circ\text{C} \pm 1$ (91°C)
Shape fixity temperature (°C)	Ambient temperature ( $T_a$ )
Recovery temperature (°C)	$T_r$
Load cell	500N
Loading speed	5mm/min
Thickness (mm)	$1.8 \pm 0.1$
width (mm)	32
Length (mm)	170

The composite sample is placed on 2-supporting spans, which are 90 mm apart. A load cell of 500N (accuracy of 0.01N) is employed to measure the precise forces. For the temperature measurement, thermocouples of type K are used. As all the composite plates used in this work have an active layer of eight carbon yarns, so, for each test, one thermocouple is put on the carbon yarn whereas the second thermocouple is put in between the two carbon yarns. Both the thermocouples are put on the upper side of the composite plate. The temperature for the



thermocouple on the carbon yarn is always greater than the second one. These thermocouples are connected to DAQ system which works with the LabVIEW software. Hence, different temperatures are visible in LabVIEW software that can be exported to Excel sheets (see Figure 62).

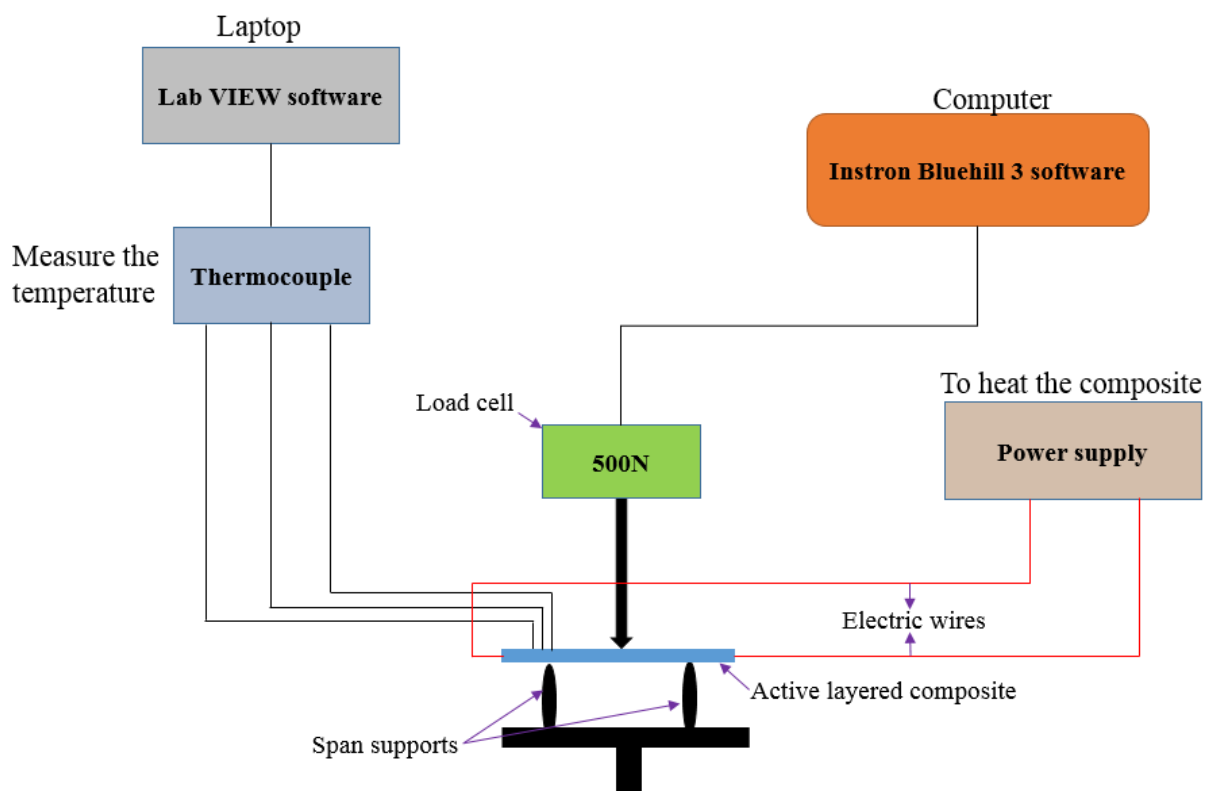


Figure 62: Illustration of experimental assembly used to characterize the morphing behavior of active layer

Complete thermos mechanical cycle can be seen from the Figure 63. Firstly, a preload of 0.1 N is applied in order to make sure the contact between load cell and sample. In the meantime, specimen is heated up to deformation temperature  $T_d$  ( $T_d = T_g + 5^\circ\text{C}$  ( $91^\circ\text{C}$ )) for 950s in order to obtain the thermal stabilization that is measured by thermocouple placed on upper surface. This corresponding position point B of the specimen is taken as a reference position for measurements of all displacement. Then, a load with speed of 5mm/min is applied to obtain the prescribed displacement of 50mm. The said displacement is maintained and the composite specimen is allowed to cool down for 700s in order to chase the ambient temperature with an intent to maintain the initial fixity. After cooling of deformed composite structure, no delamination is seen on upper

surface of composite structure. Furthermore, shape recovery capability is investigated of largely deformed composite structure at same heating condition (recovery temperature  $T_r = T_d$ ).

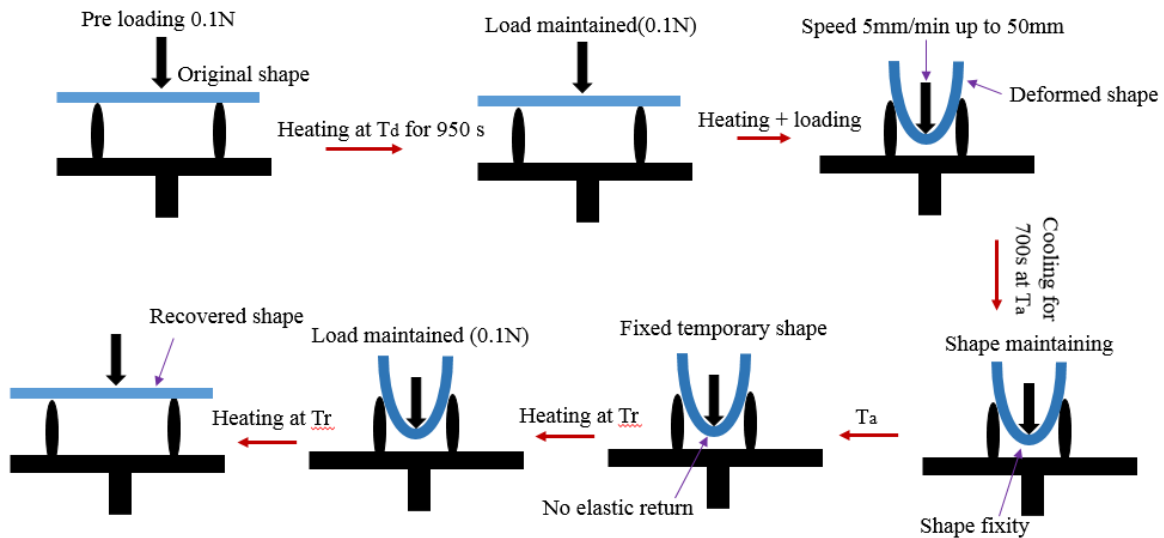


Figure 63: Illustration of complete mechanism of thermomechanical cycle of active layer

The thermo-mechanical cycle contains two steps, the first step is the shape programming cycle and the second is the shape recovery cycle. The temporary shape of the sample is obtained by the shape programming cycle, whereas, the obtained temporary shape is recovered to its original permanent shape in the shape recovery cycle. The complete thermomechanical cycle can be seen from Figure 64. Firstly, a preload of 0.1 N (A) is applied in order to make sure the contact between the load cell and the sample. In the meantime, the specimen is heated up to the deformation temperature  $T_d$  ( $T_d = T_g + 5^\circ\text{C}$ ) for 950 s in order to obtain the thermal stabilization that is measured by the thermocouple placed on the upper surface. This corresponding position point B of the specimen is taken as a reference position for measurements of all displacements. Then, a load with a speed of 5 mm/min is applied to obtain the prescribed displacement of 50 mm (B to C). The said displacement is maintained, and the composite specimen is allowed to cool down for 700 s (C to D) in order to chase the ambient temperature with an intent to maintain the initial fixity. At this point (D), no delamination is seen in the composite structure. Furthermore, the shape recovery capability is investigated of a largely deformed composite structure at the same heating condition (recovery temperature  $T_r = T_d$ ). At point A to C, sliding of the specimen is observed, which is recorded by the sensor.

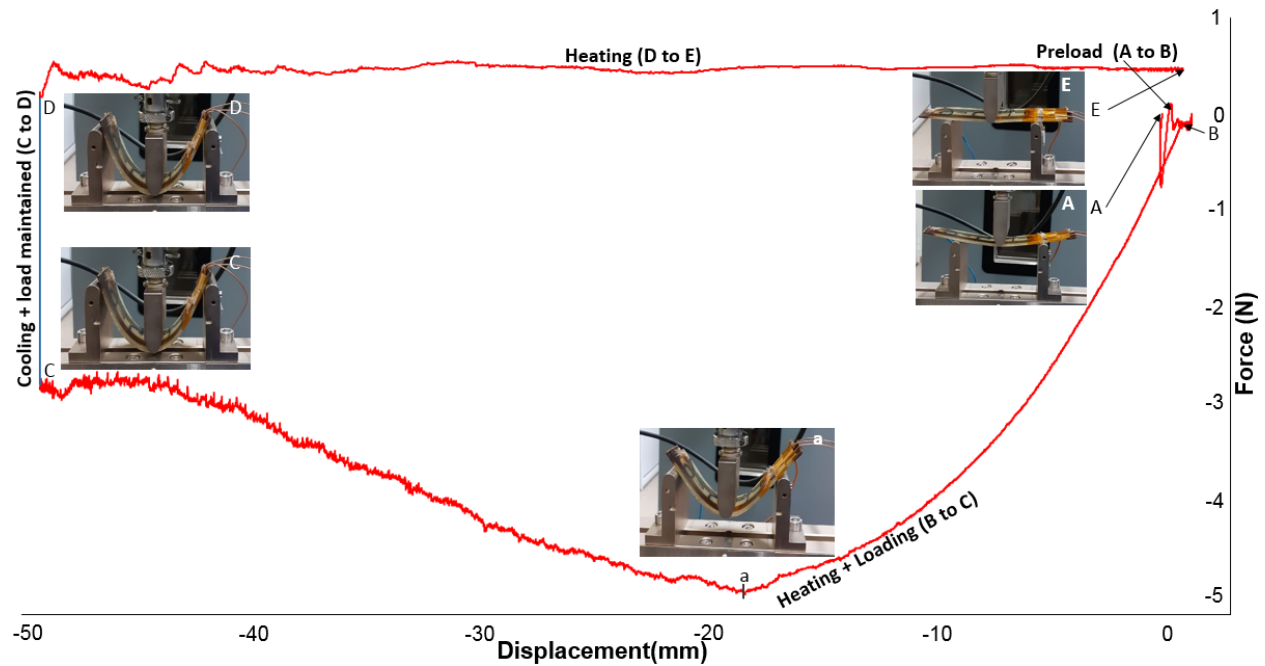


Figure 64: Complete recording of thermo-mechanical cycle of shape programming and shape recovery by 500N load sensor

#### 4.6.2 Different heating, loading and cooling cycles

Upon heating from A to B (Fig. 65), the average free-displacement 0.82mm is obtained, corresponding to 91°C. The displacement is due to the unsymmetrical gradient property, which is inherent during manufacturing process and uncontrollable [27]. During programming cycle, upon heating + loading (B to C), deformation recorded very smoothly until point a, but after, during large deformation from point a to C the value of charge is found deflative due to sliding of sample on two span sports. Because, the specimen is placed freely on two sports and the limitation of experiment is to hold the sample on these sports. In addition, the load cell is very sensitive which recorded all the sensitive motion of specimen. Increment in temperature is also observed during large deformation of specimen (a to C) due to heat transfer. However, the prescribed large displacement (50mm-1.7mm) is obtained without any delamination or cracks. Moreover, chased temporary shape is fixed upon cooling and 100% shape fixity (D) is achieved because no elastic return is recorded by sensor. Furthermore, to study the shape-recovery behavior, deformed specimen is subjected to apply the  $T_r$  in order to restore its original shape. Complete shape recovery cycle is recorded by sensor from point D to E. Sample recovered almost its original shape completely (E), which is very impressive shape recovery behavior.

In this work, it can be conclude that the 3D-reinforced fabricated composite structure exhibited superior thermo-responsive shape memory and shape recovery behavior. Upon heating (above  $T_g$ ) and loading at same time, matrix molecular chains could be stretched and programmed with a new temporary shape. When the specimen is cooled below its  $T_g$ , the deformed shape at high temperature could be fixed because of the frozen chain-segments (known as shape fixity). For shape recovery, without any external force, the stored strain-energy is released upon heating which reactivate the chain-mobility and thus determines shape recovery of composite [119].

During cooling cycle, (as the illustrated in Figure 65) the reaction of material is found very different at point k ( $90^\circ\text{C}$ ) to k' ( $60^\circ\text{C}$ ). From point k to g, the curing rate found higher as compare to values at k' to D and the values of charge is observed to be decreasing constantly. But suddenly, the value of charge is found to be increasing from point g to k' that indicates the  $T_g$  range of polymer. Because near  $T_g$  curing of polymer occurred due to the hardening of molecular chains which makes the polymer more stronger. Therefore, typically maximum toughness occurs at a testing-temperature slightly below or at the  $T_g$  of polymer's [120]. It can be concluded that the range (k to k') indicates the glass transition range of polymer.

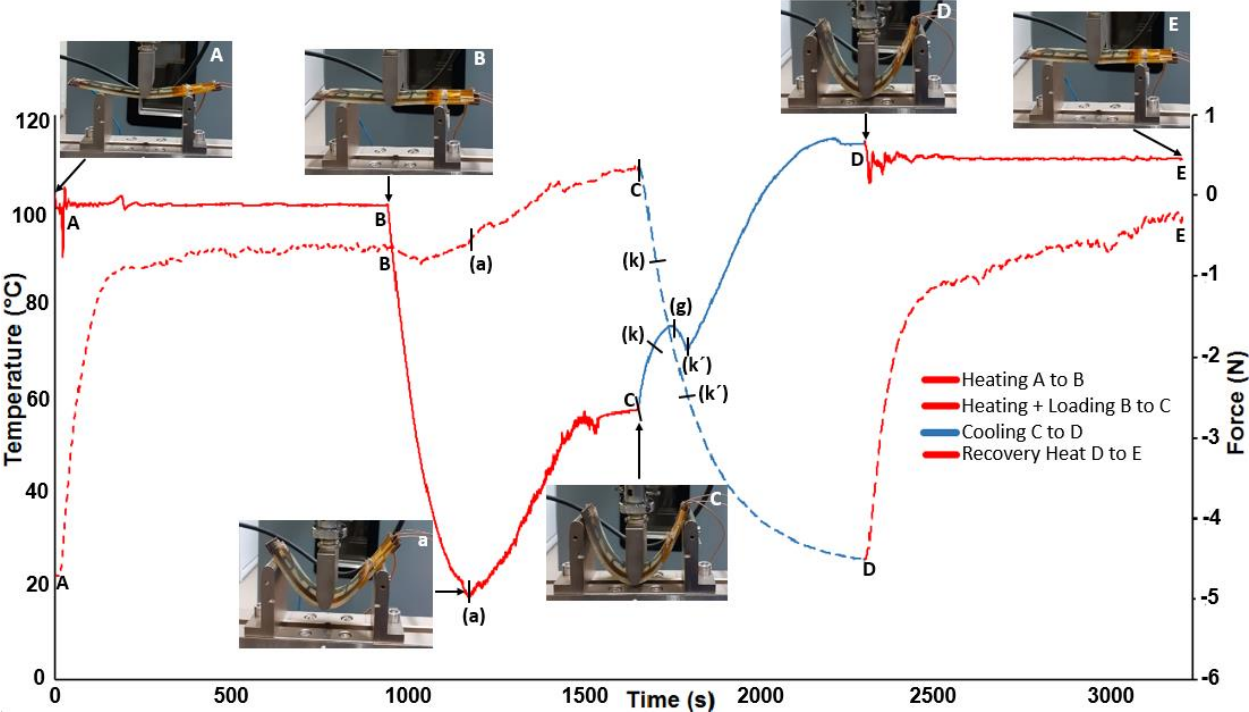


Figure 65: Complete illustration of heating and loading, during shape programming and recovery cycle

### 4.6.3 Shape recovery speed and recovery displacement

Shape recovery speed also investigated with respect to temperature, by using following equation

$$V = \frac{x_1 - x_0}{t_1 - t_0}$$

shape recovery (as illustrated in Figure 66 ), initially upon heating (from point A to B), speed is found to be higher in start because due to larger curvature lot of forces are exerted on the structure (stored strain recovery). After that (from point B to k), the observed shape recovery started to decrease and from point k to k' near polymer  $T_g$  the forces increases due to hardening of molecular chains. Furthermore, constant decrement of shape recovery can be seen from k' to C, and then very slow and stabilized shape recovery (as seen from C to D) is recorded. This is because, the specimen moves ahead from the curvature so there remain no significant forces to be exerted on the structure. Recovery is also the function of temperature so temperature helps the structure to recover its original shape completely.

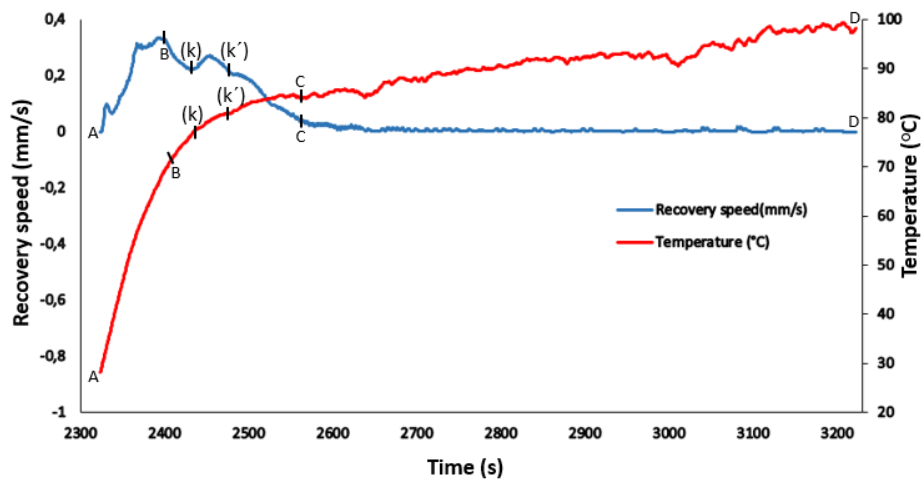


Figure 66: Illustration of shape recovery speed vs temperature

It is evident from Figure 67, that the specimen recover its 89.7% displacement very quickly from A to B. It is because, from point A to B, most of stored forces in the deformed structure are released upon temperature. In addition, from point B to C, specimen recover only 10.04% shape recovery( $S_R$ ) of total recovery ( $T_R = 99.74\%$ ) because sample did not have enough stored energy in its structure, it is due to only the temperature effect.

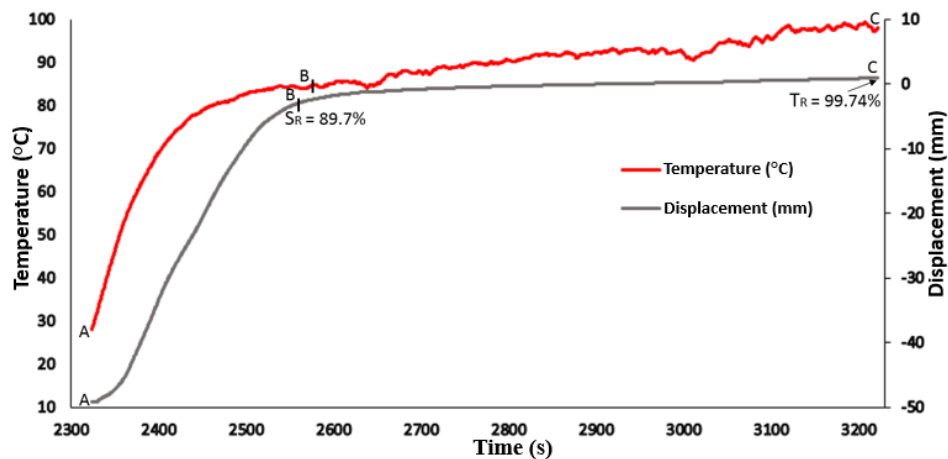


Figure 67: Illustration of shape recovery displacement vs temperature

#### 4.7 Conclusion

Flexural modulus and ILSS (which provides the reinforcement-matrix binding strength) are investigated for developed 3D multilayer woven fabric at different temperatures. Failure mode in flexural and ILSS is analyzed by SEM at different temperatures, in which damage is not observed in multilayer fabric but in matrix. Also during the investigation of shape memory and shape recovery capability of epoxy resin, high shape fixity displacement is obtained in epoxy resin at different span length, and the shape recovery capability of resin is found very impressive. Moreover, different shape memory capability of 3D reinforced SMPC is investigated in which the specimens are deformed into different shapes varying from simple(U-shaped, S-shaped and loop) to complex shapes(M-shaped, twisted and spiral). All samples are successfully deformed into temporary shape no fracture observed during programming cycle. Furthermore, shape recovery capability of SMPC is investigated in which all SMPC specimen recover to nearly their original permanent shapes within less than 1 min. After shape recovery investigation, the top surface appearance of all SMPCs are investigated by using SEM. There is no damage found on surface area of all shape memory specimens. Finally shape fixity and shape recovery capability of 3D multilayer woven fabric composite specimen is investigated by using different techniques (3-point bending test and non-contact 3D optical scanner). In said techniques, the complete shape memory/shape fixity and shape recovery cycle is recorded successfully. Conclusively, a very remarkable shape fixity and shape memory properties have been obtained from this composite system.

So far, the thermomechanical bending and interlaminar shear properties of the fabricated multilayer SMP composite are investigated. Shape memory properties are also studied under the programmed thermomechanical cycle test. 3D deployment behavior is, in addition, quantitatively characterized using 3D scanning technology. It has been shown that the developed multilayer SMP composite can be willingly reshaped by deforming it at an elevated temperature and then cooling in the deformed state. When reheating, the composite almost fully returns towards the original cured shape without delaminating or degrading the material.

---

## **General Conclusion**

---



In present research work, all what related to the physical and mechanical properties of the constituents of the SMP composite materials either for the matrix or reinforcements are deeply investigated and discussed. Based on the performed characterizations on the layered reinforcements, we find that the design of triple layer fabric of type A3 24 which has a plain weave pattern in all layers and high filling densities in warp and weft directions, possesses overall good physical and mechanical performances compared to other layered fabric types. Therefore, the fabric design(A3 24) that showed superior mechanical properties is consequently incorporated with epoxy resin to produce SMP composite samples whose shape recovery behaviors are investigated.

Furthermore, the thermomechanical properties of the fabricated SMP composite have been evaluated by using three-point bending and interlaminar shear strength. Three-point bending tests under different temperatures have been conducted, in order to demonstrate the variable flexural stiffness and strength properties of the deployable composite samples. The SMP composite samples have shown temperature dependent flexural modulus and strength, with important differences between 50°C and 30°C. Interestingly, short beam shear testing has also been performed on the developed SMP composite at different temperatures to determine their interlaminar shear strength that would be a measure of reinforcement-matrix binding strength. Upon increasing the test temperature from 30°C to 80°C, a significant loss in interlaminar shear strength property was observed.

Furthermore, this study is evident that the pure epoxy resin exhibits the impressive shape memory property at different span lengths. Actuation property of specimens of different widths is almost same at same span length. However, the shape fixity displacement increases by decreasing the span length, because, when the specimen is deformed at less span length then it provides the more curvature, which results in increase of actuation property.

The shape recovery behavior of the SMP composite has been systematically examined and analyzed under unconstrained condition. The composite was initially deformed at an elevated temperature and different temporary shapes varying from simple to complex were achieved. Then, the composite was cooled to ambient temperature to fix its temporary configuration; this comprises U-shaped, S-shaped, twisted, folded and spiral shapes. Upon reheating, the composite is returned to its original shape. The obtained results have shown that the present SMP composite exhibits

excellent shape recovery without visible damage, regardless of the level of applied deformation and desired temporary shape. Shape memory functionality (shape fixity and shape recovery) of the developed SMP composite has been further analyzed using different methods like controlled three point bending mechanism and an optical 3D scanner. This is done by measuring the 3D shape of a sample submitted to bending during the course of these steps (before deformation, after applying deformation at high temperature, after cooling and unloading and after recovery). Also by recording all steps of shape memory and recovery cycle (shape deformation, shape fixity and shape recovery) using sensitive sensor during three point bending investigation. The results showed that this composite sample had high shape retention and shape recovery capabilities.

In conclusion, the experimental results conducted in the present study are very promising, showing that the developed 3D multilayer woven SMP composite can provide some preliminary reference for SMP composites based deployable structures in future aerospace applications.

---

## **Future recommendations**

---

In future recommendation, it would be interesting to develop the mast structure for space application in order to reduce the volume of structure that ease the transportation.

it would also be interesting to investigate the shape memory capability of more rigid 3D-fabric (Carbon, Glass, Kevlar etc.). These fibers enhance the mechanical properties of shape memory polymer composite to another high level.

---

## References

---

- [1] M. S. P. Shaffer and A. H. Windle, 'Fabrication and Characterization of Carbon Nanotube/Poly(vinyl alcohol) Composites', p. 5.
- [2] B. Das, K. Eswar Prasad, U. Ramamurty, and C. N. R. Rao, 'Nano-indentation studies on polymer matrix composites reinforced by few-layer graphene', *Nanotechnology*, vol. 20, no. 12, p. 125705, Mar. 2009, doi: 10.1088/0957-4484/20/12/125705.
- [3] M. Yoonessi *et al.*, 'Graphene Polyimide Nanocomposites; Thermal, Mechanical, and High-Temperature Shape Memory Effects', *ACS Nano*, vol. 6, no. 9, pp. 7644–7655, Sep. 2012, doi: 10.1021/nn302871y.
- [4] E. T. Thostenson and T.-W. Chou, 'Aligned multi-walled carbon nanotube-reinforced composites: processing and mechanical characterization', *J. Phys. Appl. Phys.*, vol. 35, no. 16, pp. L77–L80, Aug. 2002, doi: 10.1088/0022-3727/35/16/103.
- [5] J. Leng, H. Lv, Y. Liu, and S. Du, 'Electroactivate shape-memory polymer filled with nanocarbon particles and short carbon fibers', *Appl. Phys. Lett.*, vol. 91, no. 14, p. 144105, Oct. 2007, doi: 10.1063/1.2790497.
- [6] J. Leng, H. Lv, Y. Liu, and S. Du, 'Synergic effect of carbon black and short carbon fiber on shape memory polymer actuation by electricity', *J. Appl. Phys.*, vol. 104, no. 10, p. 104917, Nov. 2008, doi: 10.1063/1.3026724.
- [7] C.-S. Zhang and Q.-Q. Ni, 'Bending behavior of shape memory polymer based laminates', *Compos. Struct.*, vol. 78, no. 2, pp. 153–161, Apr. 2007, doi: 10.1016/j.compstruct.2005.08.029.
- [8] P. Turner, T. Liu, and X. Zeng, 'Collapse of 3D orthogonal woven carbon fibre composites under in-plane tension/compression and out-of-plane bending', *Compos. Struct.*, vol. 142, pp. 286–297, May 2016, doi: 10.1016/j.compstruct.2016.01.100.
- [9] M. F. Yahya, F. M. Z. Nasrun, S. A. Ghani, and M. R. Ahmad, 'Factors Affecting Tensile Performance of 2D & 3D Angle Interlock Woven Fabric Composite: A Review', *Adv. Mater. Res.*, vol. 1134, pp. 147–153, Dec. 2015, doi: 10.4028/www.scientific.net/AMR.1134.147.
- [10] K. R. Hart, P. X. L. Chia, L. E. Sheridan, E. D. Wetzel, N. R. Sottos, and S. R. White, 'Mechanisms and characterization of impact damage in 2D and 3D woven fiber-reinforced composites', *Compos. Part Appl. Sci. Manuf.*, vol. 101, pp. 432–443, Oct. 2017, doi: 10.1016/j.compositesa.2017.07.004.
- [11] I. Goda and J.-F. Ganghoffer, 'Construction of first and second order grade anisotropic continuum media for 3D porous and textile composite structures', *Compos. Struct.*, vol. 141, pp. 292–327, May 2016, doi: 10.1016/j.compstruct.2016.01.061.
- [12] Y. Rahali, M. Assidi, I. Goda, A. Zghal, and J. F. Ganghoffer, 'Computation of the effective mechanical properties including nonclassical moduli of 2.5D and 3D interlocks by micromechanical approaches', *Compos. Part B Eng.*, vol. 98, pp. 194–212, Aug. 2016, doi: 10.1016/j.compositesb.2016.04.066.
- [13] Y. Rahali, I. Goda, and J. F. Ganghoffer, 'Numerical identification of classical and nonclassical moduli of 3D woven textiles and analysis of scale effects', *Compos. Struct.*, vol. 135, pp. 122–139, Jan. 2016, doi: 10.1016/j.compstruct.2015.09.023.
- [14] A. Elias, F. Laurin, M. Kaminski, and L. Gornet, 'Experimental and numerical investigations of low energy/velocity impact damage generated in 3D woven composite

- with polymer matrix', *Compos. Struct.*, vol. 159, pp. 228–239, Jan. 2017, doi: 10.1016/j.compstruct.2016.09.077.
- [15] Xiaogang Chen, L. W. Taylor, and L.-J. Tsai, 'An overview on fabrication of three-dimensional woven textile preforms for composites', *Text. Res. J.*, vol. 81, no. 9, pp. 932–944, Jun. 2011, doi: 10.1177/0040517510392471.
- [16] C. Liu, H. Qin, and P. T. Mather, 'Review of progress in shape-memory polymers', *J. Mater. Chem.*, vol. 17, no. 16, pp. 1543–1558, Apr. 2007, doi: 10.1039/B615954K.
- [17] M. Behl and A. Lendlein, 'Shape-memory polymers', *Mater. Today*, vol. 10, no. 4, pp. 20–28, Apr. 2007, doi: 10.1016/S1369-7021(07)70047-0.
- [18] D. Ratna and J. Karger-Kocsis, 'Recent advances in shape memory polymers and composites: a review', *J. Mater. Sci.*, vol. 43, no. 1, pp. 254–269, Jan. 2008, doi: 10.1007/s10853-007-2176-7.
- [19] M. Babaahmadi, M. Sabzi, G. R. Mahdavinia, and M. Keramati, 'Preparation of amorphous nanocomposites with quick heat triggered shape memory behavior', *Polymer*, vol. 112, pp. 26–34, Mar. 2017, doi: 10.1016/j.polymer.2017.01.074.
- [20] Y. Liu, K. Gall, M. L. Dunn, and P. McCluskey, 'Thermomechanics of shape memory polymer nanocomposites', *Mech. Mater.*, vol. 36, no. 10, pp. 929–940, Oct. 2004, doi: 10.1016/j.mechmat.2003.08.012.
- [21] F. Ji, Y. Zhu, J. Hu, Y. Liu, L.-Y. Yeung, and G. Ye, 'Smart polymer fibers with shape memory effect', *Smart Mater. Struct.*, vol. 15, no. 6, pp. 1547–1554, Dec. 2006, doi: 10.1088/0964-1726/15/6/006.
- [22] R. Vaia, 'Remote-controlled actuators', *Nat. Mater.*, vol. 4, no. 6, pp. 429–430, Jun. 2005, doi: 10.1038/nmat1400.
- [23] Z. Wang and Z. C. Kang, *Functional and Smart Materials: Structural Evolution and Structure Analysis*. Springer US, 1998.
- [24] Z. G. Wei, R. Sandstrom, and S. Miyazaki, 'Shape memory materials and hybrid composites for smart systems: Part II Shape-memory hybrid composites', *J. Mater. Sci.*, vol. 33, no. 15, pp. 3763–3783, Aug. 1998, doi: 10.1023/A:1004674630156.
- [25] P. Gaudenzi, *Smart Structures: Physical Behaviour, Mathematical Modelling and Applications*. 2009.
- [26] C. A. Rogers and I. Ahmad, 'U.S. Army Research Office Workshop on Smart Materials, Structures and Mathematical issues', *Virginia Polytechnic Institute & State University*, pp. 1–12, 1988.
- [27] A. Basit, 'Development and characterization of a shape memory polymer composite actuator for morphing structures', *Université de Haute Alsace - Mulhouse*, Dec. 2012, [Online]. Available: <https://tel.archives-ouvertes.fr/tel-01267578>.
- [28] C. A. Rogers, 'Intelligent Material Systems and Structures', *Honolulu Hawaii*, pp. 11–33, 1990.
- [29] W. M. Huang, Z. Ding, C. C. Wang, J. Wei, Y. Zhao, and H. Purnawali, 'Shape memory materials', vol. 13, no. 7, p. 8, 2010.
- [30] F. E. Feninat, G. Laroche, M. Fiset, and D. Mantovani, 'Shape Memory Materials for Biomedical Applications', *Adv. Eng. Mater.*, no. 3, p. 14, 2002.
- [31] E. Hornbogen, 'Comparison of Shape Memory Metals and Polymers', *Adv. Eng. Mater.*, vol. 8, no. 1–2, pp. 101–106, Feb. 2006, doi: 10.1002/adem.200500193.

- [32] I. S. Gunes and S. C. Jana, 'Shape Memory Polymers and Their Nanocomposites: A Review of Science and Technology of New Multifunctional Materials', *J. Nanosci. Nanotechnol.*, vol. 8, no. 4, pp. 1616–1637, Apr. 2008, doi: 10.1166/jnn.2008.038.
- [33] H. Funakubo and J. Kennedy, 'Shape memory alloys', *Gordon Breach*, 1987.
- [34] L. Sun and W. M. Huang, 'Mechanisms of the multi-shape memory effect and temperature memory effect in shape memory polymers', *Soft Matter*, vol. 6, no. 18, pp. 4403–4406, Sep. 2010, doi: 10.1039/C0SM00236D.
- [35] L. Sun, W. M. Huang, and J. Y. Cheah, 'The temperature memory effect and the influence of thermo-mechanical cycling in shape memory alloys', *Smart Mater. Struct.*, vol. 19, no. 5, p. 055005, May 2010, doi: 10.1088/0964-1726/19/5/055005.
- [36] H. Lv, J. Leng, Y. Liu, and S. Du, 'Shape-Memory Polymer in Response to Solution', *Adv. Eng. Mater.*, vol. 10, no. 6, pp. 592–595, 2008, doi: 10.1002/adem.200800002.
- [37] C. Liang, C. Rogers, and E. Malafeev, 'Investigation of shape memory polymers and their hybrid composites (Reprinted from proceedings of the second joint Japan/US conference on adaptive structures)', *J. Intell. Mater. Syst. Struct.*, pp. 789–802, Nov. 1997.
- [38] N. Scheerbaum, D. Hinz, and O. Gutfleisch, 'Textured polymer bonded composites with Ni–Mn–Ga magnetic shape memory particles', *Acta Mater.*, p. 7, 2007.
- [39] H. Tobushi, E. Pieczyska, Y. Ejiri, and T. Sakuragi, 'Thermomechanical Properties of Shape-Memory Alloy and Polymer and Their Composites', *Mech. Adv. Mater. Struct.*, vol. 16, no. 3, pp. 236–247, Apr. 2009, doi: 10.1080/15376490902746954.
- [40] D. C. Hofmann, 'Shape Memory Bulk Metallic Glass Composites', *Science*, vol. 329, no. 5997, pp. 1294–1295, Sep. 2010, doi: 10.1126/science.1193522.
- [41] L. Sun *et al.*, 'Stimulus-responsive shape memory materials: A review', *Mater. Des.*, 2012.
- [42] T. H. H. T., and H. S., 'Thermomechanical Constitutive Modeling in Shape Memory Polymer of Polyurethane Series', Aug. 1997.
- [43] H. Tobushi, K. Okumura, S. Hayashi, and N. Ito, 'Thermomechanical constitutive model of shape memory polymer', *Mech. Mater.*, p. 10, 2001.
- [44] C. Liu, S. B. Chun, P. T. Mather, L. Zheng, E. H. Haley, and E. B. Coughlin, 'Chemically Cross-Linked Polycyclooctene: Synthesis, Characterization, and Shape Memory Behavior', *Macromolecules*, vol. 35, no. 27, pp. 9868–9874, Dec. 2002, doi: 10.1021/ma021141j.
- [45] J. L. Willett, 'Humidity-Responsive Starch-Poly(methyl acrylate) Films', *Macromol. Chem. Phys.*, vol. 209, no. 7, pp. 764–772, 2008, doi: 10.1002/macp.200700495.
- [46] S. Hayashi, 'Technical report on preliminary investigation of shape memory polymers.' Japan: Mitsubishi Heavy Industries Inc, 1990.
- [47] L. Jinsong, L. Haibao, L. Yanju, H. Wei Min, and D. Shanyi, 'Shape memory polymers – a class of novel smart material', *J. Mater. Res. Technol.*, vol. 34, Nov. 2009.
- [48] J. Hu, *Shape Memory Polymers and Textiles*. Elsevier, 2007.
- [49] J. Leng, X. Lan, Y. Liu, and S. Du, 'Shape-memory polymers and their composites: Stimulus methods and applications', *Prog. Mater. Sci.*, vol. 56, no. 7, pp. 1077–1135, Sep. 2011, doi: 10.1016/j.pmatsci.2011.03.001.
- [50] R. Langer and D. A. Tirrell, 'Designing materials for biology and medicine', *Nature*, vol. 428, no. 6982, pp. 487–492, Apr. 2004, doi: 10.1038/nature02388.
- [51] P. Miaudet *et al.*, 'Shape and temperature memory of nanocomposites with broadened glass transition', *Science*, vol. 318, no. 5854, pp. 1294–1296, Nov. 2007, doi: 10.1126/science.1145593.



- [52] J. Leng, H. Lu, Y. Liu, W. M. Huang, and S. Du, 'Shape-Memory Polymers—A Class of Novel Smart Materials', *MRS Bull.*, vol. 34, no. 11, pp. 848–855, Nov. 2009, doi: 10.1557/mrs2009.235.
- [53] J. Leng, X. Lan, Y. Liu, and S. Du, 'Electroactive thermoset shape memory polymer nanocomposite filled with nanocarbon powders', *Smart Mater. Struct.*, vol. 18, no. 7, p. 074003, Jun. 2009, doi: 10.1088/0964-1726/18/7/074003.
- [54] Y.-C. Chen and D. C. Lagoudas, 'A constitutive theory for shape memory polymers. Part I: Large deformations', *J. Mech. Phys. Solids*, vol. 56, no. 5, pp. 1752–1765, May 2008, doi: 10.1016/j.jmps.2007.12.005.
- [55] Y.-C. Chen and D. C. Lagoudas, 'A constitutive theory for shape memory polymers. Part II: A linearized model for small deformations', *J. Mech. Phys. Solids*, vol. 56, no. 5, pp. 1766–1778, May 2008, doi: 10.1016/j.jmps.2007.12.004.
- [56] J. Leng and S. Du, *Shape-Memory Polymers and Multifunctional Composites*. CRC Press, 2010.
- [57] S. Kelch, S. Steuer, A. M. Schmidt, and A. Lendlein, 'Shape-Memory Polymer Networks from Oligo[( $\epsilon$ -hydroxycaproate)-co-glycolate]dimethacrylates and Butyl Acrylate with Adjustable Hydrolytic Degradation Rate', *Biomacromolecules*, vol. 8, no. 3, pp. 1018–1027, Mar. 2007, doi: 10.1021/bm0610370.
- [58] A. Lendlein, A. M. Schmidt, and R. Langer, 'AB-polymer networks based on oligo( $\epsilon$ -caprolactone) segments showing shape-memory properties', *Proc. Natl. Acad. Sci. U. S. A.*, vol. 98, no. 3, pp. 842–847, Jan. 2001, doi: 10.1073/pnas.031571398.
- [59] A. Lendlein, A. M. Schmidt, M. Schroeter, and R. Langer, 'Shape-memory polymer networks from oligo( $\epsilon$ -caprolactone)dimethacrylates', *J. Polym. Sci. Part Polym. Chem.*, vol. 43, no. 7, pp. 1369–1381, 2005, doi: 10.1002/pola.20598.
- [60] S. Ahn, R. M. Kasi, S.-C. Kim, N. Sharma, and Y. Zhou, 'Stimuli-responsive polymer gels', *Soft Matter*, vol. 4, no. 6, pp. 1151–1157, 2008, doi: 10.1039/B714376A.
- [61] S. Zhang, Y. Feng, L. Zhang, J. Sun, X. Xu, and Y. Xu, 'Novel interpenetrating networks with shape-memory properties', *J. Polym. Sci. Part Polym. Chem.*, vol. 45, no. 5, pp. 768–775, 2007, doi: 10.1002/pola.21832.
- [62] H. M. Jeong, B. K. Kim, and Y. J. Choi, 'Synthesis and properties of thermotropic liquid crystalline polyurethane elastomers', *Polymer*, vol. 41, no. 5, pp. 1849–1855, Mar. 2000, doi: 10.1016/S0032-3861(99)00334-1.
- [63] H. M. Jeong, S. Y. Lee, and B. K. Kim, 'Shape memory polyurethane containing amorphous reversible phase', *J. Mater. Sci.*, vol. 35, no. 7, pp. 1579–1583, Apr. 2000, doi: 10.1023/A:1004761206709.
- [64] S. H. Lee, J. W. Kim, and B. K. Kim, 'Shape memory polyurethanes having crosslinks in soft and hard segments', *Smart Mater. Struct.*, vol. 13, no. 6, p. 1345, Oct. 2004, doi: 10.1088/0964-1726/13/6/007.
- [65] B. K. Kim *et al.*, 'Polyurethane ionomers having shape memory effects', *Polymer*, vol. 39, no. 13, pp. 2803–2808, Jun. 1998, doi: 10.1016/S0032-3861(97)00616-2.
- [66] A. Lendlein and S. Kelch, 'Shape-Memory Polymers', *Angew. Chem. Int. Ed.*, vol. 41, no. 12, pp. 2034–2057, 2002, doi: 10.1002/1521-3773(20020617)41:12<2034::AID-ANIE2034>3.0.CO;2-M.
- [67] K. Gall, M. L. Dunn, Y. Liu, G. Stefanic, and D. Balzar, 'Internal stress storage in shape memory polymer nanocomposites', *Appl. Phys. Lett.*, vol. 85, no. 2, pp. 290–292, Jul. 2004, doi: 10.1063/1.1769087.

- [68] X. Luo and P. T. Mather, 'Conductive shape memory nanocomposites for high speed electrical actuation', *Soft Matter*, vol. 6, no. 10, pp. 2146–2149, 2010, doi: 10.1039/C001295E.
- [69] A. J. W. McClung, G. P. Tandon, and J. W. Baur, 'Deformation rate-, hold time-, and cycle-dependent shape-memory performance of Veriflex-E resin', *Mech. Time-Depend. Mater.*, vol. 17, no. 1, pp. 39–52, Feb. 2013, doi: 10.1007/s11043-011-9157-6.
- [70] I. A. Rousseau and T. Xie, 'Shape memory epoxy: Composition, structure, properties and shape memory performances', *J. Mater. Chem.*, vol. 20, no. 17, pp. 3431–3441, 2010, doi: 10.1039/B923394F.
- [71] D. M. Feldkamp and I. A. Rousseau, 'Effect of the Deformation Temperature on the Shape-Memory Behavior of Epoxy Networks', *Macromol. Mater. Eng.*, vol. 295, no. 8, pp. 726–734, 2010, doi: 10.1002/mame.201000035.
- [72] X. Wu, Y. Liu, and J. Leng, 'Investigation of mechanical behavior of epoxy shape memory polymers', in *Behavior and Mechanics of Multifunctional Materials and Composites 2009*, Mar. 2009, vol. 7289, p. 72890Z, doi: 10.1117/12.815706.
- [73] V. A. Beloshenko and Yu. V. Voznyak, 'Shape memory effect in the epoxy polymer composites with aggregated filler', *Polym. Sci. Ser. A*, vol. 51, no. 4, pp. 416–423, Apr. 2009, doi: 10.1134/S0965545X09040075.
- [74] H. Deng, J. P. Gao, X. F. An, and X. S. Yi, 'Tailoring of Thermal Transition Temperature and Toughening of Shape Memory Epoxy Polymer', *Applied Mechanics and Materials*, 2012. <https://www.scientific.net/AMM.182-183.93> (accessed Feb. 26, 2020).
- [75] G. P. Tandon, K. Goecke, K. Cable, and J. Baur, 'Durability Assessment of Styrene- and Epoxy-based Shape-memory Polymer Resins', *J. Intell. Mater. Syst. Struct.*, vol. 20, no. 17, pp. 2127–2143, Nov. 2009, doi: 10.1177/1045389X09348255.
- [76] J. Xu and J. Song, 'Thermal Responsive Shape Memory Polymers for Biomedical Applications', in *Biomedical Engineering - Frontiers and Challenges*, R. Fazel, Ed. InTech, 2011.
- [77] T. Xie and I. A. Rousseau, 'Facile tailoring of thermal transition temperatures of epoxy shape memory polymers', *Polymer*, vol. 50, no. 8, pp. 1852–1856, Apr. 2009, doi: 10.1016/j.polymer.2009.02.035.
- [78] M. A. Di Prima *et al.*, 'Deformation of epoxy shape memory polymer foam: Part II. Mesoscale modeling and simulation', *Mech. Mater.*, vol. 42, no. 3, pp. 315–325, Mar. 2010, doi: 10.1016/j.mechmat.2009.11.002.
- [79] L. B. Vernon, Beaver, and H. M. Vernon, 'Process of manufacturing articles of thermoplastic synthetic resins', *U. S. Pat. 2234993*, Mar. 1941.
- [80] R. William C, Barrington, R. Edward M, A. W. Sloan, and W. D. Stewart, 'Polyethylene product and process', *U. S. Pat. 3144398*, Aug. 1964.
- [81] W. Sokolowski, S. Tan, and M. Pryor, 'Lightweight Shape Memory Self-Deployable Structures for Gossamer Applications', presented at the 45th AIAA/ASME/ASCE/AHS/ASC Structures, Structural Dynamics & Materials Conference, Palm Springs, California, Apr. 2004, doi: 10.2514/6.2004-1660.
- [82] J. Hu, Y. Zhu, H. Huang, and J. Lu, 'Recent advances in shape-memory polymers: Structure, mechanism, functionality, modeling and applications', *Prog. Polym. Sci.*, vol. 37, no. 12, pp. 1720–1763, Dec. 2012, doi: 10.1016/j.progpolymsci.2012.06.001.
- [83] J. Zotzmann, M. Behl, D. Hofmann, and A. Lendlein, 'Reversible triple-shape effect of polymer networks containing polypentadecalactone- and poly(epsilon-caprolactone)-

- segments', *Adv. Mater. Deerfield Beach Fla*, vol. 22, no. 31, pp. 3424–3429, Aug. 2010, doi: 10.1002/adma.200904202.
- [84] J. R. Lin and L. W. Chen, 'Study on shape-memory behavior of polyether-based polyurethanes. I. Influence of the hard-segment content', *J. Appl. Polym. Sci.*, vol. 69, no. 8, pp. 1563–1574, Aug. 1998, doi: 10.1002/(SICI)1097-4628(19980822)69:8<1563::AID-APP11>3.0.CO;2-W.
- [85] J. R. Lin and L. W. Chen, 'Study on shape-memory behavior of polyether-based polyurethanes. II. Influence of soft-segment molecular weight', *J. Appl. Polym. Sci.*, vol. 69, no. 8, pp. 1575–1586, 1998, doi: 10.1002/(SICI)1097-4628(19980822)69:8<1575::AID-APP12>3.0.CO;2-U.
- [86] F. L. Ji, J. L. Hu, and J. P. Han, 'Shape memory polyurethane-ureas based on isophorone diisocyanate', *High Perform. Polym.*, vol. 23, no. 3, pp. 177–187, May 2011, doi: 10.1177/0954008311398323.
- [87] S. Chen, J. Hu, Y. Liu, H. Liem, Y. Zhu, and Y. Liu, 'Effect of SSL and HSC on morphology and properties of PHA based SMPU synthesized by bulk polymerization method', *J. Polym. Sci. Part B Polym. Phys.*, vol. 45, no. 4, pp. 444–454, 2007, doi: 10.1002/polb.21046.
- [88] B. S. Lee, B. C. Chun, Y.-C. Chung, K. I. Sul, and J. W. Cho, 'Structure and Thermomechanical Properties of Polyurethane Block Copolymers with Shape Memory Effect', *Macromolecules*, vol. 34, no. 18, pp. 6431–6437, Aug. 2001, doi: 10.1021/ma001842l.
- [89] S. Chen, J. Hu, Y. Liu, H. Liem, Y. Zhu, and Q. Meng, 'Effect of molecular weight on shape memory behavior in polyurethane films', *Polym. Int.*, vol. 56, no. 9, pp. 1128–1134, 2007, doi: 10.1002/pi.2248.
- [90] F. L. Ji and J. L. Hu, 'Comparison of shape memory polyurethanes and polyurethane-ureas having crystalline reversible phase', *High Perform. Polym.*, vol. 23, no. 4, pp. 314–325, Jun. 2011, doi: 10.1177/0954008311405868.
- [91] R. Xiao, C. Zhan, and W. M. Huang, *Programming of Shape-Memory Polymers: The Temperature Memory Effect and Triple/Multiple-Shape-Memory Effect in Polymers*. William Andrew Publishing, 2017.
- [92] A. Lendlein and S. A. Madbouly, 'Shape-Memory Polymer Composites', in *Advanced Polymer Science*, 2009.
- [93] M. Nishikawa, K. Wakatsuki, A. Yoshimura, and N. Takeda, 'Effect of fiber arrangement on shape fixity and shape recovery in thermally activated shape memory polymer-based composites', *Compos. Part Appl. Sci. Manuf.*, vol. 43, no. 1, pp. 165–173, Jan. 2012, doi: 10.1016/j.compositesa.2011.10.005.
- [94] T. Ohki, Q.-Q. Ni, N. Ohsako, and M. Iwamoto, 'Mechanical and shape memory behavior of composites with shape memory polymer', *Compos. Part Appl. Sci. Manuf.*, vol. 35, no. 9, pp. 1065–1073, Sep. 2004, doi: 10.1016/j.compositesa.2004.03.001.
- [95] K. Gall, M. L. Dunn, Y. Liu, D. Finch, M. Lake, and N. A. Munshi, 'Shape memory polymer nanocomposites', *Acta Mater.*, p. 12, 2002.
- [96] I. S. Gunes, F. Cao, and S. C. Jana, 'Evaluation of nanoparticulate fillers for development of shape memory polyurethane nanocomposites', *Polymer*, vol. 49, no. 9, pp. 2223–2234, Apr. 2008, doi: 10.1016/j.polymer.2008.03.021.
- [97] S. Mondal and J. L. Hu, 'Shape Memory Studies of Functionalized MWNT-reinforced Polyurethane Copolymers', *Iran. Polym. J.*, vol. 15, no. 2, p. 9, 2006.

- [98] J. M. Cuevas, R. Rubio, J. M. Laza, J. L. Vilas, M. Rodriguez, and L. M León, ‘Shape memory composites based on glass-fibre-reinforced poly(ethylene)-like polymers’, *Smart Mater. Struct.*, vol. 21, no. 3, p. 035004, Mar. 2012, doi: 10.1088/0964-1726/21/3/035004.
- [99] C.-S. Zhang and Q.-Q. Ni, ‘Bending behavior of shape memory polymer based laminates’, *Compos. Struct.*, vol. 78, no. 2, pp. 153–161, Apr. 2007, doi: 10.1016/j.compstruct.2005.08.029.
- [100] X. Luo and P. T. Mather, ‘Triple-Shape Polymeric Composites (TSPCs)’, *Adv. Funct. Mater.*, vol. 20, no. 16, pp. 2649–2656, Aug. 2010, doi: 10.1002/adfm.201000052.
- [101] H. Tamagawa, ‘Thermo-responsive two-way shape changeable polymeric laminate’, *Mater. Lett.*, vol. 64, no. 6, pp. 749–751, Mar. 2010, doi: 10.1016/j.matlet.2009.12.053.
- [102] W. Wagermaier, K. Kratz, M. Heuchel, and A. Lendlein, ‘Characterization Methods for Shape-Memory Polymers’, in *Shape-Memory Polymers*, vol. 226, A. Lendlein, Ed. Berlin, Heidelberg: Springer Berlin Heidelberg, 2009, pp. 97–145.
- [103] M. Rajanish, N. V. Nanjundaradhya, and R. S. Sharma, ‘An Investigation On ILSS Properties of Unidirectional Glass Fibre / Alumina Nanoparticles Filled Epoxy Nanocomposite At Different Angles Of Fibre Orientations’, *Procedia Mater. Sci.*, vol. 10, pp. 555–562, 2015, doi: 10.1016/j.mspro.2015.06.006.
- [104] J. Goldstein *et al.*, *Scanning Electron Microscopy and X-ray Microanalysis*. New York, USA.: Springer, 2007.
- [105] Z. Wang, J. Liu, J. Guo, X. Sun, and L. Xu, ‘The Study of Thermal, Mechanical and Shape Memory Properties of Chopped Carbon Fiber-Reinforced TPI Shape Memory Polymer Composites’, *Polymers*, vol. 9, no. 11, Nov. 2017, doi: 10.3390/polym9110594.
- [106] F. DA, ‘Shape memory polymer intravascular delivery system with heat transfer medium’, *U. S. Pat. 6224610*, 2001.
- [107] H. M. Wache, D. J. Tartakowska, A. Hentrich, and M. H. Wagner, ‘Development of a polymer stent with shape memory effect as a drug delivery system’, *J. Mater. Sci.*, p. 4, 2003.
- [108] R. Dhanasekaran, S. Sreenatha Reddy, B. Girish Kumar, and A. S. Anirudh, ‘Shape Memory Materials for Bio-medical and Aerospace Applications’, *Mater. Today Proc.*, vol. 5, no. 10, pp. 21427–21435, 2018, doi: 10.1016/j.matpr.2018.06.551.
- [109] M. Behl and A. Lendlein, ‘Actively moving polymers’, *Soft Matter*, vol. 3, no. 1, pp. 58–67, 2007, doi: 10.1039/B610611K.
- [110] P. Keller, M. Lake, D. Codell, R. Barrett, R. Taylor, and M. Schultz, ‘Development of Elastic Memory Composite Stiffeners for a Flexible Precision Reflector’, presented at the 47th AIAA/ASME/ASCE/AHS/ASC Structures, Structural Dynamics, and Materials Conference<BR> 14th AIAA/ASME/AHS Adaptive Structures Conference<BR> 7th, Newport, Rhode Island, May 2006, doi: 10.2514/6.2006-2179.
- [111] M. Love, P. Zink, R. Stroud, D. Bye, S. Rizk, and D. White, ‘Demonstration of Morphing Technology through Ground and Wind Tunnel Tests’, presented at the 48th AIAA/ASME/ASCE/AHS/ASC Structures, Structural Dynamics, and Materials Conference, Honolulu, Hawaii, Apr. 2007, doi: 10.2514/6.2007-1729.
- [112] L. Santo, F. Quadrini, and D. Bellisario, ‘Shape memory composite antennas for space applications’, *IOP Conf. Ser. Mater. Sci. Eng.*, vol. 161, no. 1, p. 012066, Nov. 2016, doi: 10.1088/1757-899X/161/1/012066.

- [113] J. Zhu, G. Fang, Z. Cao, X. Meng, and H. Ren, 'A Self-Folding Dynamic Covalent Shape Memory Epoxy and Its Continuous Glass Fiber Composite', *Ind. Eng. Chem. Res.*, vol. 57, no. 15, pp. 5276–5281, Apr. 2018, doi: 10.1021/acs.iecr.8b00222.
- [114] H. M. Hussein and D. M. Harrison, 'Investigation into the use of engineering polymers as actuators to produce "automatic disassembly" of electronic products', 2004.
- [115] G. Akovali, *Handbook of Composite Fabrication*. iSmithers Rapra Publishing, 2001.
- [116] 'Alali - Contribution à l'étude de tissus multicouches CAO.pdf'. Accessed: Jun. 25, 2020. [Online]. Available: <https://tel.archives-ouvertes.fr/tel-01249557/document>.
- [117] N. Zheng, G. Fang, Z. Cao, Q. Zhao, and T. Xie, 'High strain epoxy shape memory polymer', *Polym. Chem.*, vol. 6, no. 16, pp. 3046–3053, Apr. 2015, doi: 10.1039/C5PY00172B.
- [118] Y. Liu, C. Han, H. Tan, and X. Du, 'Thermal, mechanical and shape memory properties of shape memory epoxy resin', *Mater. Sci. Eng. A*, vol. 527, no. 10, pp. 2510–2514, Apr. 2010, doi: 10.1016/j.msea.2009.12.014.
- [119] E. Wang *et al.*, 'A novel reduced graphene oxide/epoxy sandwich structure composite film with thermo-, electro- and light-responsive shape memory effect', *Mater. Lett.*, vol. 238, pp. 54–57, Mar. 2019, doi: 10.1016/j.matlet.2018.11.138.
- [120] K. E. Smith, S. Sawicki, M. A. Hyjek, S. Downey, and K. Gall, 'The effect of the glass transition temperature on the toughness of photopolymerizable (meth)acrylate networks under physiological conditions', *Polymer*, vol. 50, no. 21, pp. 5112–5123, Oct. 2009, doi: 10.1016/j.polymer.2009.08.040.